GENERAL GEOLOGY AND SLOPE FAILURE ASSESSMENT OF SOIL CUT-SLOPE AT KUALA BALAH, JELI DISTRICT, KELANTAN, MALAYSIA

by

CHIAR WEI WEI

A report submitted in fulfilment of the requirements for the degree of Bachelor of Applied Science (Geoscience) with Honours

FACULTY OF EARTH SCIENCE

UNIVERSITI MALAYSIA KELANTAN

2017

DECLARATION

I declare that this thesis entitled "GENERAL GEOLOGY AND SLOPE FAILURE ASSESSMENT OF SOIL CUT-SLOPE AT KUALA BALAH, JELI DISTRICT, KELANTAN, MALAYSIA"is the result of my own research except as cited in the references. The thesis has not been accepted for any degree and is not concurrently submitted in candidature of any other degree.

Signature :
Name : Chiar Wei Wei
Date :

ACKNOWLEDGEMENT

I would like to express my sincere gratitude who had help in order to successful accomplishment of this project. A greatest appreciation to my research supervisor, Mr. Shukri bin Ma'ail for his invaluable advice and guidance along the whole period of the research.

In addition, a thank you to Mr. Hamzah bin Hussin, who acts as my supervisor in FYP 1 for his willingness and sincere advice to the successful completion of first part of this research. I would like to express my gratitude to examiners in FYP 1, Dr. Wani Sofia Binti Udin and Madam Elvaene James for their rectification in FYP 1 and willingness of the explanation.

I am deeply grateful to Mr. Arham Muchtar Achmad Bahar, Mr. Mohd Syakir Bin Sulaiman and Miss Zakiyah Binti Ainul Kamal for their encouragement and support for this study. Without them, this study would hardly to be completed.

I owe deepest gratitude to Faculty of Earth Science Universiti Malaysia Kelantan and Engineering Department of Politeknik Kota Bharu. The laboratory and facilities provided are making it to possible to carry out all the tests.

Last but not least, I would like to thank you my family members who support me to the successful completion of this project. I would also like to thank you to all my friends who direct and indirectly support and help me in this four years of study.

General Geology and Slope Failure Assessment

of Soil Cut-Slope at Kuala Balah, Jeli District, Kelantan,

Malaysia

ABSTRACT

Slope failure assessment in this research included the study of characteristics of the slope and the factor of safety of the slope. The properties of the slope forming materials are significant in the slope stability analysis. The study area is located at Kuala Balah, Jeli, Kelantan. The total area of the study are is 25km^2 and bounded within the coordinate of 5° 26' 10.80" N, 101° 54' 15.00" E and 5° 23' 28.8" N, 101° 56' 56.40" E. The objectives of this study are to update the geological map of the Kuala Balah, Jeli, Kelantan with scale of 1:25 000, to produce slope failure inventory of the study area with slope geometry, mode/ type of failure, failure geometry, origin of soil/ rock, cause of failure, type of slope stabilization protection and vegetation cover of failure and to construct slope stability analysis for soil cut-slope at study area by using Slope/ W software. Geological mapping and engineering mapping were carried out to identify the geological features and the soil-cut-slope. Geological map of Kuala Balah, Jeli, Kelantan has been updated. The lithology consists of fine-grained granite, granodiorite, fine-grained biotite granite, quartzite, fine-grained gneiss, coarse-grained quartz-plagioclase gneiss, shale, mudstone and metasandstone. There are a total eight cut-slope failure observed in the study area. The inventory of slope failure is constructed. Most of the weathering grade of soil cut-slope is five and originated from shale. The mode of failure of all slope is rotational slide and protected by vegetation or Gabion retaining wall. Major causes of the failure are weathering process and rainfall. Laboratory analysis for properties of soil had been done for the slope stability analysis. Based on the laboratory tests of soil, the classification of soil is done and the results are used in the determination of factor of safety of slope. The soil samples are categorized into three groups which area sandy silty clay, sandy lean clay and sandy high plasticity clay. The factor of safety of the selected slopes are range in 0.339 to 2.548 which indicated there has stable slope and unstable slopes.

Geologi Am dan Penilaian Kegagalan Cerun

Tanah Potong di Kuala Balah, Daerah Jeli, Kelantan

Malaysia

ABSTRAK

Penilaian kegagalan cerun dalam projek penyelidikan ini termasuk kajian ciri-ciri cerun dan faktor keselamatan cerun. Ciri-ciri bahan pembentukan cerun adalah penting dalam analisis kestabilan cerun. Kawasan kajian terletak di Kuala Balah, Jeli, Kelantan. Jumlah kawasan kajian adalah 25km^2 dengan koordinat 5° 26' 10.80" U, 101° 54' 15.00" T and 5° 23' 28.8" U, 101° 56' 56.40" T. Objektif kajian ini termasuk kemaskini peta geologi Kuala Balah, Jeli, Kelantan dengan skala 1:25 000, meghasilkan inventori kegagalan cerun dalam kawasan kajian dengan geometri cerun, mod/ jenis kegagalan, geometri kegagalan, gred luluhawa, asal tanah/ batu, sebab kegagalan, jenis perlindungan penstablilan cerun dan perlindungan tunbuh-tunbuhan kepada kegagalan dan membina analisis kestabilan cerun untuk cerun potong tanah dalam kawasan kajian dengan menggunakan Slope/W software. Pemetaan geologi dan pemetaan kejuruteraan telah dijalankan bagi mengenalpasti ciri-ciri geologi dan cerun potong tanah. Analisis makmal tentang ciri-ciri tanah telah dilakukan untuk analisis kestabilan cerun. Peta geologi Kuala Balah, Jeli, Kelantan telah dikemaskini dan mengandungi batuan seperti granit berbutir halus, granodiorite, biotit granit berbutir halus, kuarzit, gneis berbutir halus, kuarza-plagioklas gneis berbutir kasar, syal, batu lumpur dan batu pasir yang termetamorf. Dalam kawasan kajian, jumlah lapan kegagalan cerun telah diperhatikan. Inventori kegagalan cerun telah dibina. Kebanyakan gred luluhawa creun tanah adalah ged lima dan berasal daripada syal. Jenis kegagalan cerun adalah gelinciran putaran dan dilindungi dengan tumbuh-tumbuhan atau dinding penahan gabion. Sebab kegagalan utama termasuk proses luluhawa dan hujan. Berdasarkan ujian makmal tanah, klassifikasi tanah telah diperlakukan dan keputusan digunakan dalam penentuan faktor keselamatan cerun. Sampel tanah telah dibahagikan kepada tiga kumpulan iaitu lempung berlanau berpasir, lempung "kurus" berpasir, dan lempung keplastikan tinggi berpasir. Faktor keselamatan cerun bagi cerun terpilih adalah dalam julat 0.339 hingga 2.548. Nilai faktor keselamatan cerun menunjukkan cerun tersebut adalah stabil dan tidak stabil.

TABLE OF CONTENT

LIST OF TABLES

LIST OF FIGURES

LIST OF ABBREVIATIONS

cm	Centimeter
etc.	Et Cetera
ha	Hectare
km	Kilometer
km^2	Kilometer Square
m	Meter
mm	Millimeter
Afs	Alkali Feldspar
Bt	Biotite
Cpx	Clinopyroxene
Grt	Garnet
Hlb	Hornblende
Opx	Orthopyroxene
Plg	Plagioclase
ASTM	American Section of the International Association for Testing Materials
CH	Clay of Low Plasticity, Lean Clay
E	East
GIS	Geographic Information System
IUGS	International Union of Geological Sciences
K-feldspar	Potassium Feldspa
MH	Silt of High Plasticity, Elastic Silt
ML	Silt
N	North

NW	Northwest
NNE	North- Northeast
NNW	North- Northwest
PPL	Plane Polarized Light
QAP	Quartz, Alkali Feldspar, Plagioclase
RM	Ringgit Malaysia
S	South
SE	Southeast
SSW	South- Southwest
SSE	South- Southeast
TRB	Transportation Research Board
W	West
XPL	Cross Polarized Light

LIST OF SYMBOLS

°	Degree
’	Minute
”	Second
%	Percent
c	Cohesion
$\emptyset$	Angle of friction
τ	Shear strength
E	Interslice shear force
λ	Percentage of the function used
$f(x)$	Function

CHAPTER 1

INTRODUCTION

1.1 General Background

Slope failure also known as mass movement or mass wasting as well as the term landslide. Slope failure is downslope phenomenon of material under influence of gravity in vertical, horizontal or combination of both movement. The slope failure often occurred at the cut-slope on the highway or the residential area. There are numerous factors that caused the occurrence of slope failure such as slope angle, water content of the materials, vegetation, overloading, weathering and climate.

Kelantan is one of the state in Malaysia that located at the north-east coast of Peninsular Malaysia. The north of Kelantan is Thailand, south-east is Terengganu, West is Perak and Pahang is located south to the Kelantan. There are total of ten districts divided in Kelantan. These districts named, Kota Bharu, Pasir Mas, Tumpat, Pasir Puteh, Bachok, Kuala Krai, Machang, Jeli, Gua Musang and Tanah Merah. Generally, Kelantan consists of sedimentary and metasedimentary rocks on the west and east and granites of the Main Range and Boundary Range surround the sedimentary and metasedimentary rocks.

The study area of this research is located at the Jeli district of Kelantan and it covers 25 km^2 and both 5 km for the width of sides. The distance from Universiti Malaysia Kelantan Campus Jeli to the Kuala Balah is around 38 km. This area is a part of Stong Migmatite Complex with granitoids. Stong

Migmatite Complex is divided into three components which are Berangkat Tonalite, Kenerong Leucogranite and Noring Granite by Singh *et al.* (1984). Figure 1.1 referred to granitoid rocks of the Stong Migmatite Complex (Singh *et al*., 1984). The study area of this research is consists two of the components which are Noring Granite and Kenerong Leucogranite. According to the deformation of the rock, the Noring Granite is younger than Kenerong Leucogranite because Noring Granite is undeformed compared to Kenerong Leucogranite. The cutting of foliated Kenerong Leucogranite by Noring Granite as the evidence of the younging order (Singh *et al*., 1984). The largest component of the Stong Migmatite Complex is Noring Granite.

1.2 Problem Statements

Slope failure occur frequently in Malaysia. The number of slope failure in Malaysia is increase every year even though there is no any actual data recorded either slope failure in cut-slope or fill-slope (Jamaluddin, 2006). Since there had an extreme flood occurred in Kelantan in December 2014, the slope stabilization had been affected due to the water content in the soils or rocks. Even some of the areas have no flood occurred, the rainfall also had increased the water content instead caused some slope to failed.

This research is carried out to identify the type and distribution of the lithology of the study area via field studies. The main goal of this research is to carry out the slope stability analysis on selected soil cut-slope within 25 km^2 of the study area. With the analysis, it can help to design slope failure mitigation with the proper way. There are several factors that caused the slope

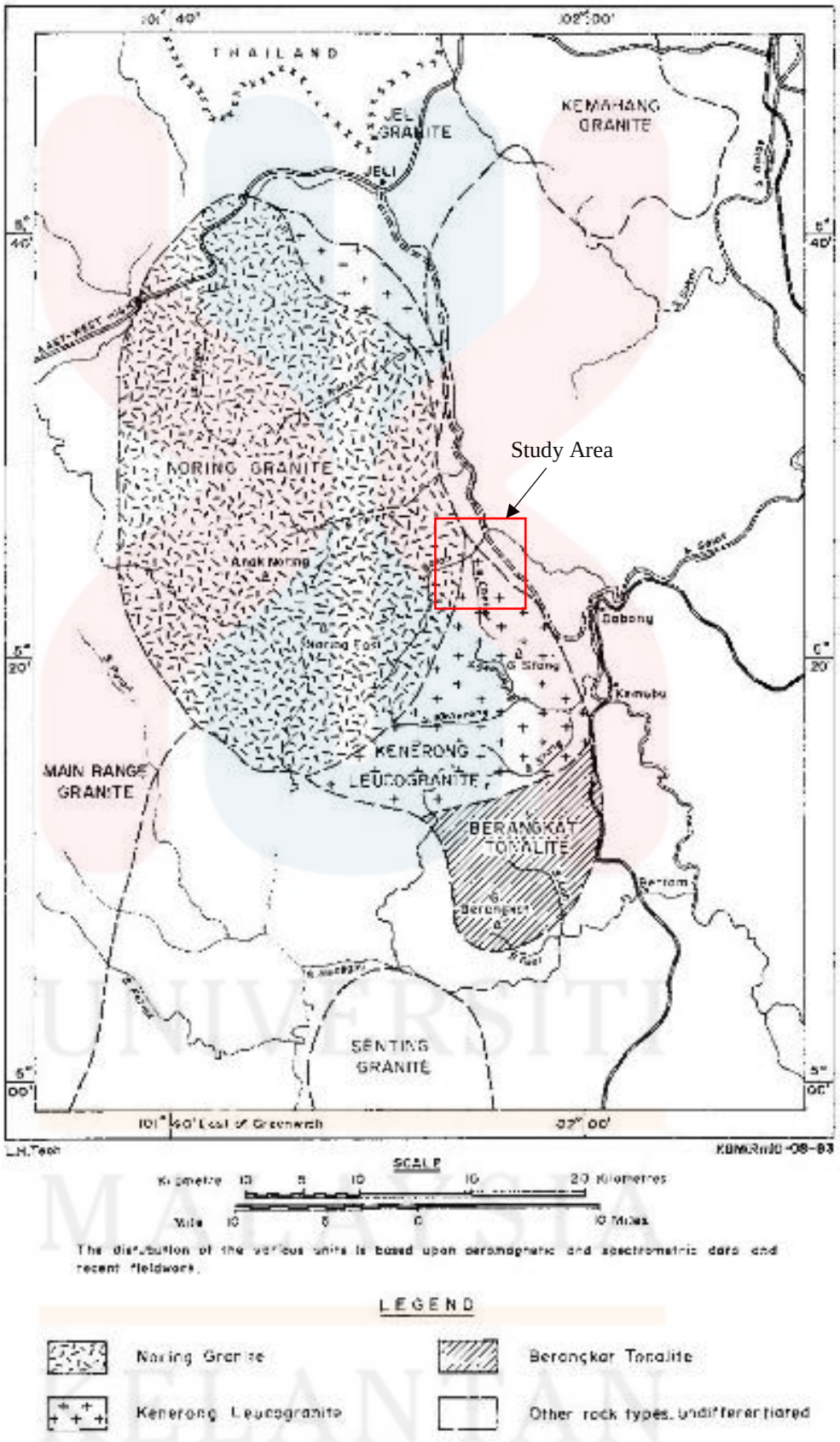

Figure 1.1: Granitoid rocks of the Stong Migmatite Complex (Singh *et al.*, 1984).

failure in Malaysia such as relict structure (Jamaluddin & Deraman, 2000), rainfall (Ng, 2012), and human factors (Jamaluddin, 2006).

With the research on the characteristics of the slope failure and the properties of soil, the factor of safety of the slope of the particular area can be determined based on the properties of soil. This can be as a guideline for the protection process for the further slope failure occur later.

Based on the previous research, the lithology identified are acid intrusive and sedimentary rocks. There is only a few research discussed about the metamorphic rocks of Stong Migmatite Complex. In the past, there was few times of extreme flood occurred. Some of the villages are not existed nowadays. Hence, the updated geological map can provide the latest information about the general geology of study area.

1.3 Research Objectives

The research objectives are as follow:

i. To update the geological map of the Kuala Balah, Jeli, Kelantan with scale of 1:25 000
ii. To produce slope failure inventory of the study area with slope geometry, mode/ type of failure, failure geometry, origin of soil/ rock, cause of failure, type of slope stabilization protection and vegetation cover of failure
iii. To construct slope stability analysis for soil cut-slope at study area using Slope/W software

1.4 Study Area

In this part, it is included details of the location of study area, demography, rainfall distribution, land use, social economic and road connection in the study area.

1.4.1 Location

The selected study area is of Kuala Balah in Jeli District, Kelantan. The location map is shown in Figure 1.2. The main road of this area is known as Malaysia Federal Route 66 connected Jeli- Dabong- Gua Musang. The study area covers 25 km^2 that bounded by coordinate of 5° 26' 10.80" N, 101° 54' 15.00" E and 5° 23' 28.8" N, 101° 56' 56.40" E.

Within this 25 km^2 area, the elevation is range from 40 m to 740 m. The elevation indicates that this area is a mountainous area. There are a few villages and main stream in this area. The villages showed on the map Kampung Kuala Balah, Kampung Kula, and Kampung Batu Lembu. The main stream named Sungai Pergau, Sungai Balah, Sungai Kanuwing and Sungai Chenor. The base map is shown in Figure 1.3.

From the geological map as presented in Figure 1.4, this area consists two main type of lithologies. They are intrusive rock and sedimentary rock. The intrusive rock are represented by Noring Granite and Kenerong Leucogranite which the Kenerong Leucogranite is metamorphosed. The box drawn in Figure 1.4 represented the study area of this research.

Figure 1.2: Location map of study area.

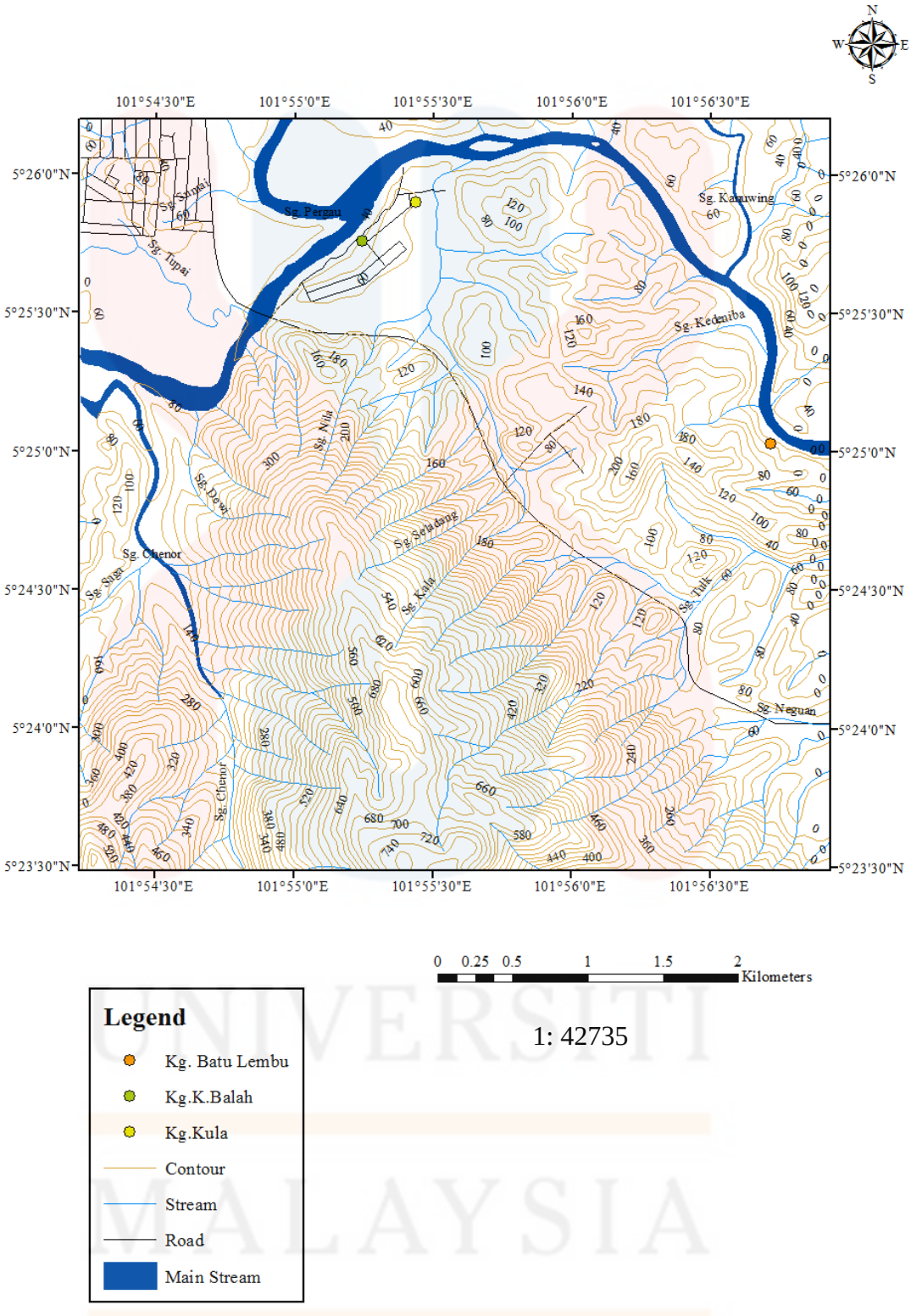

Figure 1.3: Base map of Kuala Balah, Jeli, Kelantan.

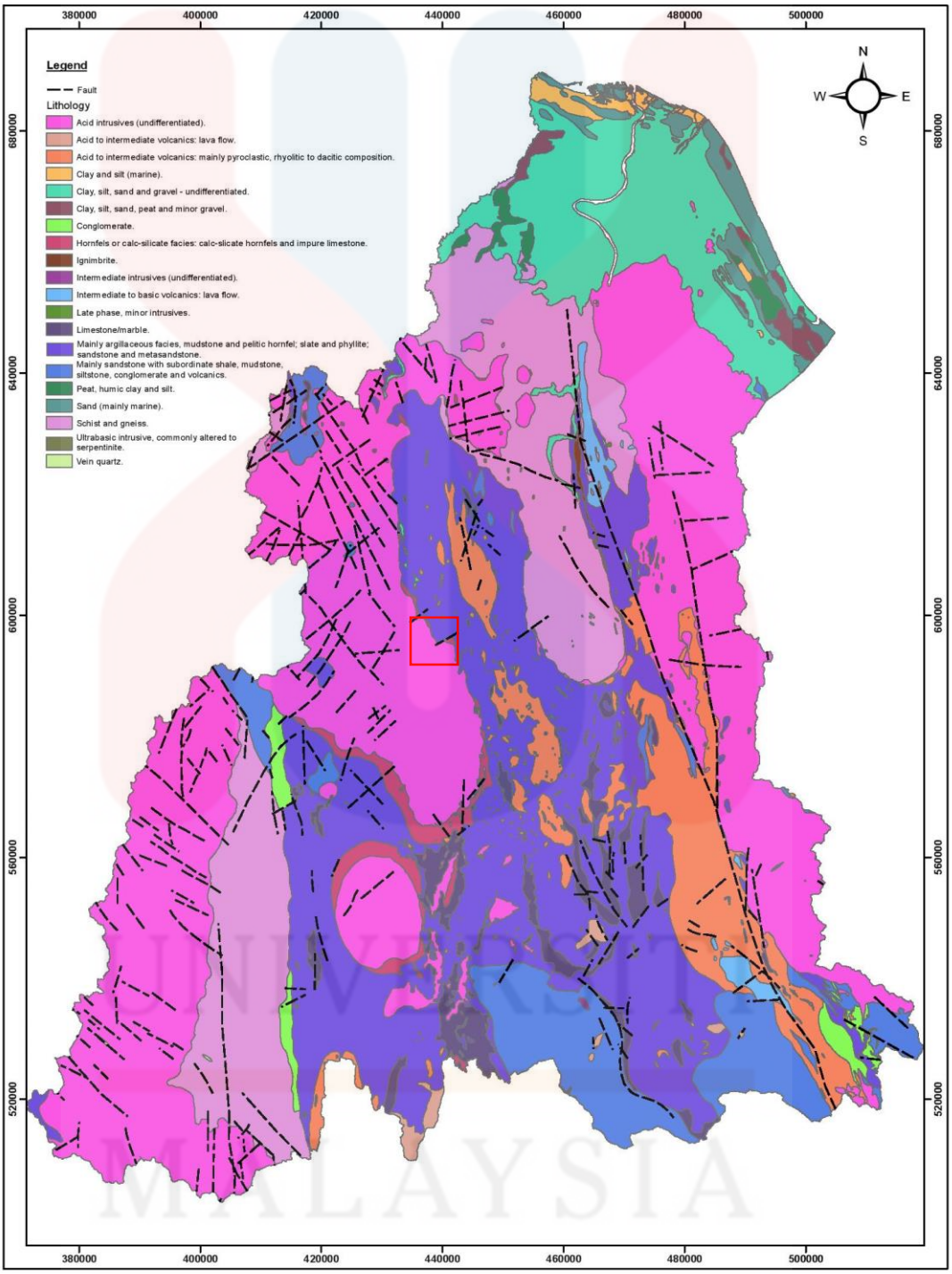

Figure 1.4: Geological map of Kelantan (Source: Department of Minerals and Geoscience Malaysia, 2010).

1.4.2 Demography

The graph of population of Kelantan is showed in Figure 1.5. From the Table 1.1, the population of Kelantan has increased from 1991 to 2010 by 198,542 person. The population for all the districts in Kelantan are increased except Bachok, Machang and Jeli. Bachok and Machang are decreased in people distribution gradually from 1991 to 2010. Jeli district went through raising in population from 1991 to 2000 but declined from 2000 to 2010 by 3,314 person.

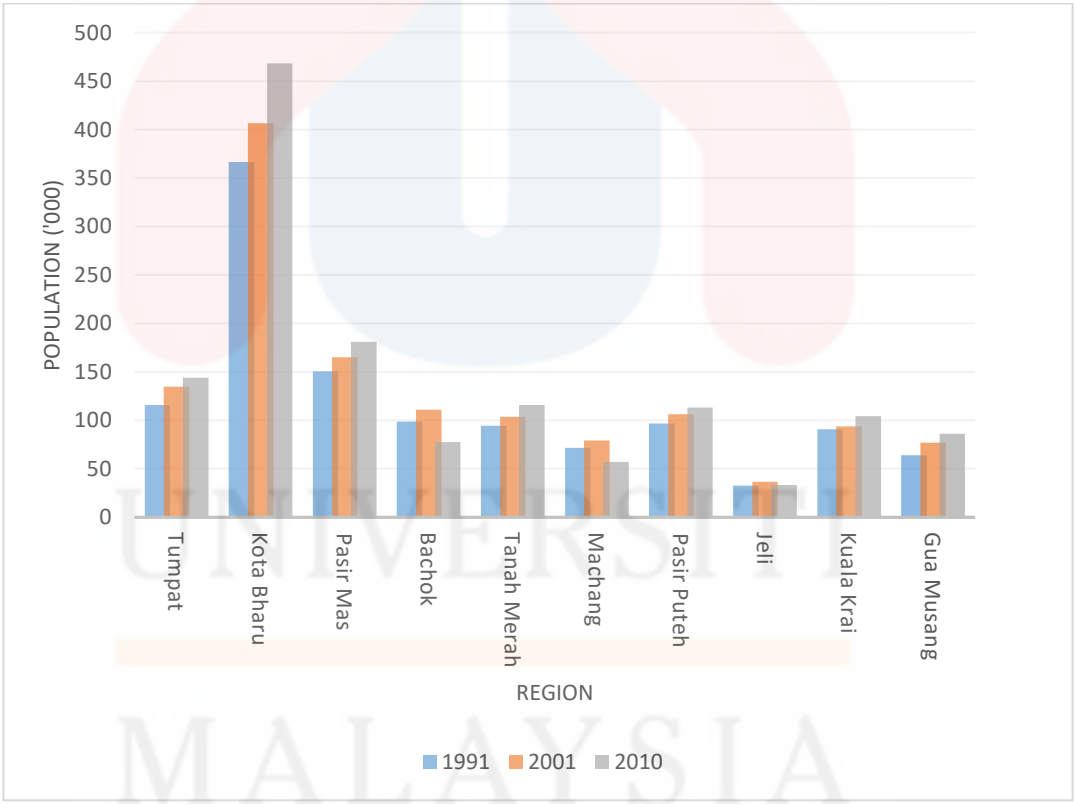

Figure 1.5: Population of Kelantan.

Table 1.1: Population of Kelantan 1991, 2000 and 2010 (Modified from Department of Mineral and Geoscience, 2003 and People Distribution Information, 2013).

Region	District	Population ('000)			Area (Hectare)
		1991	2001	2010	
Northern Kelantan	Tumpat	115.9	134.8	143,793	17,700
	Kota Bharu	366.8	406.7	468,438	39,400
	Pasir Mas	150.4	165.1	180,878	56,900
	Bachok	98.6	111.0	77,447	27,900
	Tanah Merah	94.3	103.5	115,949	88,000
	Machang	71.5	79.0	56,937	52,700
	Pasir Puteh	96.8	106.1	113,191	42,400
Southern Kelantan	Jeli	32.7	36.5	33,186	131,800
	Kuala Krai	90.8	93.6	104,234	227,700
	Gua Musang	63.9	76.7	86,189	817,700
KELANTAN		1,181.70	1,313.00	1,380.242	1,502,200

1.4.3 Rainfall

From the rain distribution provided by Department of Irrigation and Drainage Kelantan, It included rain distribution in 2015 and January to April in 2016. The station number is 5718033 which named Kg. Jeli in Jeli Kelantan Malaysia. It located at the Rergau River and it belongs to Kelantan river basin. In 2015, the minimum rainfall is 0.0 mm while the maximum is 78.8 mm which recorded in December. February 2015 has least rainfall which is only 37.0 mm. The total rainfall distribution of Kampung Jeli station is 2376.4 mm. Since there is only has complete rainfall record for January, February and March for 2016, the minimum rainfall is 0.0 mm while the maximum rainfall is 58.3 mm. March has the least rainfall which is only 10.0 mm for the whole month. February of 2016 recorded the maximum rainfall with 291.5 mm. Figure 1.6 showed rain distribution of Kg. Jeli station Kelantan 2015.

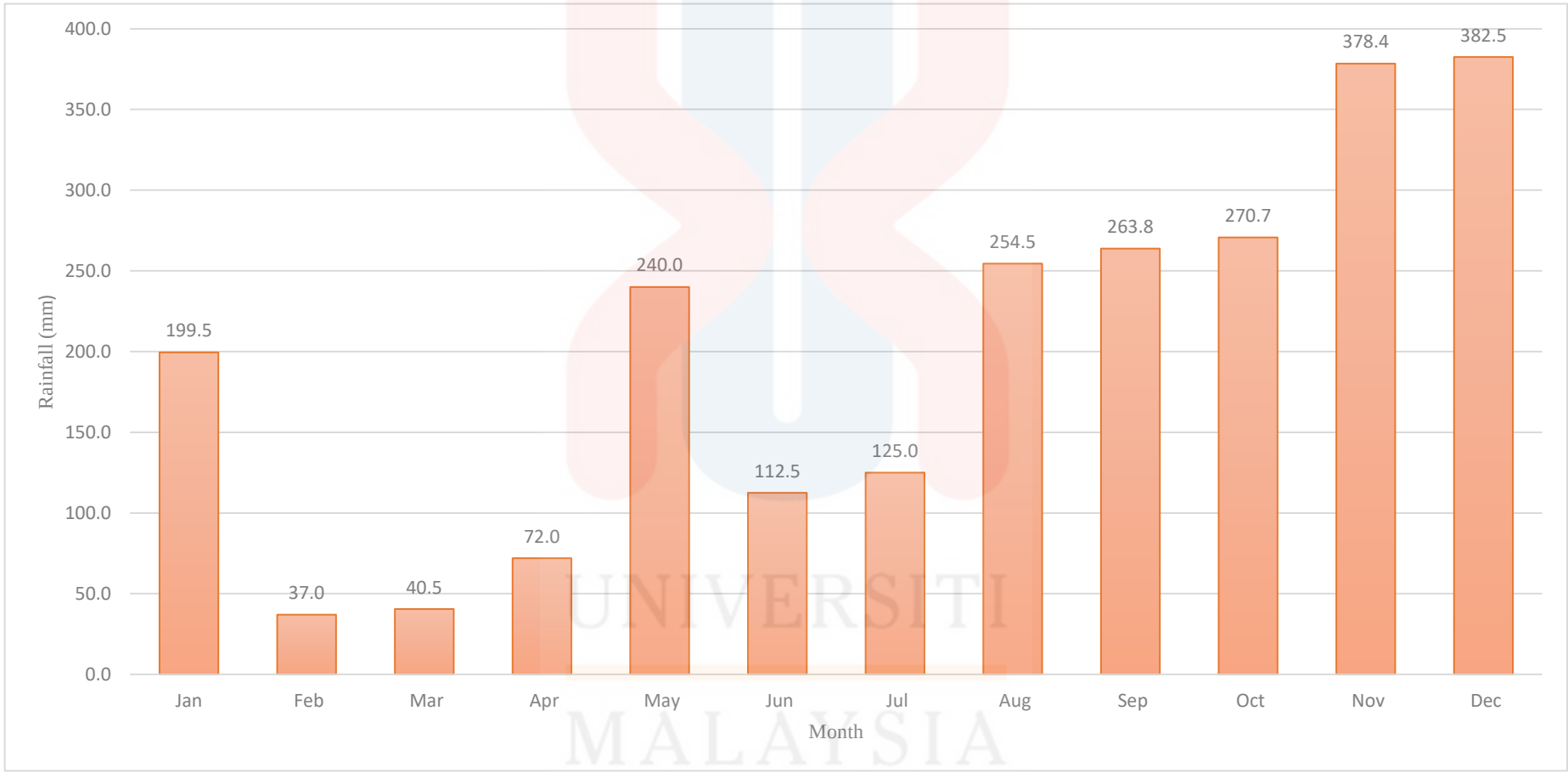

Figure 1.6: Rain distribution of Kampung Jeli station, Kelantan 2015

1.4.4 Land Use

Land use in Kelantan state is dominant by the forest reserve. It covered around 59.5 % in 2001 while forest and water body has covered total of 72.7% of Kelantan total land area in 2002. It followed by agriculture which is 335,600 ha (22.3%) and 380,279.3 ha (25.35%) respectively in 2001 and 2002. The urban area and mining area both cover 0.3% of Kelantan land while the other land use category covers 17.6% in 2001. Hassan (2004) stated that the urban change in the land use category has been changing gradually from the 1970s to 1990s with growth of 7% and after the 1990s there were very slow developments in the area with only 1.4% of growth. Table 1.2 showed the category of land use of Kelantan in 2001 while Table 1.3 showed land use by Kelantan district in the year of 2002.

Within the study area the land use is dominant by forest which covered around 50% of the total land use. It followed by rubber and others. The other categories of land use included river, mines and tailings, municipal and related, mixed plantations, various plants, clearings area, swamp forest ,and idle grass or weeds. In this area, it is only minor land use for municipal purpose while other land is major use for vegetation. The map of land use of Kuala Balah, Jeli, Kelantan is shown in Figure 1.7.

Table 1.2: Category of land use of Kelantan in 2001 (Department of Mineral and Geoscience, 2003).

Category	Area (hectare)	Percentage
Forest Reserve	894,271	59.5 %
Agriculture	335,660	22.3 %
Urban	4,967	0.3 %
Mining	3,737	0.3 %
Others - river, water ways and dam reservoir areas - grazing areas - cleared areas - mangrove areas - secondary jungle	263,565	17.6 %
Total	1,502,200	100 %

Source: Kelantan Socio-Economic Profile 2001, State Economic Planning Unit, Kelantan

Table 1.3: Land use by Kelantan district in the year of 2002 in hectare (Adnan, 2010).

District	Land Use Categories (hectare)				Total Land Area (hectare)
	Built Up	Agriculture	Forest Reserve & Water Body	Others	
Kota Bharu	6,288.4	32,743.4	854.0	54.0	39,939.00
Tumpat	2,630.3	12,869.3	2,065.0	558.0	18,122.6
Pasir Mas	2,546.9	44,626.0	10,206.3	141.4	57,520.6
Machang	861.8	25,472.3	25,525.3	1,096.0	52,955.4
Pasir Puteh	308.1	29,901.7	11,535.8	533.8	42,279.4
Bachok	4,125.0	19,691.4	2,960.6	763.0	27,540.0
Gua Musang	1,506.0	82,921.4	730,663.1	1,261.0	816,351.5
Jeli	661.5	18,500.4	114,097.2	72.6	133,331.7
Kuala Krai	988.3	59,350.6	165,393.1	413.2	266,145.2
Tanah Merah	2,230.0	54,202.8	29,593.2	1,127.0	87,153.0
Total	22,146.3	380,279.3	1,092,893.6	6,020.0	1,502,600.6

Source: Adapted from Technical Report of RSN Kelantan, 2003-2020

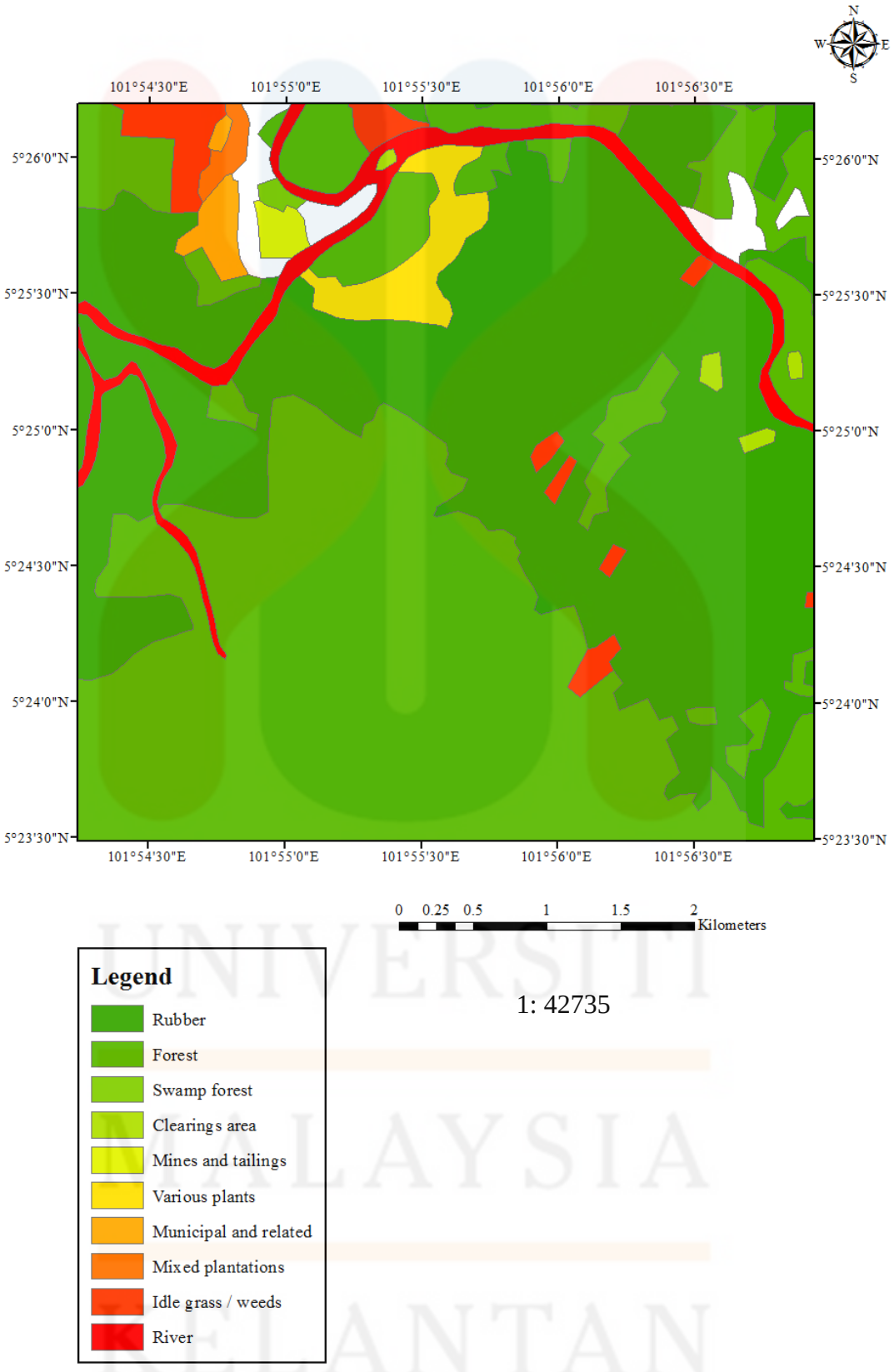

Figure 1.7: Land use of Kuala Balah, Jeli, Kelantan.

1.4.5 Social Economic

The Gross Domestic Product (GDP) per state and GDP per capita for Kelantan is RM 5,404 million and RM 6,720. For the national average, GDP per state is RM 15,457 million and RM 14,100 for GDP per capita. The wholesale and retail trade, hotel and restaurant subsector (29.0 %) and agriculture sector (15.2 %) are the main contributor to the GDP. The agriculture yields are rubber, oil palm, paddy, tobacco, fruits, vegetables, forestry and fishery. The industrial sector produces wood-based, food-based, textile, electrical and non-metallic mineral products. For the period 1991 to 1995, the economy grew at an annual rate of 6.2 % while 3.2 % for 1996 to 2000 due to downturn in the economy in 1997 and 1998 (Department of Minerals and Geoscience Malaysia, 2003). Table 1.4 showed the GDP by economic sectors for 2001.

Table 1.4: GDP by economic sectors for 2001 (Department of Minerals and Geoscience Malaysia, 2003) Source: State Economic Planning Unit, Kelantan

Sector		Share of GDP-2001	
		RM (million)	%
Agriculture		823	15.2
Mining & Quarrying		38	0.7
Industrial (Manufacturing)		495	9.2
Construction		107	2.0
Services	Electricity, Gas & Water	221	4.1
	Transport & Storage	563	10.4
	Wholesale & Retail Trade, Hotel & Restaurant	1569	29.0
	Finance, Insurance & Real Estate	324	6.0
	Government Services	471	8.7
	Other Services	793	14.7
TOTAL		5,404	100.0

1.4.6 Road Connection

The main road within this 25 km^2 is connected Jeli – Dabong – Gua Musang and named as Malaysia Federal Route 66. It is around 7 km in the study area. The other roads in the study area are connected to the villages and part of the Kuala Balah town. Figure 1.8 represented the road connection of Kuala Balah, Jeli, Kelantan.

1.5 Scope of the Study

In this research, it is concerned on the general geology and the slope failure assessment of the study area. In the part of general geology, the type of lithology, structural geology and the geomorphology of the study area is identified. The various maps of the study area is produced according to the analysis such as geological map, map of lineament, drainage pattern, landform classification, contour pattern, resistance pattern, and watershed. The analysis of the structural geology of the study area also will be carry out in this research.

For the part of the slope failure assessment, the characteristics in terms of size, geometry, steepness, mode and types of the slope failure of the soil cut-slope is identified and an inventory of the slope failure is produced based on the characteristics. The factor of safety of slope also determined from the slope stability analysis.

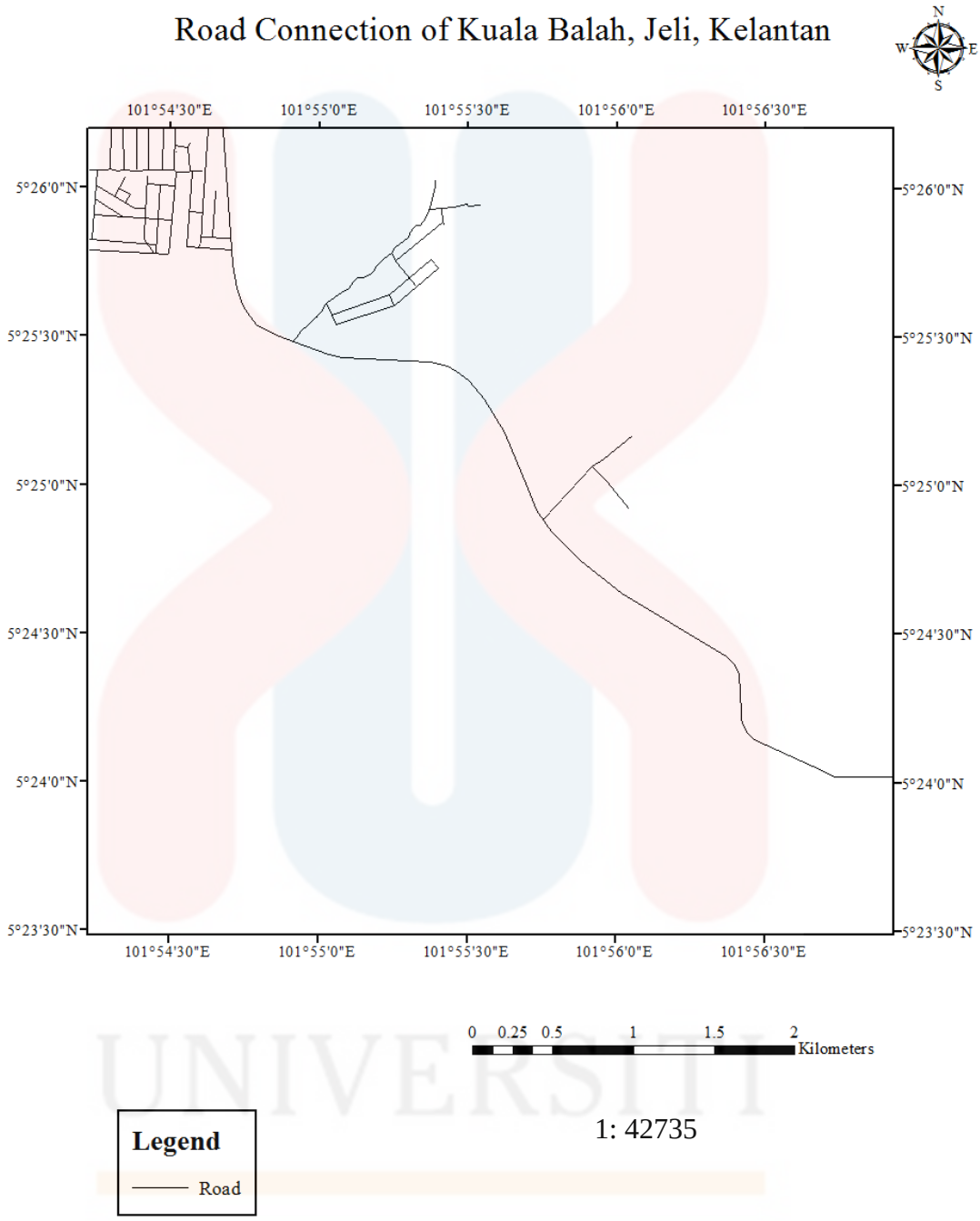

Figure 1.8: Road connection of Kuala Balah, Jeli, Kelantan.

1.6 Research Importance

This research is important due to the previous geological information has not been updated and most of the slope failure occur in highly to completely weathered cut-slope. This indicates that there are high potential for the slope failure to occur because the slope failure likely to occur on the loose and weathered materials. The factor of safety of slope is determined based on the properties of soil by using Morgenstern-Price method.

CHAPTER 2

LITERATURE REVIEW

2.1 Introduction

In this chapter, it is divided into two parts which are geological and engineering geology review. In the geological review, there are several topic included such as regional geology and tectonic setting, historical geology, structural geology, stratigraphy, geomorphology and petrography. All of these geological reviews are related to Peninsular Malaysia as well as Kelantan sate and study area.

The second part is the specification of this research which is engineering analysis of slope. The topics included are terminology of slope failure, slope failure classification, factors and triggering mechanisms of slope failure, weathering grade, slope failure inventory, properties of soil, classification of soil and factor of safety by Morgenstern-Price Method.

2.2 Geological Review

2.2.1 Regional Geology and Tectonic Setting

Hutchison (1977) has proposed that Peninsular Malaysia consist four major tectonic regions: Western Stable Shelf, the Main Range Belt, the Central Graben and the Eastern Belt. The Western Stable Shelf consists the oldest rocks

of Peninsular Malaysia. At Langkawi islands, Perlis and Kedah, the exposed Lower and Upper Palaeozoic miogeoclinal sedimentary formations are slightly folded and un-metamorphosed. Granite is not rich in this tectonic zone. The Main Range Belt is categorized by huge Main Range batholith that forms the mountain range extending from the region of Malacca towards Thailand. The country rocks of the Main Range are predominantly of isoclinally folded phyllitic lower Palaeozoic metasediments including marble, and small amount of strongly folded Upper Palaeozoic formations.

The Central Graben has more strongly folded Permian rocks overlying by gently folded Triassic and Mesozoic sedimentary formations. The dominant rock are pyroclastic rocks while the minor type of rock is granitic rock. The Central Graben separated from Main Range Belt by the Bentong-Raub ophiolite line and from the Eastern Belt by Lebir Fault and its southern extensions. The Eastern Belt consists mainly Permo-Carboniferous sedimentary formations with associated pyroclastic and acid to intermediate composition volcanic rocks. It is characterized by several elongate granitic plutons intruded through slightly deformation (Hutchison, 1977).

According to Hutchison (2009a), Peninsular Malaysia is an integral part of the Eurasian Plate, the south-East Asian part known as Sundaland. Peninsular Malaysia is divided into three major belts known as Western Belt, Central Belt and Eastern Belt. The Western Belt covers Perlis, Kedah, Penang, Langkawi, Selangor, Malacca, half part of Negeri Sembilan and some part of Kelantan and Pahang area. Most area of Kelantan, Pahang and Johor are categorized as Central Belt. Eastern Belt covers the whole Terengganu and some part of Kelantan, Pahang and Johor.

Kelantan is located at the Central Belt or Central Graben from the division. Along a small line through Gunung Benom and Gunung Stong which have granites and gneiss with a variety of uplifted high-grade metamorphic rocks is the exception for the Central Graben that lack of granitic rock (Hutchison, 1977).

2.2.2 Historical Geology

According to Hutchison (2014), the prominent N-S Paleo- Tethys Bentong- Raub suture divides Peninsular Malaysia into a Sibumasu block on the west and an Indochina block on the east, known locally as East Malaya. The Indochina and South China terranes had drifted from Gondwanaland in the Early Devonian and were spared the Upper Palaeozoic glaciation and instead developed equatorial Gigantopteris flora. Sibumasu collided with East Malaya and Indochina in the Late Triassic also known as the Indosinian Orogeny, causing crustal thickening resulting in important tin-bearing S-type granites, characterized by the Main Range of the Peninsula, the 'tin islands' of Indonesia and parts of central Thailand.

The Palaeo- Tethys became narrower as it subducted beneath East Malaya- Indochina giving rise to Permo- Triassic volcanic rocks and I-type granites. Permian andesitic volcanic rocks are abundant on East Malaya but totally absent in Sibumasu. It indicated that the subduction was eastwards beneath East Malaya (Hutchison, 2009b). The timing of rifting and collision of the Sibumasu and Indochina terranes opening and closure of the Palaeo- Tethys Ocean as shown in Figure 2.1.

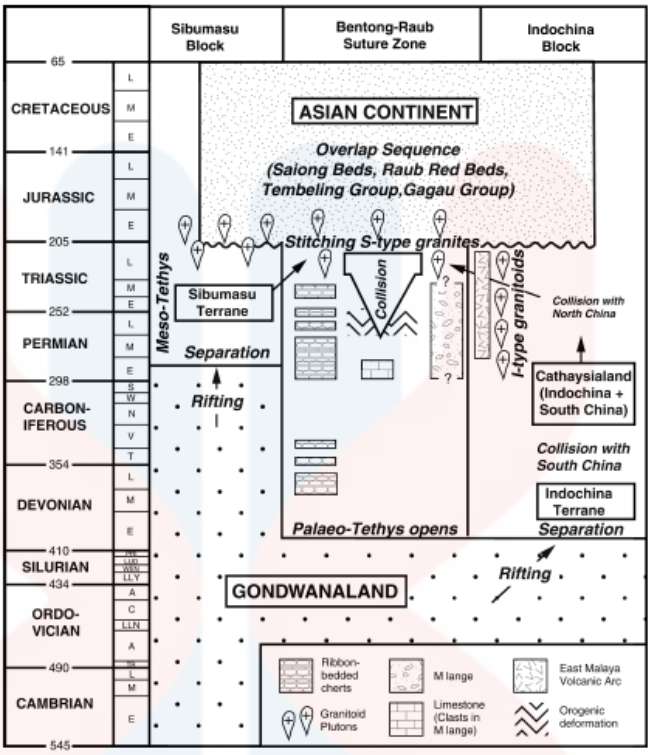

Figure 2.1: The timing of rifting and collision of the Sibumasu and Indochina terranes opening and closure of the Palaeo- Tethys Ocean (Metcalfe, 2000)

2.2.3 Structural Geology

In Peninsular Malaysia, the distribution of the Main Range Granite affected the NNW-SSE general structural trend which later overlaid by N-S, NW-SE, NNE-SSW, and E-W major faults. These major faults are undergone complex repeated movements. The irregularity of the surface topography and the coastlines controlled by these structures associated with bedrock lithologies. The faults identified in Peninsular Malaysia are divided into three such as terrane-bounding faults, terrane-parallel faults and terrane-crossing faults. These faults are distributed around the states in Peninsular Malaysia in different locations (Shuib, 2009a).

Shuib (2009b) stated that Peninsular Malaysia has undergone at least six deformation events between Cambrian to Eocene according to the regional stratigraphy and detailed localised structural analysis, overprinting relationships, structural vergences, tectonic transport directions and stratigraphic relationships. Most of these deformation are related to the major faults of different directions.

Kenerong Leucogranite, one of the component of Stong Migmatite Complex is undergone at least four phases of deformation which produce variety of deformation structures. Foliation and reverse fault are developed during first phase of deformation. Most of the structures are formed during the second and third phase of deformation such as lateral fault, pinch and swell, boundinage, drag folds and small-scale kink folds. Only normal fault is developed for the forth phase of deformation (Ibrahim Abdullah & Jatmika Setiawan, 2003).

2.2.4 Stratigraphy

The stratigraphy of Peninsular Malaysia divided into Palaeozoic stratigraphy, Mesozoic stratigraphy and Cenozoic stratigraphy. In the Western Belt, it consists of the oldest rock of Malaysia which represented by the Upper Cambrian arenaceous Machinchang Formation overlying by the Setul Formation composed dominantly by limestone with detrital bands of the age of Ordovician- Silurian. The Tertiary rocks are represented by small basinal rocks of shale and other clastics with coal beds (Khoo and Tan, 1983).

The Central Belt is mostly underlain by rocks of the Mesozoic and Permian. The oldest rocks at this belt are schists, amphibolites, conglomerates,

other clastics and small bodies of serpentinite associated with the schists. Marine Permian and Triassic rocks cover most of the area at Central Belt. The rocks are shale, mudstone, fine sandstone, limestone and volcanic rocks (Khoo and Tan, 1983). The Gua Musang and Aring Formations represented the Upper Palaeozoic rocks in south Kelantan (Lee, 2009).

For the Eastern Belt, the Palaeozoic sediments of mostly Carboniferous to Permian age are distributed from east Kelantan through Terengganu and east Pahang into east Johor (Lee, 2009). The oldest sediments are represented by clastics, limestone and volcanic rocks. The unconformity between the older Carboniferous and Permian sediments and sediments of Jurassic to Cretaceous age like Gagau Group is formed by the deposition of the continental deposits (Khoo and Tan, 1983). Stratigraphic correlation chart for the Palaeozoic of Peninsular Malaysia and stratigraphic correlation chart for the Permian and Triassic of Peninsular Malaysia are shown in Figure 2.2 and Figure 2.3 respectively.

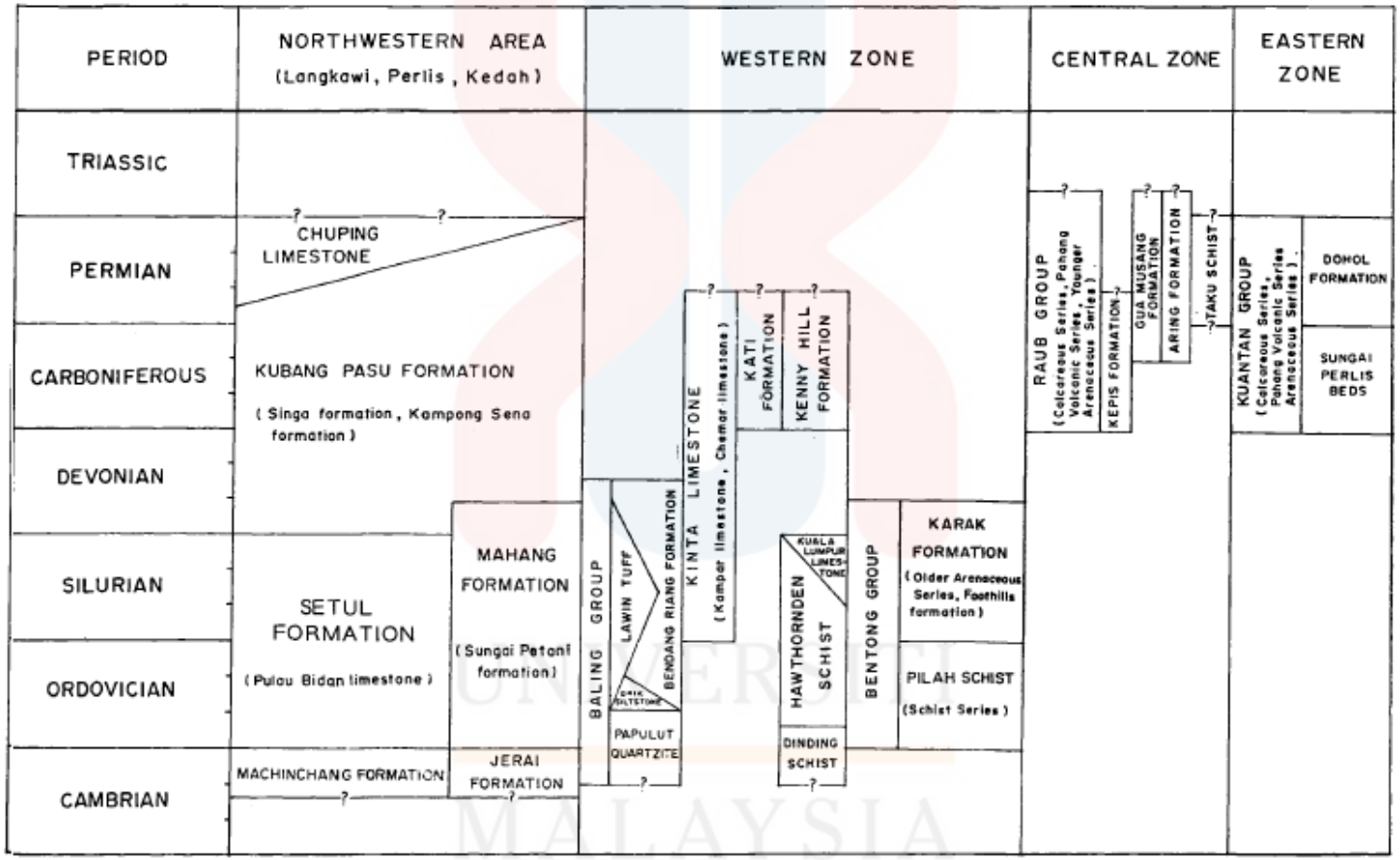

Figure 2.2: Stratigraphic correlation chart for the Palaeozoic of Peninsular Malaysia (Foo, 1983)

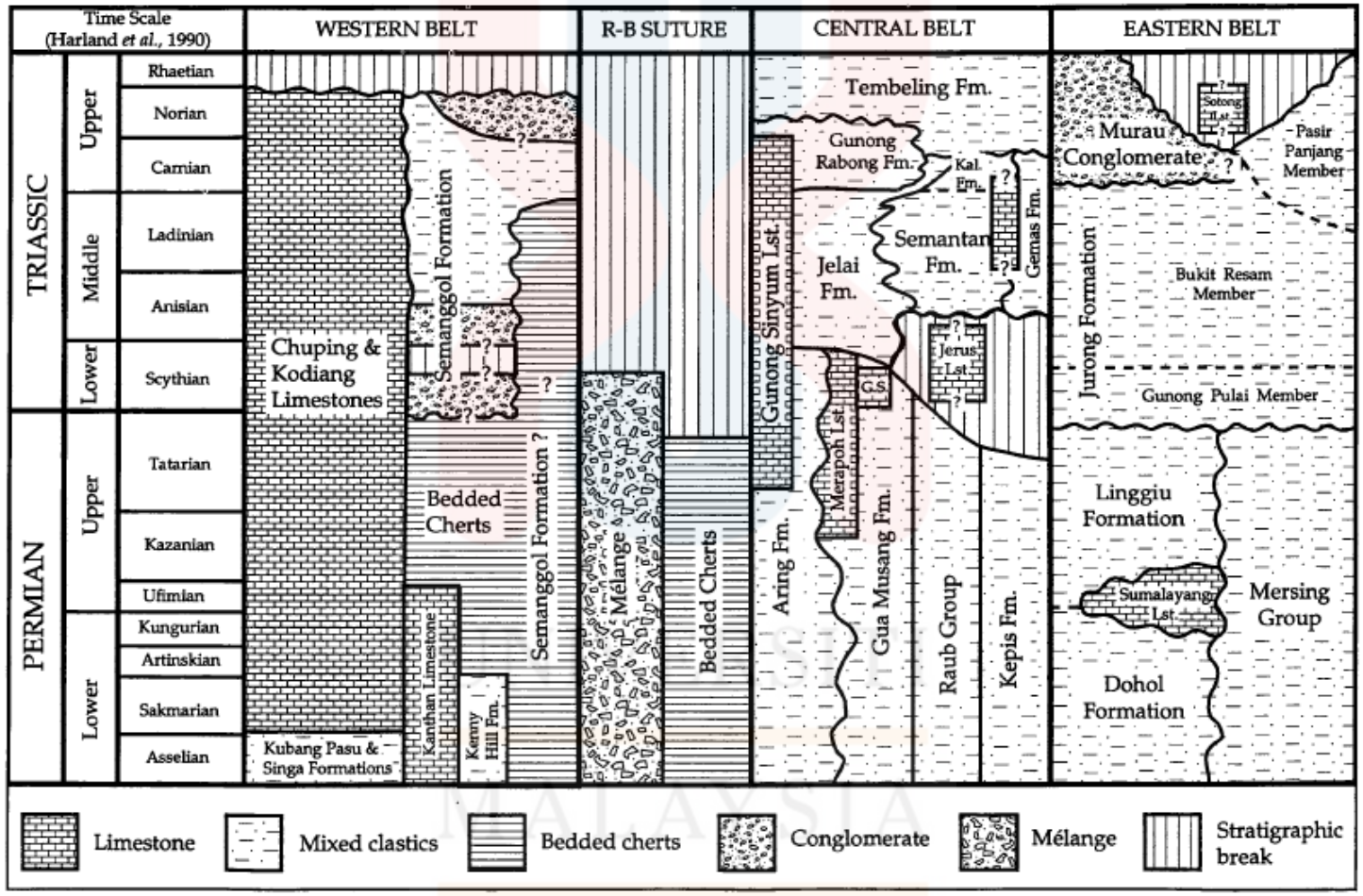

Figure 2.3: Stratigraphic correlation chart for the Permian and Triassic of Peninsular Malaysia (Metcalfe and Azhar, 1994).

2.2.5 Geomorphology

The geomorphology of Kelantan is formed by the combination of seven types of lithology. The major geomorphology in Kelantan are mountainous area, hilly area, plains and coastal plains. Stong Migmatite Complex, Main Range igneous rock and Bentong Schist formed mountainous areas. The hilly areas are Gunung Reng, Gua Musang, Gua Madu, Bukit Panau, Bukit Keterah and etc. The hot spring is one of the features found in plain areas that located between hilly area and coastal plain within the Kelantan state in Gua Musang, Jeli, Machang, and Kota Bahru. The coastal plains in Kelantan have been highly eroded because of the wave actions especially in Pantai Cahaya Bulan where the coastal plains consist of sandbar, lagoon and estuary (Tanot Unjah *et al*., 2001).

2.2.6 Petrography

Kelantan state has the oldest rock with Silurian to Ordovician age. Kelantan has second highest percentage of intrusive rock overall. The study area of this research is one of the place of plutonic intrusion known as Stong Mignatite Complex. Singh *et al.* (1984) stated that the earliest age of the granite in Stong Migmatite Complex is Carboniferous to Triassic while an intrusion and metamorphism of Cretaceous age occurred for at least last part of the Stong Migmatite Complex. Ibrahim Abdullah and Jatmika Setiawan (2003) also stated that the metasedimentary enclaves which are original the country rock of

Kenerong Leucogranite are considered to be Permo-Carboniferous to Early Triassic, probably originated from the Gua Musang Formation.

The three elements of the Stong Migmatite Complex have different minerals content and physical characteristics due to the formation and deformation process. Berangkat Tonalite is grey, rather mafic, in part highly foliated, megacrystic tonalite-granodiorite. Kenerong Leucogranite is highly deformed and highly foliated that made up of sequence veins of leucogranite and biotite granite, pegmatite and aplite while Noring Granite is unfoliated pink megacrystic biotite granite (Singh *et al*., 1984). Azman (2009) stated that the mineralogy of the Berangkat Tonalite is similar to Noring Granite which both contain the main mafic phase of hornblende compared to the Kenerong Leucogranite that only contain biotite.

Noring Granite is coarse grained with average size of mineral between 0.55 mm to 3 cm. Noring Granite made up of plagioclase, pinkish K- feldspar megacryst, quartz, hornblende, biotite, apatite, sphene, allanite, epidote and magnetite. The plagioclase crystals are euhedral to subhedral in shape and 1 mm to 8 mm in size (Azman, 2000).

2.3 Engineering Analysis of Slope

2.3.1 Terminology of Slope Failure

The terms of landslide, mass wasting and mass movement is used to describe slope failure. All these terms are defined as the vertical, horizontal or

combination of two of the downslope movement of materials like rock, soil, clay or combination due to the gravity.

Slope failure is divided into several parts even though there have many types of slope failure that have been classified. Figure 2.4 showed the components of slope failure of slump-earth flow that used the common nomenclature. The definition of the common components of slope failure are enumerated in APPENDIX-A.

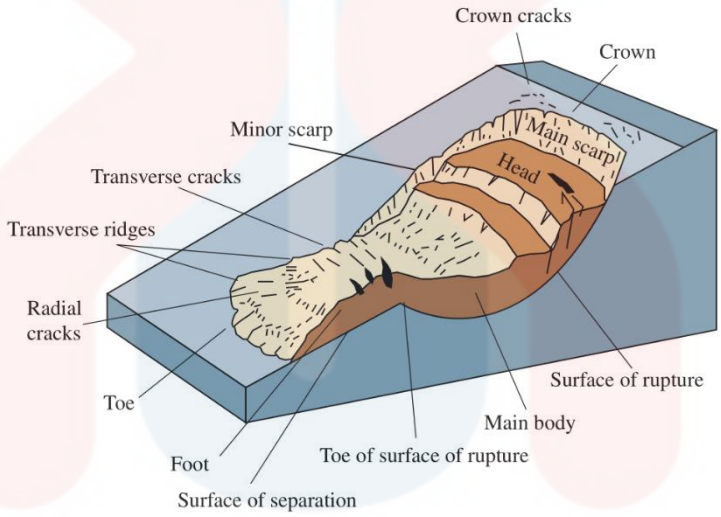

Figure 2.4: Common nomenclature used for labelling the slope failure of slump-earth flow (Highland, 2004)

2.3.2 Slope Failure Classification

The types of slope failure movement include falls, slides, flows, topples, spreads, and complex movements. The classification was produced by United States Geological Society (USGS) according to the types of materials and mode of mass movement. This classification also known as Varne's classification. The classification of several types of slope failure is represented

in Table 2.1. The figure of the types of slope failure showed in APPENDIX-B from Highland, 2004.

Table 2.1: Classification of landslides (Cruden and Varnes, 1996)

<table>
<tr><td colspan="2" rowspan="3">TYPE OF MOVEMENT</td><td colspan="3">TYPE OF MATERIAL</td></tr>
<tr><td rowspan="2">BEDROCK</td><td colspan="2">ENGINEERING SOILS</td></tr>
<tr><td>Predominantly Coarse</td><td>Predominantly fine</td></tr>
<tr><td colspan="2">FALLS</td><td>Rock fall</td><td>Debris fall</td><td>Earth fall</td></tr>
<tr><td colspan="2">TOPPLES</td><td>Rock topple</td><td>Debris topple</td><td>Earth topple</td></tr>
<tr><td rowspan="2">SLIDES</td><td>ROTATIONAL</td><td rowspan="2">Rock slide</td><td rowspan="2">Debris slide</td><td rowspan="2">Earth slide</td></tr>
<tr><td>TRANSLATIONAL</td></tr>
<tr><td colspan="2">LATERAL SPREADS</td><td>Rock spread</td><td>Debris spread</td><td>Earth spread</td></tr>
<tr><td colspan="2" rowspan="2">FLOWS</td><td rowspan="2">Rock flow (deep creep)</td><td>Debris flow</td><td>Earth flow</td></tr>
<tr><td colspan="2">(soil creep)</td></tr>
<tr><td colspan="2">COMPLEX</td><td colspan="3">Combination of two or more principal types of movement</td></tr>
</table>

a. Falls

Falls are sudden movement of geological materials such as rocks, soils and debris that break away from the bedrock in steep slopes and falls freely due to the gravity of Earth. Generally, the failure surface is planar, wedged shaped or vertical (Subinoy, 2013). The rapid mass movement that occur along steep canyons, cliffs and road cuts is categorized as rock fall which are most common type of falls have a wide range of size from small rocks to massive falls.

b. Slides

The slides is defined as the movement of materials along one or more surfaces of failure which include soil, rock or combination of the two. The masses often slide along the geological structures like faults, joints, bedding or foliation planes and shear zones. Slide is divided into two categories, rotational slide and translational slide. The movement of the rotational slide is controlled by the rotation of slide material parallel to the ground slope. The surface of rupture is concave upward and commonly occurs in soil zone. The translational slide moves along a more or less planar surface downward with slightly rotation. The contact planes between hard rock and loose materials, layered rock, or weak plane of rock are the surface of rupture for the translational slide.

c. Flows

The flows are categorized into five common types: rock flow, debris flow, mudflow, earthflow and creep. The flows defined as mass movement of materials that behave like viscous flow and plastic movement. Hungr *et al*. (2001) defined that rock flow as known as rock avalanche with the meaning of movement of massive fragmented rock from a large rock slide or rock fall that flow in extremely rapid speed. According to the description of (Hungr *et al*., 2001) the motion of both debris flow and mudflow are very rapid to extremely rapid but in different materials, such as debris flow contain saturated non plastic debris with plasticity index less than 5 percent while mudflow contain saturated plastic debris with plasticity index more than 5 percent. Earthflow

and creep are both slow motion of flow. The detail landslide flow classification is shown in Table 2.2.

Table 2.2: Landslide flow classification based on the material (Hungr *et al.*, 2001)

Material	Water Content	Special Condition	Velocity	Name
Silt, Sand, Gravel, Debris (talus)	dry, moist or saturated	no excess pore-pressure; limited volume	various	Non-liquefied sand (silt, gravel, debris) flow
Silt, Sand, Debris, Weak rock	saturated at rupture surface content	liquefiable material; constant water	Ex. Rapid	Sand (silt, debris, rock) flow slide
Sensitive Clay	at or above liquid limit	liquefaction *in situ*; constant water content	Ex. Rapid	Clay flow slide
Peat	saturated	excess pore-pressure	Slow to very rapid	Peat flow
Clay or Earth	near plastic limit	slow movements; plug flow (sliding)	< Rapid	Earth flow
Debris	saturated	established channel; increased water content	Ex. Rapid	Debris flow
Mud	at or above liquid limit	fine-grained debris flow	> Very Rapid	Mud flow
Debris	free water present	flood	Ex. Rapid	Debris flood
Debris	partly or fully saturated	no established channel; relatively shallow, sleep source	Ex. Rapid	Debris avalanche
Fragmented Rock	various, mainly dry	intact rock at source; large volume	Ex. Rapid	Rock avalanche

d. Topples

Topples are caused by an overturning motion about a pivot point below the centre of gravity of block and commonly occur on rock blocks (West, 2010). The initial failure surface can be either single or multiple.

e. Spreads

Spreads also known as lateral spreads is defined as the mass movement occurs in flat or less steep areas of saturated soil that contain loose sediments that fail by liquefaction (Subinoy, 2013).

f. Complex

The complex movement is the combination of two or more types of failures. TRB classification has stated six specific combinations included rock fall- debris fall, slump and topple, rock slide- rock fall, cambering spreading and bending overflow, slump- earthflow, and mudslide.

2.3.3 Factors and Triggering Mechanisms of Slope Failure

The factors that caused the slope failure is categorized into three parts: geological causes, morphological causes and human causes. There are five geological causes included weak or sensitive materials, weathered materials,

sheared, jointed, or fissured materials, discontinuity, and permeability and stiffness of materials. Morphological causes are tectonic or volcanic uplift, glacial rebound, erosion, deposition loading slope, vegetation removal, thawing, and weathering. Excavation and loading of slope, deforestation, irrigation, mining, and water leakage are the example of human causes (Highland, 2004). Jamaluddin (2006) also stated that the slope failures caused by human factors in form of negligence, incompetence, lack of and poor maintenance system, ignorance of geological inputs, unethical practice, and various negative attitudes of human self.

Monroe *et al*. (2006) stated that the causes of mass wasting due to five major factors. These factors are slope angle, weathering and climate, water content, vegetation and overloading. The greater the gradient of the slope, the higher the probability for the slope failure to occur. The steepness of slope often affected by the excavations for either road cuts or hillside building and undercutting of stream. Weathering process increase the possibility of slope failure by decrease the shear strength of the materials especially for the high grade weathering zone. The water content of the rocks or soils increase will decrease the slope stability. The cohesion between the grains loss due to the reduction of friction of grains. The function of vegetation is to decrease the water saturation of the material by water absorption. The root of vegetation also play a role to stabilize the slope by holding the soil to bedrock and compact the soil's particles close to each other. Overloading is one of the human causes that caused by dumping, filling or piling up of materials which decrease their shear strength by raise the water pressure within the materials.

Discontinuities is defined as any break or fracture within a rock mass which cause the tensile strength across the fracture planes to be approach zero or be lower than that of rock material. Joints, faults, fissures, fault zones, bedding planes, cleavage and foliation are the example of discontinuities (Aziman & Husaini, 2001). Discontinuities categorized into two major types of modes of origin, those that occur in sets, for example bedding planes, joints, cleavage, foliations and those that are unique, for example individual joints or faults (Dearman, 1991). According to Jamaluddin and Deraman (2000), the soil overhangs can fail in form of earth falls, earth topples, earth slumps, planar slides, wedge or complex failures depending on the presence and orientation of the relict discontinuities. The common discontinuities related to slope stability are joint, fault, shear zone, bedding surfaces and foliation.

The triggering mechanisms often refer to the natural causes. The example for the triggering mechanisms are earthquake's vibrations, excessive water content from heavy rainfall, volcanic eruptions, explosions and loud claps of thunder (Monroe *et al*., 2006). Ng (2012), Raj (2000) and Chow & Mohamad (2003) stated that rainfall is the main factor that caused the slope failure in Malaysia. Figure 2.5 showed the distribution of landslide triggering factors based on selective Malaysia case history. Prolonged rainfall during the months of October and November also one of the factor that cause the landslides occurred in Hulu Kelang, Selangor Malaysia (Low *et al*, 2012).

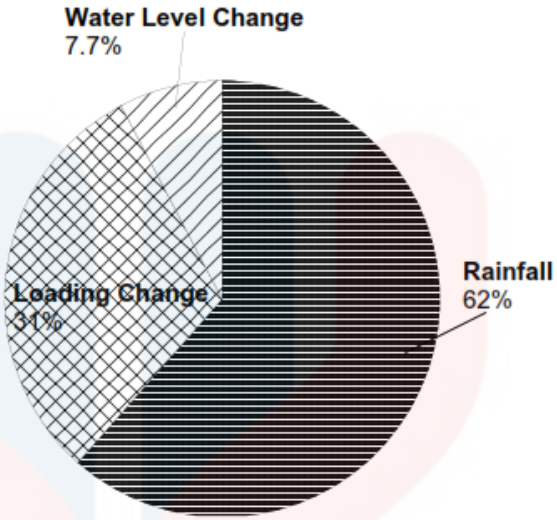

Figure 2.5: Distribution of landslide triggering factors based on selective Malaysia case history (Ng, 2012)

2.3.4 Weathering Grade

Weathering grade is the classification based on the degree of chemical, biological or physical weathering in a given rock type. It is widely used in modern rock mass classification. The weathering grade is divided into six ranging from fresh rock to residual soil (Robert and Jerome, 1988). Table 2.3 showed the classification of weathering grades.

Table 2.3: Classification of weathering grade (Robert and Jerome, 1988)

Term	Description	Grade
Fresh	No visible sign of rock material weathering.	IA
Faintly weathered	Discoloration on major discontinuity surfaces.	IB
Slightly weathered	Discoloration indicates weathering of rock material and discontinuity surfaces. All the rock material may be discoloured by weathering and may be somewhat weaker than in its fresh condition	II
Moderately weathered	Less than half of the rock material is decomposed and/ or disintegrated to a soil. Fresh or discoloured rock is present either as a continuous framework or as core stones.	III
Highly weathered	More than half of the rock material is decomposed and/ or disintegrated to a soil. Fresh or discoloured rock is present either as a continuous framework or as core stones.	IV
Completely weathered	All rock material is decomposed and/ or disintegrated to soil. The original mass structure is still largely intact.	V
Residual soil	All rock material is converted to soil. The mass structure and material fabric are destroyed. There is a large change in volume, but the soil has not been significantly transported.	VI

2.3.5 Slope Failure Inventory

Slope failure inventory is a table that recorded the characteristics of slope failure investigated with several parameters. Hussin *et al.* (2015) stated that the parameters recorded for each slope failure are discontinuity, lithological type, size of slope failure, weathering grade, seepage and the factors that cause the slope failure as well as geometry of slope failure and type of stabilization and slope protection used on the slope. Based on the classification by Tajul Anuar Jamaluddin (1990) in Table 2.4, the scale of slope failure can be determined.

Table 2.4: Classification of slope failure size (Jamaluddin, 1990)

Scale of slope failure	Volume of failure (m^3)
Small	< 100
Medium	100 – 1000
Large	1000 – 5000
Very large	> 5000

Tajul Anuar Jamaluddin and Muhammad Fauzi Deraman (2000) constructed the slope failure inventory according to several parameters which are slope geometry, mode or type of failure, failure geometry, dominant structures, weathering grade and slope protection.

2.3.6 Properties of Soil

The properties of soil is important in the classification of soil which included moisture content, liquid and plastic limits, particle size distribution and soil strength. These properties can be measure via laboratory test and in-situ test. Moisture content is the water content in the soil which can be removed by the drying process in the laboratory. The equation for the moisture content as below:

$$w = \frac{W_w}{W_s}\, x\, 100\% \qquad (2.1)$$

which

w = moisture content,

W_w = weight of water, and

W_s = weight of solid (soil).

The liquid limit and plastic limit are part of the Atterberg limits which use to measure the water content in the fine-grained soil. Liquid limit is the limit that the soil change from plastic behaviour to liquid behaviour which measure by the water content in the soil when the change of state. The plastic limit is the determined by water content in the soil when the soil is change from solid behaviour to plastic behaviour and can be rolling into a thread. Plasticity index is the difference between liquid limit and plastic limit. Figure 2.6 represented the plasticity chart of plasticity chart against liquid limit. The plasticity limit is calculated by:

$$\text{Plasticity Index} = \text{Liquid Limit} - \text{Plastic Limit} \qquad (2.2)$$

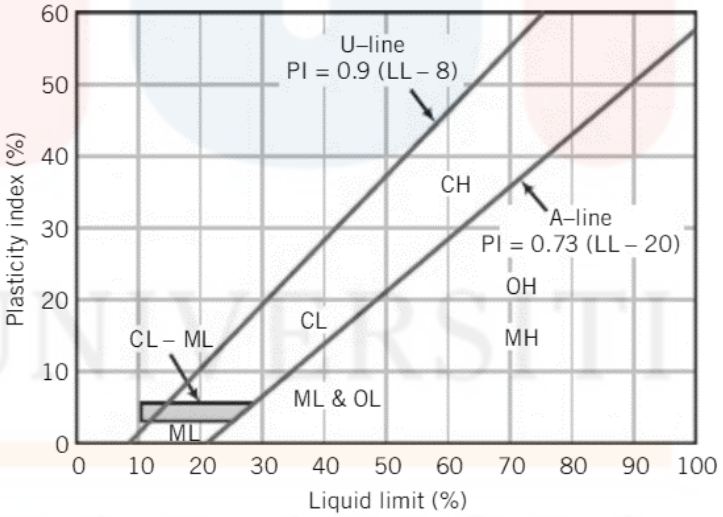

Figure 2.6: Plasticity chart (Budhu, 2007)

According to Head *et al.* (1980), particle size distribution analysis referred to the proportions by weight of the various size of particles present in the soil quantitatively. Soil is divided into six categories based on the size of

particles. The particle which 200mm and more in size is boulders, 60mm to 200mm is cobbles, gravel is range from 2mm to 60mm, sand size is 0.006mm to 2mm, silt is 0.002 to 0.006mm in size and the clay is 0.002mm and less in size. Table 2.5 showed the classification of particle size. It is important for the soil classification.

Table 2.5: Classification of particle size (Head *et al*., 1980)

Particle Size (mm)		Designation	
>200			
	200	BOULDERS	
60		COBBLES	
	20	Coarse	GRAVEL
		Medium	
	6	Fine	
2			
	0.6	Coarse	SAND
		Medium	
	0.2	Fine	
0.06			
	0.02	Coarse	SILT
		Medium	
	0.006	Fine	
0.002 and less			CLAY

Budhu (2007) stated that shear strength of soil is defined as the maximum internal resistance to apply the shearing forces. For cemented soils, they possess shear strength even the normal effective stress is zero while for unsaturated soils, when the pore water pressure is negative, the effective stress increases. The in-situ tests for shear strength of soil are vane shear test (VST), standard penetration test (SPT), cone penetrometer test (CPT) and Mackintosh probe test.

Vane shear test also can be carry out in laboratory. Based on ASTM (2000), the undrained shear strength for soil from laboratory test is calculated by following equation:

$$\tau = \frac{T}{K} \quad (2.3)$$

where

τ = undrained shear strength (Pa),

T = torque (Nm), and

K = vane blade constant (m^3).

$$K = \frac{\pi D^2 H}{2\times 10^6}\left[1 + \frac{D}{3H}\right] \quad (2.4)$$

where

D = diameter of vane (mm), and

H = height of vane (mm).

2.3.7 Classification of Soil

According to Unified Soil Classification System by ASTM (2006), the soils are classified into coarse-grained and fine-grained. It is based on the percentage of soil which can pass No.200 (75μm) sieve. It also depend on the plasticity index for the fine-grained soil. The flow chart for classifying coarse-grained and fine-grained soil are attached in APPENDIX-C.

2.3.8 Factor of Safety by Morgenstern- Price Method

Duncan (1996) stated that the factor of safety is the ratio of the shear strength to the shear stress required for equilibrium of the slope.

$$F = \frac{\text{shear strength}}{\text{shear stress required for equilibrium}} \quad (2.5)$$

$$F = \frac{c + \sigma \tan \emptyset}{\tau_{eq}} \quad (2.6)$$

which

F = factor of safety,

c = cohesion intercept on Mohr-Coulomb strength diagram,

$\emptyset$ = angle of internal friction of soil,

σ = normal stress on slip surface, and

τ_{eq} = shear stress required for equilibrium.

Factor of safety of a slope is based on various factors such as geological conditions, density, types and density of existing and anti-participated structures, reliability of soil parameters, groundwater and environmental conditions. The typical value of factor of safety is 1.15 to 1.50 for all the conditions (Budhu, 2007).

Morgenstern – Price method is based on formulations of limit equilibrium. Based on the Stability Modeling with SLOPE/W (2012), Morgenstern and Price (1965) had been suggested the equation for the interslice shear forces in the GLE formulation:

$$X = E\ \lambda\ f(x) \qquad (2.7)$$

where

X = interslice shear force,

E = interslice normal force,

λ = percentage of the function used (in decimal form), and

$f\ (x)$ = function.

In the SLOPE/W software, the interslice functions available are constant, half-sine, clipped-sine, trapezoidal and data-point specified. The advantages of Morgenstern – Price method are deliberates shear and normal interslice forces, satisfies moment and force equilibrium, and allows for diversity of user-selected interslice force function.

CHAPTER 3

MATERIALS AND METHODOLOGIES

3.1 Introduction

The methods used to carry out the study are included preliminary study, field mapping or studies, laboratory investigation, data analysis and interpretation, and report writing. After the preliminary research is done, the writing of literature review is carry out as well as site selection. During the field mapping or studies, there are two things need to be done which are geological mapping and engineering geological mapping. The GIS study also carry out to determine the geomorphology of the study area such as drainage pattern and topography as well as lineament.

During the geological mapping, the rock sample is taken from the selected study area for the making of thin section. The thin section is used for the petrography analysis and interpretation by using the polarizing microscope. The structure such as joint, fracture, fault, folding and bedding is measured by taking strike and dip for structural analysis. The data collected in the engineering mapping are used to carry out slope failure inventory and soil cut-slope stability assessment. Soil sampling is done during engineering mapping for the laboratory test of soil's properties. The final step in the methodology is report writing. The flow chart of this research is shown in Figure 3.1.

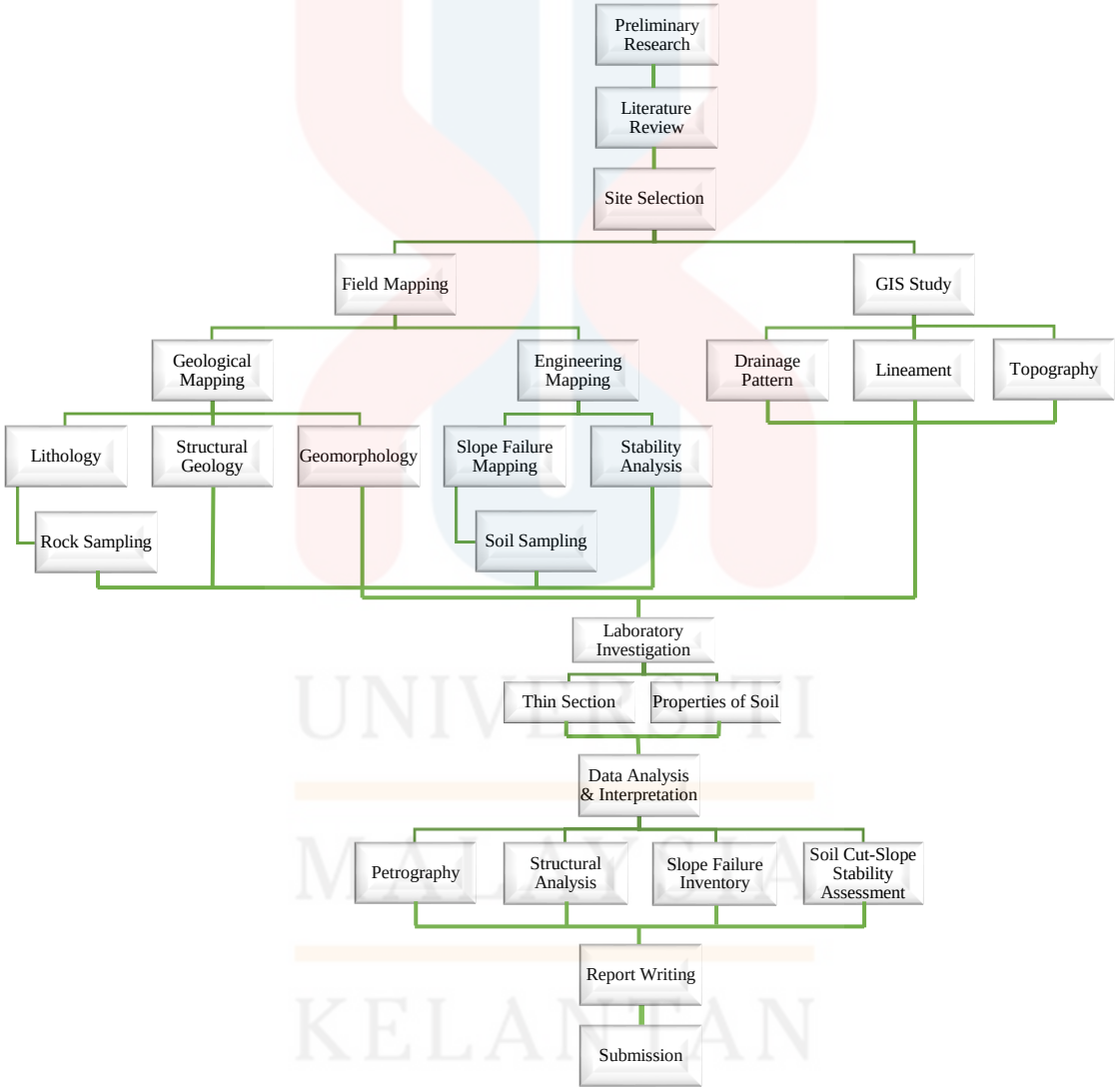

Figure 3.1: Methodology flow chart of overall research

3.2 Preliminary Researches

The preliminary researches are the desk study before doing the research regarding to the finalized topic. In this stage, it included the study of the selected study area, preparing the base map of the study area for the mapping purpose and planning the process to carry out the research. The sources for preliminary researches are information from Department of Mineral and Geoscience Malaysia, journals, articles, proceeding papers, bulletin, books and from internet.

From the numerous of the journals, articles, e-bulletin as well as e-book can be obtained. The published thesis also can downloaded via internet. All the information related to the selected topic are taken as the references. Moreover, the geological features of the study area can be found in these sources. It acts as a preliminary information before the site visit.

Other than that, a base map is generated by using ArcGIS 10 software with the data from Department of Surveying and Mapping (DSSM). In the base map, it included contour, town, river, main river and street. The values and names of these features are labelled for the use during the mapping.

3.3 Materials

3.3.1 Global Position System Equipment (Garmin 62s)

GPS showed in Figure 3.2 is a navigation system based on the satellite consists of the satellites in space, monitoring stations on earth and GPS receivers. The functions of GPS equipment are used in positioned one's position, recording traverse track, operated the interval of traverse track recording, measuring elevation, and storing the sampling location.

Figure 3.2: Global position system (GPS) equipment

3.3.2 Compass

The common compass used are Suunto compass and Brunton compass. The compass is use to get the directional degree measurements (azimuth) based on the Earth's magnetic field, measure strike and dip value of the exposed outcrop, and used in following traverse line in order to go to the pointed point as it can be set to the planned direction. Picture of compasses showed in Figure 3.3.

(a) (b)

Figure 3.3: Brunton compass (a); Suunto compass (b)

3.3.3 Measuring Tape

Measuring tape is used to measures the actual size of the lithology and structures as well as taking the measurement of the bed thickness and the grain size. It also used to measure the geometry of slope and the geometry of the slope failure.

3.3.4 Geological Hammer

There are two type of geological hammer, pointed-tip rock hammer and chisel-tip rock hammer. Pointed-tip rock hammer has a long pick-like end that usually used for the harder rock such as igneous rock and metamorphic rock. The long pick-like end useful in inserted into the cracks for levering out loose rock and digging through a thin soil cover. The chisel-tip rock hammer has a chisel-shaped blade that commonly used for sedimentary rock and sediments. The chisel end is useful for splitting the layers of sedimentary rocks, trimming rocks and digging soils and sediments. These two types of geological hammer are both important in rock sampling in the field and presented in Figure 3.4.

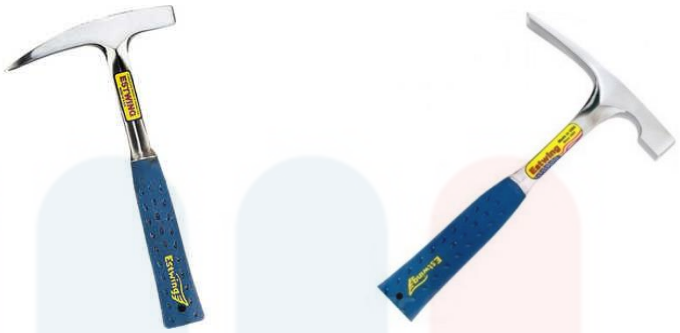

(a) (b)

Figure 3.4: Pointed-tip rock hammer (a); chisel-tip rock hammer (b)

3.3.5 Hand Lens

The hand lens is used to make the initial analysis of the rock samples in the field based on the rock types, colour, mineral compositions, textures and structure properties such as folding, foliation, intrusions or layering that cannot seen by naked eyes before the detail analysis and observation carry out in the laboratory.

3.3.6 Polarizing Microscope

The polarizing microscope commonly used for the study of rocks and minerals in the field of geology and petrography. For the observation of the rocks or minerals, a thin section of the particular sample has to be done. This microscope has three objectives with different magnification which are 4x, 10x and 40x. The analyser enables to show the thin section either in PPL or XPL. PPL is the polarisation state of the light source with lower polariser while XPL

is the polarization state of the microscope when lower and upper polarisers are inserted. Polarizing microscope is illustrated in Figure 3.5.

Figure 3.5: Polarizing microscope

3.3.7 Casagrande Apparatus

Casagrande apparatus is commonly used for liquid limit analysis. It made up of a smooth brass bowl, a carriage with cam mechanism, drop counter and a base with setting gauge. It required particle size of clay (425 micron) or smaller. It correlated the water content of the soil and the number of blows. Figure 3.6 showed the Casagrande apparatus.

Figure 3.6: Casagrande apparatus

3.3.8 Laboratory Vane Shear Strength Equipment

Laboratory vane shear strength equipment used for the undrained shear strength determination of fine-grained soil. This equipment consists four stainless steel that fixed at right angle and attached to high tensile steel rod. The laboratory vane shear strength equipment is showed in Figure 3.7.

Figure 3.7: Laboratory vane shear strength equipment.

3.3.9 GeoRose Software

GeoRose software is used to plot the structural geology rose diagram by entering the strike, dip and dip direction of structure such as joint, fault, fold, lineament and bedding. The rose diagram can be in full circle or semi-circle. The diagram can export the plot as PNG, PDF, PS and SVG formats.

3.3.10 Stereonet Software

The Stereonet Software by Richard W. Allmendinger Company used to create the stereonet diagram with the details of plane, line, line on plane, arc and small circle. There are several calculations can be done by using this

software such as poles, angle between lines or planes, apparent dips, planes from poles, two planes calculations and axial plane finder.

3.3.11 Slope/W Software

Slope/W software is one of the software by GEO-SLOPE for slope stability analysis. It can analyses simple and comples problems with different slip surfaces, geometry, material strength, pore-water pressure, reinforcement and structural components. Factor of safety can be determined by using several methods such as Ordinary, Bishop's simplified, Janbu's simplified, Spencer, Morgenstern-Price, Lowe-Karafiath and Sarma methods.

3.3.12 Topographical Map

The topographical map act as reference during the field mapping. It also important for marking the geological information on the exact location. The scale for the topographical map is 1:25 000.

3.3.13 Sample Bags

The common sample bag used is the transparent plastic bag with a resealable zip lock. It is uses to store the rock or soil sample from field. The label tag that consists information like coordinate, sample number, date and time is necessary for each sample on the sample bags.

3.3.14 Digital Camera

The digital camera or the camera on the smart phone use to record the picture of the outcrop as well as act as back up memory except the information recorded in the field notebook.

3.3.15 Field Notebook

The field notebook is important for recording all the information obtained during the field work. It must be suitable in size and easy for writing as well as sketching. All the observations must written down in the way of orderly and readable to prevent the lost and lack of information during the analysis and interpretation processes.

3.3.16 Stationery

The stationery include pencil, pen, eraser, ruler and all the necessary stationary that need for recording information and observations in the field as well as in the laboratory investigation.

3.4 Field Mapping

3.4.1 Geological Mapping

Geological mapping included the identification of all the geological aspects like lithology, structural geology and geomorphology of the selected area to produce a detailed geological report and geological map. From the observations of the lithology, the type of rocks can be determined due to their colour, texture, structures, and the mineral composition. The structural geology can be analysed by the availability of the structures within the selected area. The details of the structure such as type and strike and dip value are important and must be recorded for the interpretation of structural geology of that area. The geomorphology of an area can be identified by the observation during the geological mapping.

3.4.2 Engineering Geological Mapping

In the engineering mapping, it is concerned on the part of slope failure. The locations of the slope failure are determined and the information of the slope failures are recorded based on the parameters. The parameters are slope geometry, mode/ type of failure, failure geometry, lithology, weathering grade, causes of failure, and type of slope stabilization and protection. All of the information based on these parameters have to take as accurate as possible to avoid the error in the analysis and interpretation process of slope stability. Soil sampling is also done to carry out the laboratory test of soil's properties for the

slope stability analysis. The soil samples are took from four selected slopes and from both stable and fail slopes. Each sample is took around five kilograms from the laboratory test.

3.5 Laboratory Investigation

3.5.1 Thin Section

Thin section is slides of typically 26mm x 46mm with 0.03mm thick slice of rock attached to a glass slide epoxy. The procedure to thin section making is preparing the sample, cutting, grinding, polishing, slide mounting, final cutting, trimming, final polish and covering. The steps of producing thin section are enumerated in APPENDIX-D.

3.5.2 GIS Analysis

GIS analysis is interpretation of the selected study area by using ArcGIS software. With the software, all the features in the area are showed clearly in help to determine the geomorphology of the area. The geomorphology such as drainage pattern and topography are determined via GIS analysis and structural geology such as lineament also determined.

3.5.3 Properties of Soil

The laboratory test of properties of soil included moisture content test, liquid and plastic limits test, particle size distribution and soil strength. All of these properties of soil is determined for the slope stability assessment. The laboratory tests included moisture content, liquid and plastic limit and particle size distribution are carry out based on the Manual of Soil Laboratory Testing (1980).

3.6 Data Analysis and Interpretations

3.6.1 Petrography

The analysis and interpretation of the rock samples are carried out with the study of petrography which is based on the observation of the thin section. The thin section made will be observed under the petrographic microscope. The type of minerals, distribution of minerals, textures, and colour of the thin section are determined under the microscope.

For the igneous rock, the classification is based on the IUGS classification of felsic rock. The proportions of quartz, alkali feldspar and plagioclase is calculated to identify the type of igneous rock. The minor minerals also have to identify for the naming of the rock by using the highest proportion of the minor mineral.

The sedimentary rock is classify by using Folk's classification and Shepard's classification. The folk's classification of sandstone is based on the relative abundance of quartz, feldspar and rock fragments. Folk's carbonate classification is refer to the percentage of allochems in rock and the type of matrix.

The classification of metamorphic rock is depends on their mineral composition and texture. The textures include grain size, shape and orientation. The metamorphic rocks are divided into two major group which are foliated and non-foliated. The mineral compositions for foliated metamorphic rock are mica, quartz, feldspar, amphibole, garnet and pyroxene while the non-foliated metamorphic rocks are made up of variable minerals including the calcite or dolomite.

3.6.2 Force Analysis by Structural Data

The structural data such as orientation, strike and dip value is obtained from the discontinuities like fault, folding, bedding surface, foliation and shear zone. The force analysis and interpretation is based on the structural data collected from the field.

For the force analysis also known as dynamic analysis of the structural, the direction of the major force that driving the deformation is identified by using the structural data. Dynamic analysis seeks to reconstruct the orientation and magnitude of the stress field by studying a set of structures, typically faults and fractures (Fossen, 2010). The rose diagram is use to plotted the orientation of force and direction of the force.

3.6.3 Slope Failure Inventory

For the creation of slope failure inventory, the specific parameters identified during the slope failure mapping such as slope geometry, mode/ type of failure, failure geometry, weathering grade, origin of rock, causes of failure, type of slope stabilization protection and vegetation cover are used to construct the table with all the parameters after the data collection.

3.6.4 Soil Cut-Slope Stability Analysis

In the soil cut-slope stability analysis, it divided into properties of soil and factor of safety of the selected slope. The properties of soil tested included are moisture content, liquid and plastic limits, particle size distribution and soil strength. These properties are used for the classification of soils.

The factor of safety is computed by using Morgenstern – Price method in the SLOPE/W software. The cohesion of the soil is important in the factor of safety calculation. The value of cohesion is obtained from the laboratory tests for properties of soil. The coarse soil made up from gravel and sand is non-cohesive soil while fine soil contains silt or clay is cohesive soil.

3.7 Report Writing

Report writing is the last step for the final year project research. The final year project consists total of six chapters which are introduction, literature review, materials and methodologies, general geology, specification and conclusion. The specification referred to the main topic of the research which is soil cut-slope failure assessment of Kuala Balah for this research. All the data obtained and the findings are written into the report. The format of the report is followed by the guidelines given by Faculty of Earth Science, Universiti Malaysia Kelantan.

CHAPTER 4

GENERAL GEOLOGY

4.1 Introduction

General geology is one of the most important chapter that involved the geomorphology, stratigraphy, structural geology and historical geology of the study area. This part is done by geological mapping by traverse within the study area. Due to this area is mostly covered by the plantation, the car cannot accessed except the Malaysia Federal Route 66 and the residential area. Figure 4.1 showed the traverse map in Kuala Balah, Jeli, Kelantan.

Geomorphology is the study of the landform and its processes that related to the Earth's origin and the evolution. The geomorphology included the study of topography, drainage pattern and weathering process of an area.

Stratigraphy involved the lithostratigraphy, biostratigraphy, chronostratigraphy, sequence stratigraphy, seismic stratigraphy and magnetostratigraphy. Although there are many branch in the part of stratigraphy, in this paper only concerned on lithostratigraphy. The thin section of the lithologies is done and the analysis of the minerals and rock identification is carried out. The analysis of petrography is used to identify the type of lithologies as well as using to construct geological map of the study area.

Structural geology is carry out by the analysis of the structure found on the outcrops such as fault, joint, fracture and fold. The structural analysis is

done by plotting rose diagram using GeoRose software and stereonet by Stereonet software. The structural mechanism also done to determine the major forces that deformed the study area. Geological map of Kuala Balah, Jeli, Kelantan with cross section is constructed based on the lithostratigraphy and structural analysis.

Part of historical geology discussed about the formation and the history of the study area. This part covered the sequence of the lithology found and the deformation formed during the formation of this area.

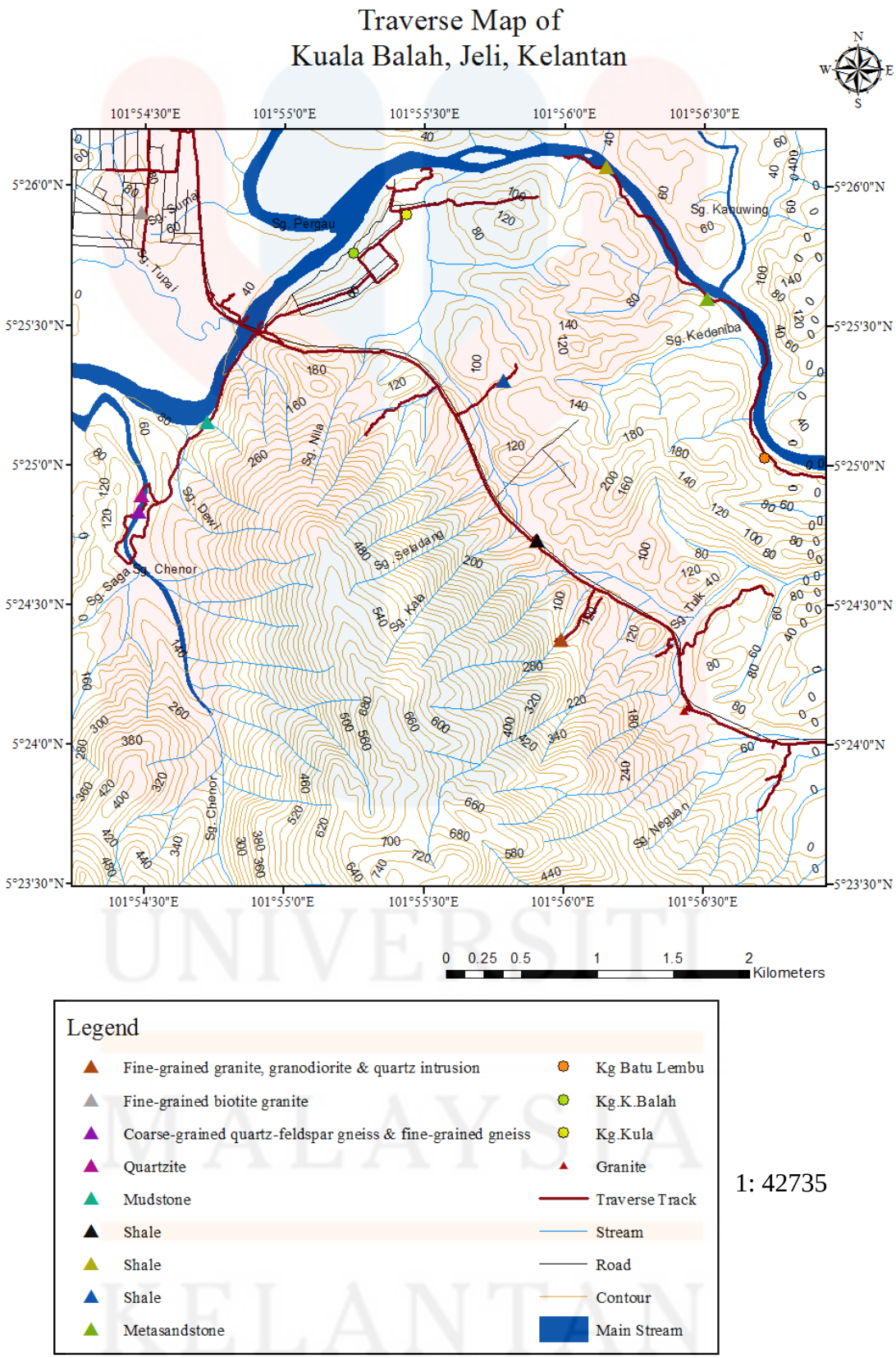

Figure 4.1: Traverse map in Kuala Balah, Jeli, Kelantan.

4.2 Geomorphology

Geomorphology referred to study of landform of the Earth. The major type of landforms included mountains, hills, plateaus and plains. The geomorphology of the Earth can be made up by either endogenic or exogenic processes. The endogenic process that create landforms is referred to volcanism, diastrophism and earthquake while exogenic process referred to the aggradation, degradation and organism action. Both of the processes take a long period to form a particular landform. Mountain is the large landform in form of a peak that rises high to its surrounding area. Plain is a landform that has flat area commonly occurs as lowland. Fluvial is a morphology formed by the processes and deposits of rivers and streams. Figure 4.2 showed the plain area with plantation, Figure 4.3 presented the mountain and plain landform and Figure 4.4 illustrated the fluvial morphology in the study area.

Figure 4.2: Plain area with plantation. (Coordinate: N 05° 25' 55.1", E 101° 55' 29.9")

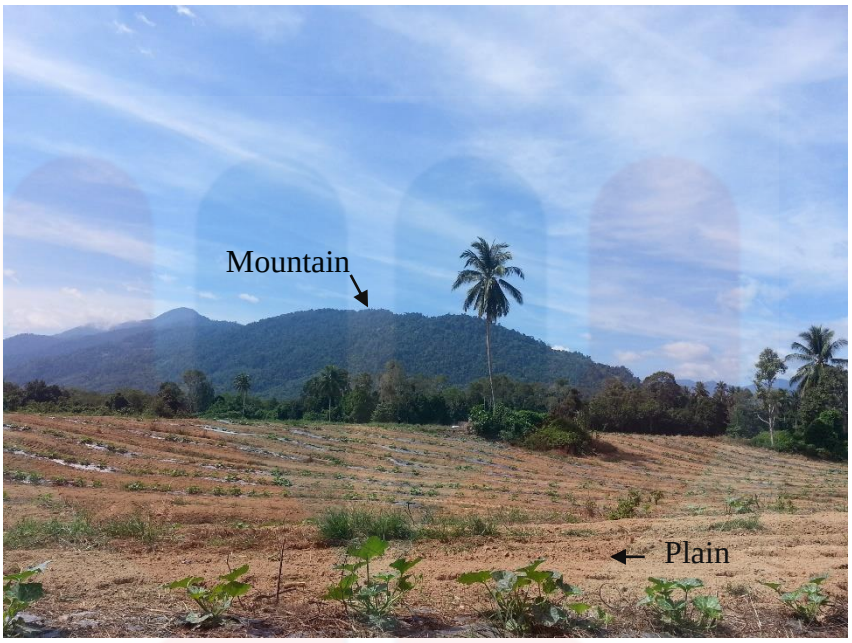

Figure 4.3: Mountain and plain landform. (Coordinate: N 05° 25' 55.1", E 101° 55' 29.9")

Figure 4.4: Fluvial morphology. (Coordinate: N 05° 24' 47.2", E 101° 54' 27.3")

4.2.1 Topography

Topography is the arrangement of the physical distribution of the Earth's surface such as shape and elevation. The topography of a particular area can show by the topographic map which included the elevation of the area.

Within this 25km^2, the landforms observed are mountain and hilly area as well as the plain area. The elevation of the mountain and hilly area is range from 40m to 740m. This area is made up of different type igneous rocks due to the intrusion and deformation and small amount of metamorphic rock. The highest elevation at south of the study area. The landform of the highest elevation is mountainous area. At this area, rubber plantation is dominant.

The plain area covered the excess part of the study area except the mountain and hilly area. This area included the river and alluvial plains. The elevation is between 40m to 200m. This area is made up of sedimentary rock and sediments which are the weathered products from weathering process. The lowest elevation located at north-west of study area. This area use as residential area.

Besides that, the closer and higher contour indicated that the area is steeper and more resistant to weathering compared to the loose and lower contour. Figure 4.5 showed the topographic map of Kuala Balah, Jeli, Kelantan in meter and Figure 4.6 presented 3D topographic map of Kuala Balah, Jeli, Kelantan in meter.

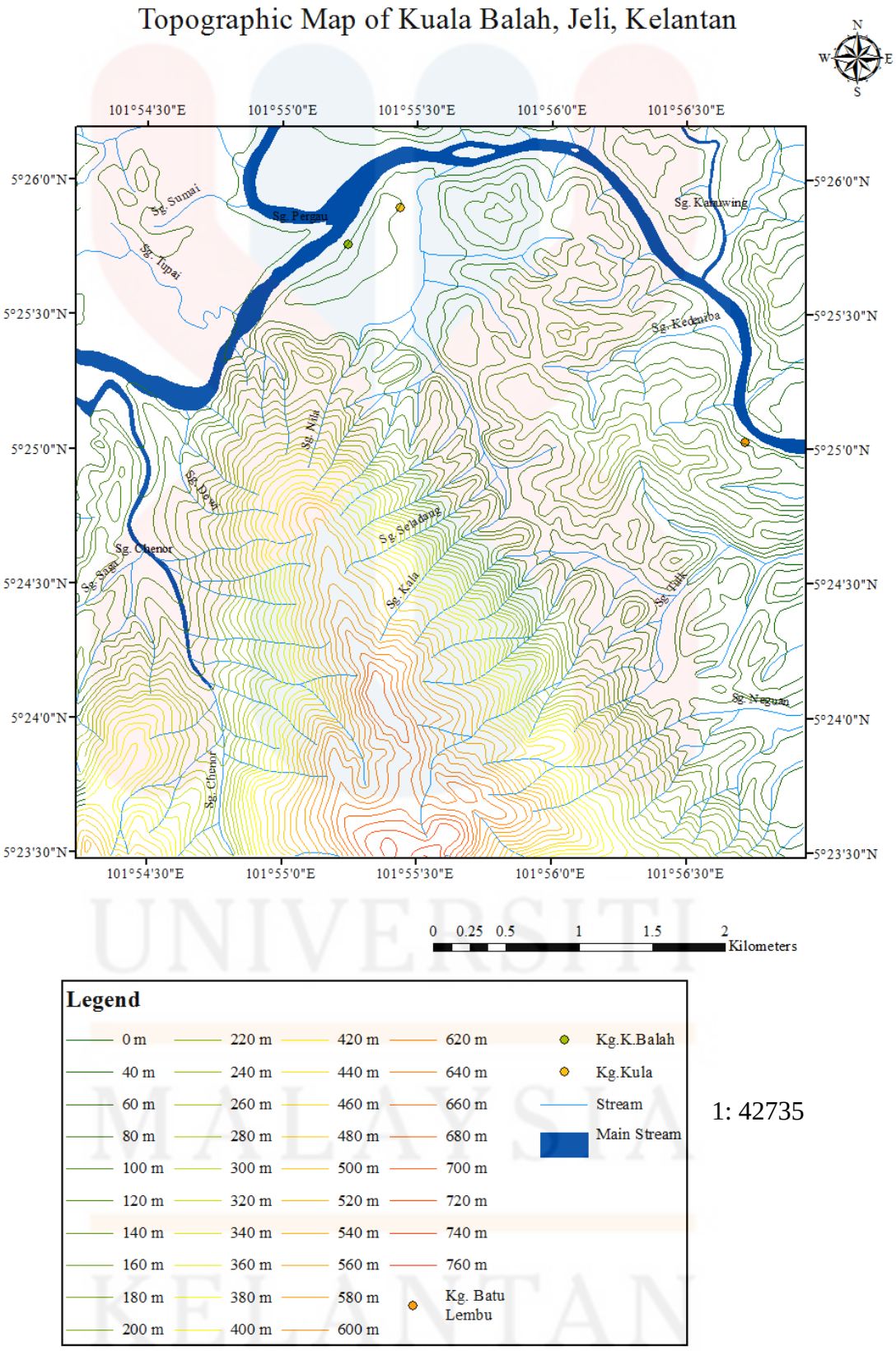

Figure 4.5: Topographic map of Kuala Balah, Jeli, Kelantan.

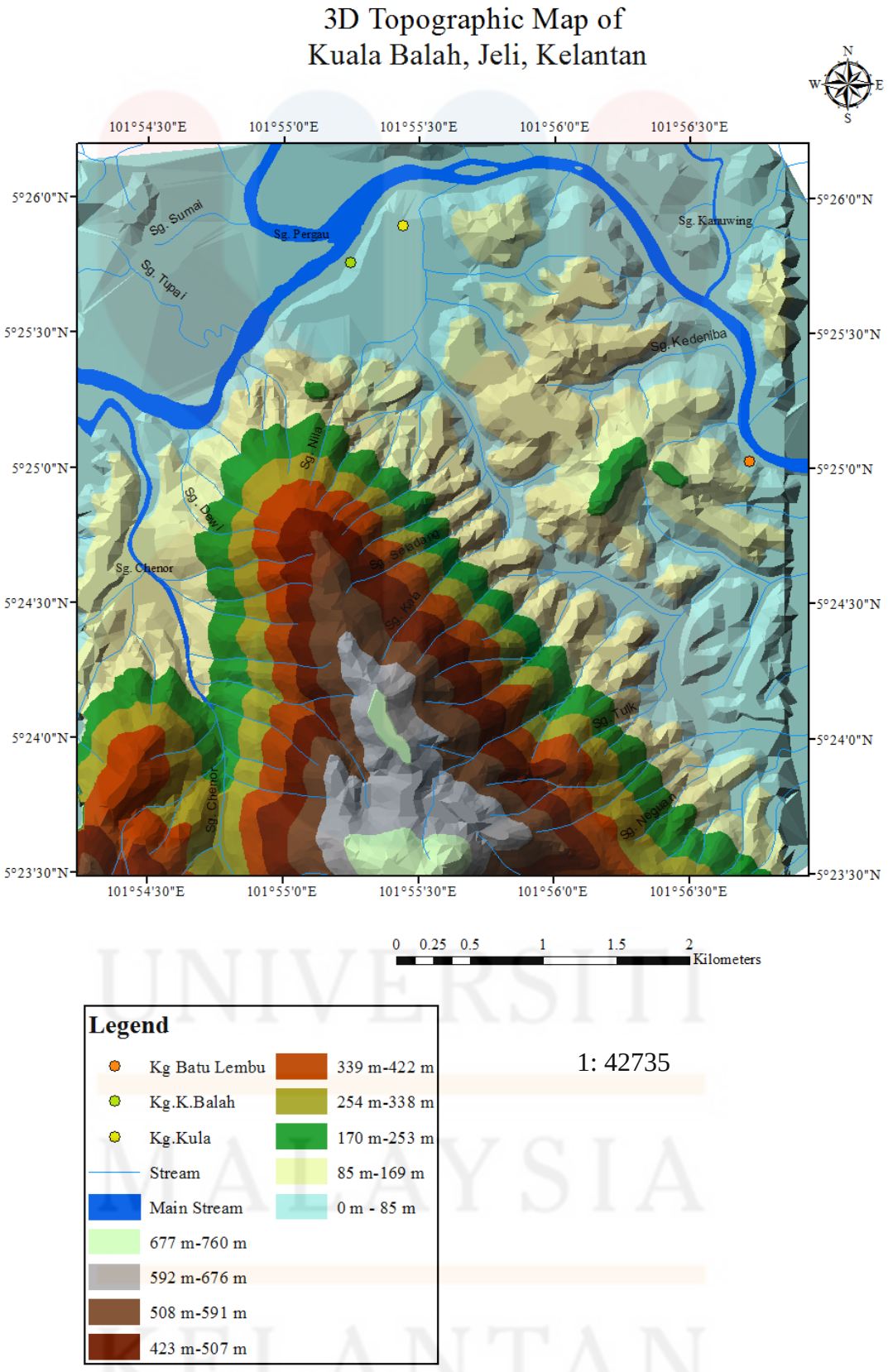

Figure 4.6: 3D topographic map of Kuala Balah, Jeli, Kelantan.

4.2.2 Drainage Pattern

Drainage pattern is the arrangement of streams on the surface of Earth by drainage system. Geologic and topographic factors of the rock beneath the Earth reflected the drainage pattern as well. The drainage pattern included dendritic, parallel, trellis, rectangular, radial, centripetal and deranged pattern. Dendritic drainage pattern is the most common drainage pattern found on the surface of Earth. The Figure 4.7 showed the radial and dendritic drainage patterns.

In the study area, the drainage patterns observed are dendritic and radial pattern. The shape of the dendritic drainage pattern (A) like branching shape of tree roots. Ritter (2006) stated that the dendritic drainage pattern develops in areas underlain by homogeneous material. The tributaries join to the larger streams at acute angle (less than 90 degrees). The dendritic drainage pattern is observed at area which sedimentary rock located. In the study area, the lithology found within dendritic drainage pattern are metasandstone, mudstone and shale. Figure 4.8 showed the dendritic drainage pattern with the label of A.

The radial drainage pattern (B) is radiate outward or inward from the centre on the hill or toward the centre of a dome. The lithology usually found in this type of drainage pattern is granite and metamorphic rock that classified as hard rock. Granite, granodiorite, quartzite and gneiss are found at the area with radial drainage pattern. The radial drainage pattern with label B presented in Figure 4.8.

Watershed is defined as the catchment area of the water from high elevation to lower elevation. It catches all the water like rain or snow and flows

into river, lake, stream and marsh. The boundary of the watershed commonly followed the contour pattern that showed the present of valley. All the distributaries are then flow into Sungai Balah which located at northern of study area. Figure 4.9 showed the watershed of Kuala Balah, Jeli, Kelantan.

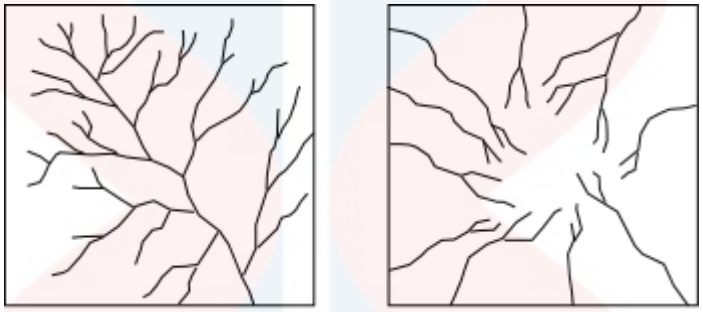

(a) (b)

Figure 4.7: Dendritic pattern (a); Radial pattern (b) Source: Streams and Drainage Systems, 2015

Along the traverse from upstream to downstream of Sungai Balah, it is found that the river water is more clearly at the upstream compared to the downstream. This phenomenon occurred because of the transportation and deposition process of the sediments. At upstream, the velocity of the water flow is high as well as the energy. The larger and denser sediments can deposited at upstream because the water cannot bring them along for the further transportation. At the downstream the water flow is slow down, the lighter and smaller sediments can be deposited. Hence, the sediments found at the downstream is smaller compared to the upstream. The cloudy water is contributed by the slit and clay-sized sediments that dominant at the downstream. At the upstream, the stage of river is mature stage because there are dominant with medium to small rock and it is U-shaped. The downstream which is Sungai Balah is old river due to broad U-shaped, wide floodplain and

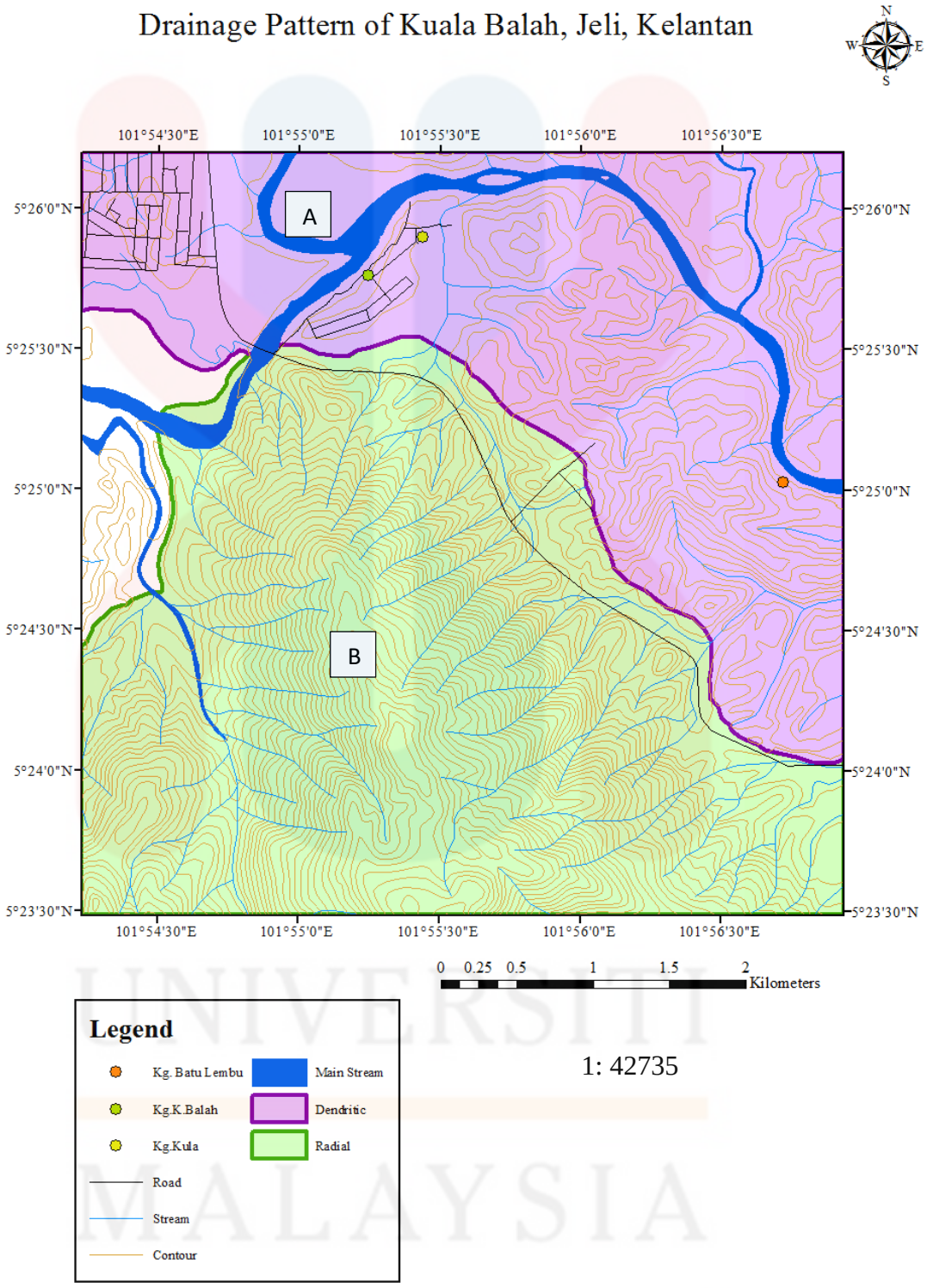

Figure 4.8: Drainage pattern of Kuala Balah, Jeli, Kelantan.

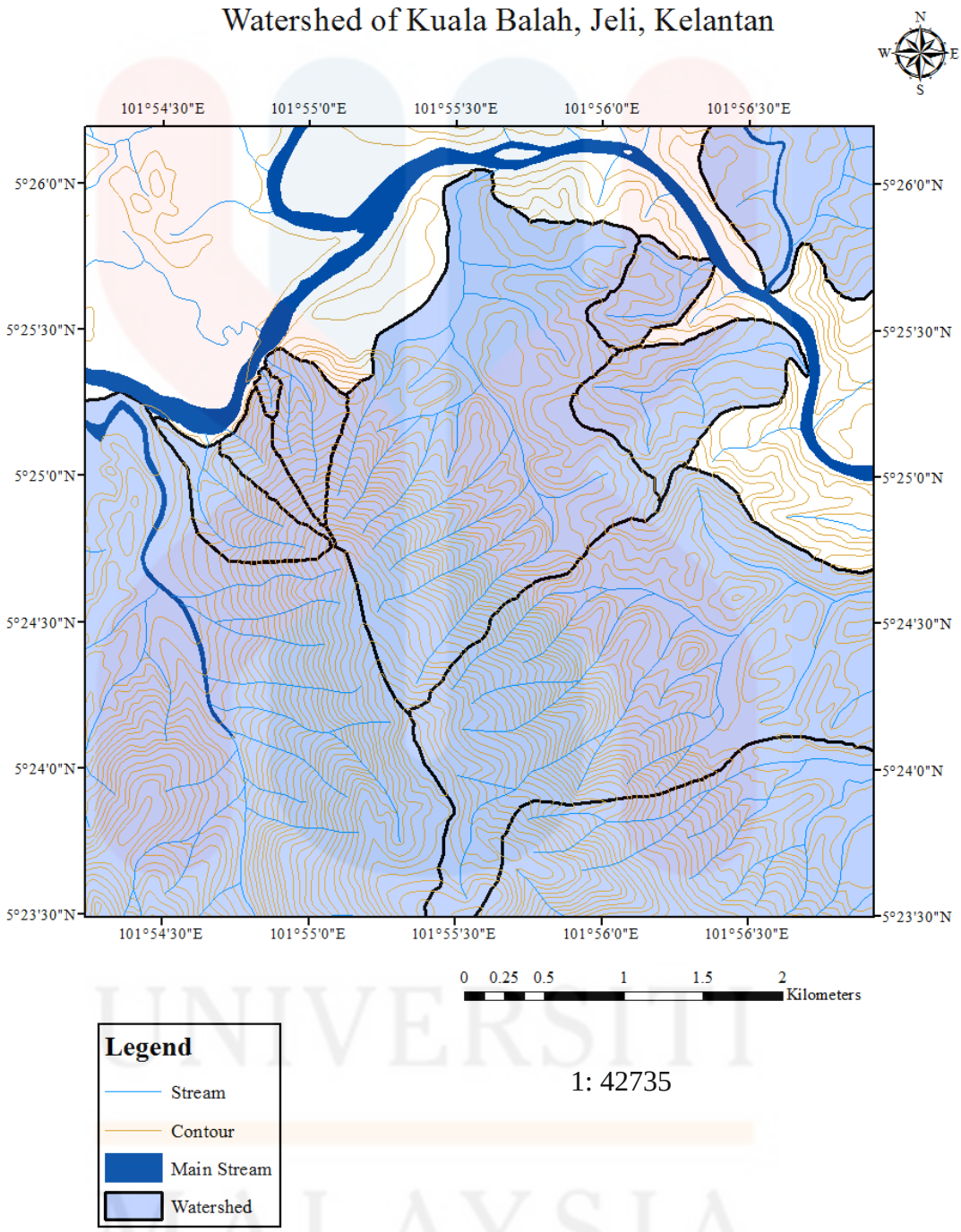

Figure 4.9: Watershed of Kuala Balah, Jeli, Kelantan.

dominant with silty sediment that caused the water become cloudy. Figure 4.10 and Figure 4.11 illustrated the river at the upstream and downstream respectively.

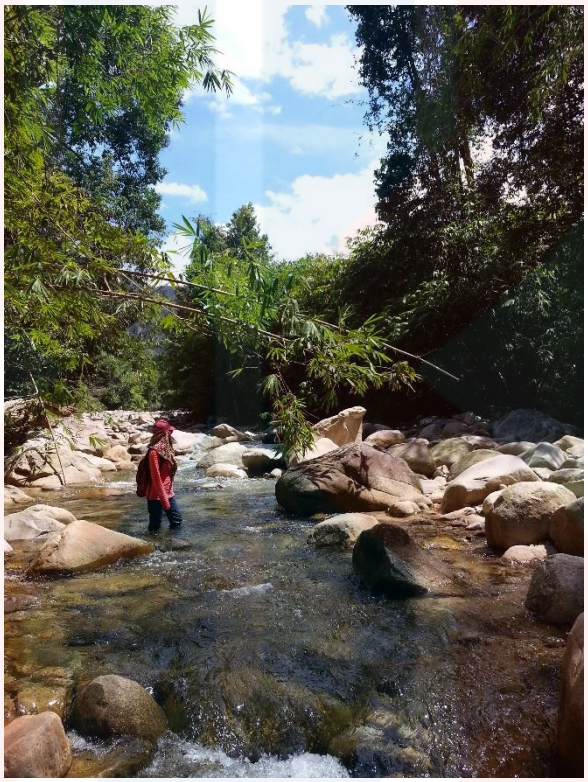

Figure 4.10: Sungai Chenor, upstream tributary of Sungai Balah. (Coordinate: N 05° 24' 47.2", E 101° 54' 27.3")

Figure 4.11: Downstream of Sungai Balah. (Coordinate: N 05° 25' 38.0", E 101° 56' 29.0")

After the extreme flood at 2014, many of the sediments are transported in to rivers and caused shallowing of river bed as well as covered the small rivers. .The sediments are transported from upstream to downstream cause some part of the river become shallow. This is due to the water flow of the river water. At the shallow part, more sediments deposited because of the velocity of water flow is decease and the sediments can be deposited easily. It will change the channel pattern by forming of the sandbar. The river may change from straight pattern to braided pattern. The river with deposited sediments showed in the Figure 4.12.

Figure 4.12: Sungai Balah with deposited sediments. (Coordinate: N 05° 25' 29.1", E 101° 54' 53.0")

The erosion of the river bank also observed during traverse along Sungai Balah. Erosion of river bank is occurred when the water level of the

river is higher than normal level and the side of the river is eroded by the high velocity of water flows. This type of erosion happened when there is heavy rainfall or flood. The erosion of river bank can change the size and the shape of the rivers. As it continuous eroded the side, the river will be enlarge. Figure 4.13 showed the erosion of the river bank.

Figure 4.13: Erosion of river bank. (Coordinate: N 05° 25' 48.2", E 101° 56' 22.3")

4.2.3 Weathering Process

Weathering process is one of the degradation process with belongs to endogenic process of the creation of geomorphology. It is break down of rocks, soil and its mineral content through natural, chemical or biological process.

Physical weathering occurred when there is changes of temperature on rocks and caused the rock to broken down without chemical properties changes. Chemical weathering is changes of chemical properties of rock through

oxidation, carbonation, hydration or hydrolysis. The biological weathering is due to the action of plants, animals, or microbes in disintegration of rocks.

Soil erosion is the removal of soil on Erath's surface by water, wind, ice and gravity. There are three types of accelerated erosion which is sheet erosion, rill erosion and gully erosion. The characteristic of gully erosion is the soil is removed along the drainage lines due to surface runoff.

In the study area, there are two types of weathering processes are found which are physical weathering and biological weathering. One of the physical weathering observed is gully erosion. Figure 4.14, Figure 4.15 and Figure 4.16 represented the gully erosion and physical weathering. Biological weathering by plant is showed in the Figure 4.17.

Figure 4.14: Gully erosion at 05°24'02.0", 101°56'47.0".

Figure 4.15: Gully erosion at 05°24'51.0", 101°55'49.0".

Figure 4.16: Potholes formed by physical weathering via running water. (Coordinate: N 05° 24' 49.7", E 101° 54' 28.5")

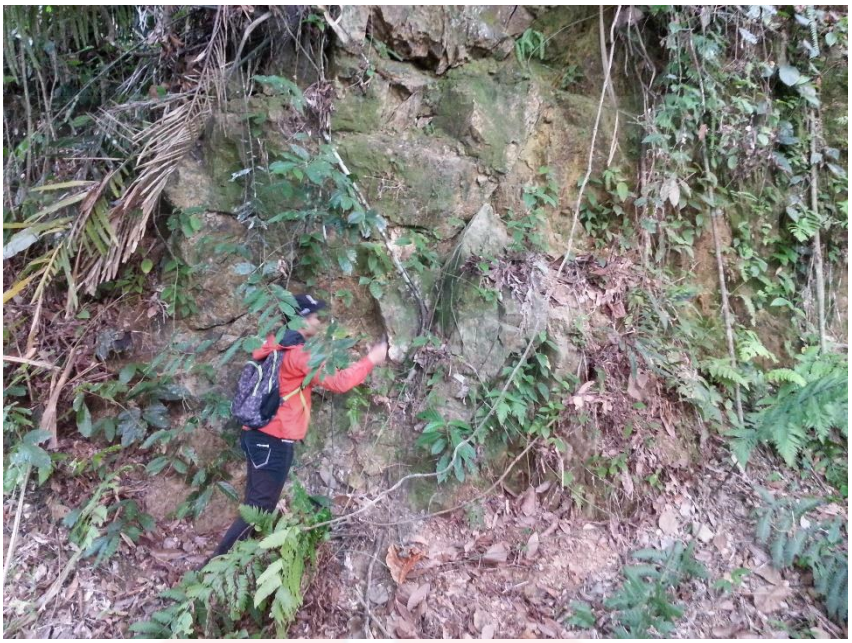

Figure 4.17: Root penetration by plants. (Coordinate: N 05° 25' 17.2", E 101° 54' 29.5")

The weathering profile consists seven parts which are loose organic matter, inorganic matter mixed with humus and much bioactivity, an eluviated zone, zone of illuviation, significantly weathered parent material, slightly weathered parent material as well as unaltered parent material.

At a location within the study area, the weathering profile is clearly seen due to the excavation of the particular area with coordinate of N 05° 24' 04.0", E 101° 56' 47.0". It does not consists all seven parts of weathering profile but the top 4 parts which are horizon O, A, E and B. Horizon O contains loose organic matter, horizon A is composes of inorganic matter that mixed with humus and much bioactivity takes place, horizon E is an eluviated zone which contains little or no organic matter and horizon B is the zone of illuviation composing materials transported from overlying horizons. Figure 4.18 showed the weathering profile of study area.

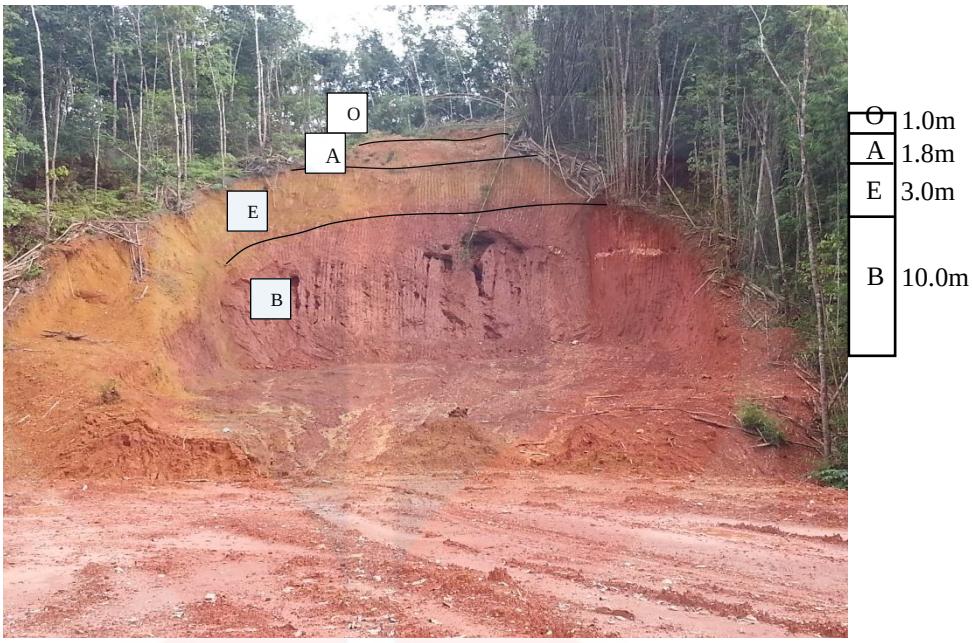

Figure 4.18: Weathering profile at N 05° 24' 04.0", E 101° 56' 47.0".

4.3 Stratigraphy

Stratigraphy is the study of the characteristics of layered rocks, relationships between the layered rocks and the relative and absolute ages of the rocks. Lithostratigraphy is one of the sub-discipline of stratigraphy which concern on the study of rock layers. It usually use to describe the relationships between the formations of igneous or sedimentary rocks. The map of rock sample location is showed in Figure 4.19. Figure 4.20 illustrated the geological map of Kuala Balah, Jeli Kelantan with cross section.

Based on Singh et al. (1984), they stated that the granites have lower age limits of Carboniferous to Triassic. The sedimentary rocks included sandstone, siltstone and shale are Triassic in age according to the geological map of Kelantan. There is also granite intrusion of Cretaceous age. The metamorphic rocks are the oldest rock in the study area followed by granite

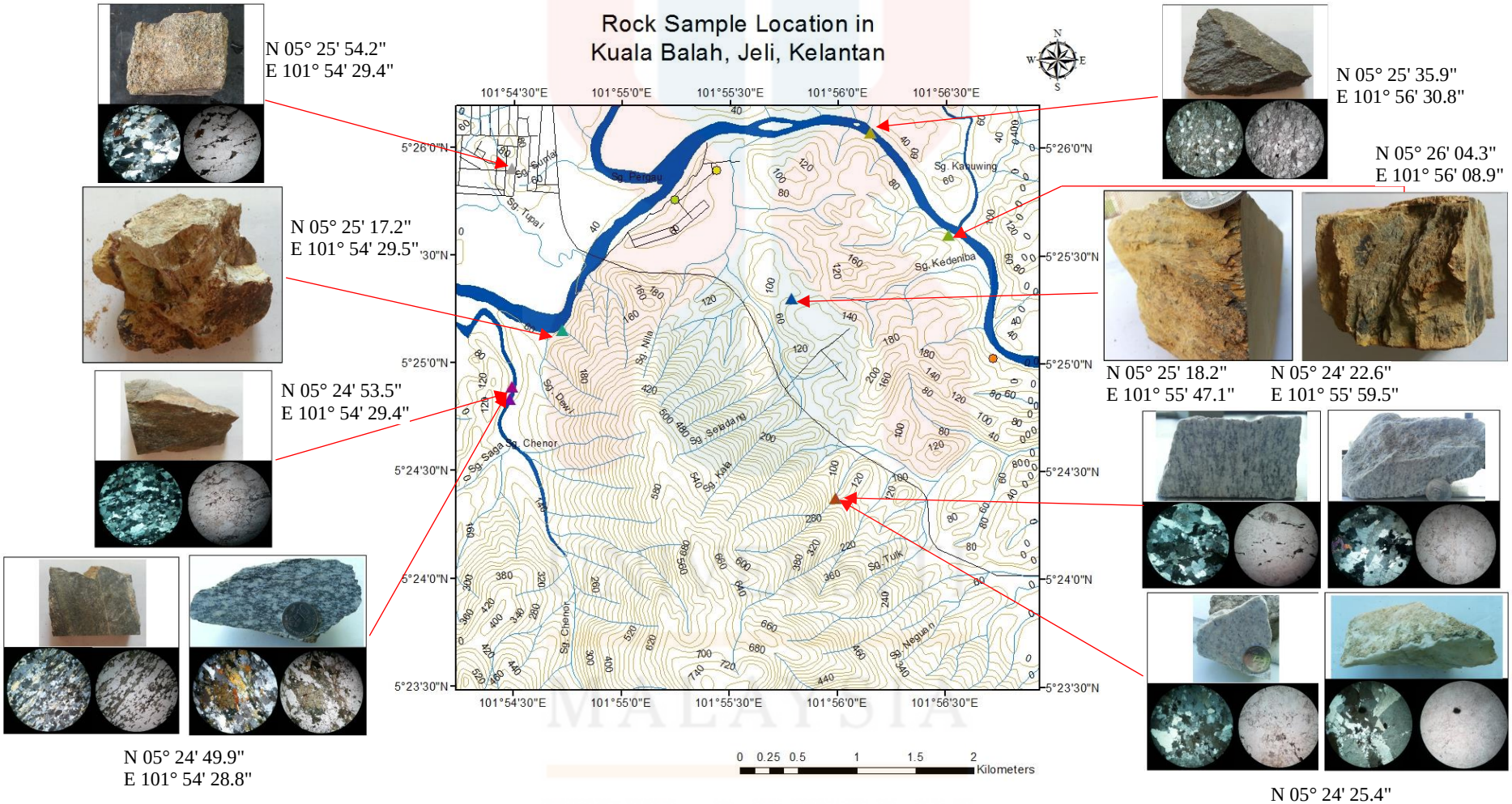

Figure 4.19: Rock sample location in Kuala Balah, Jeli, Kelantan.

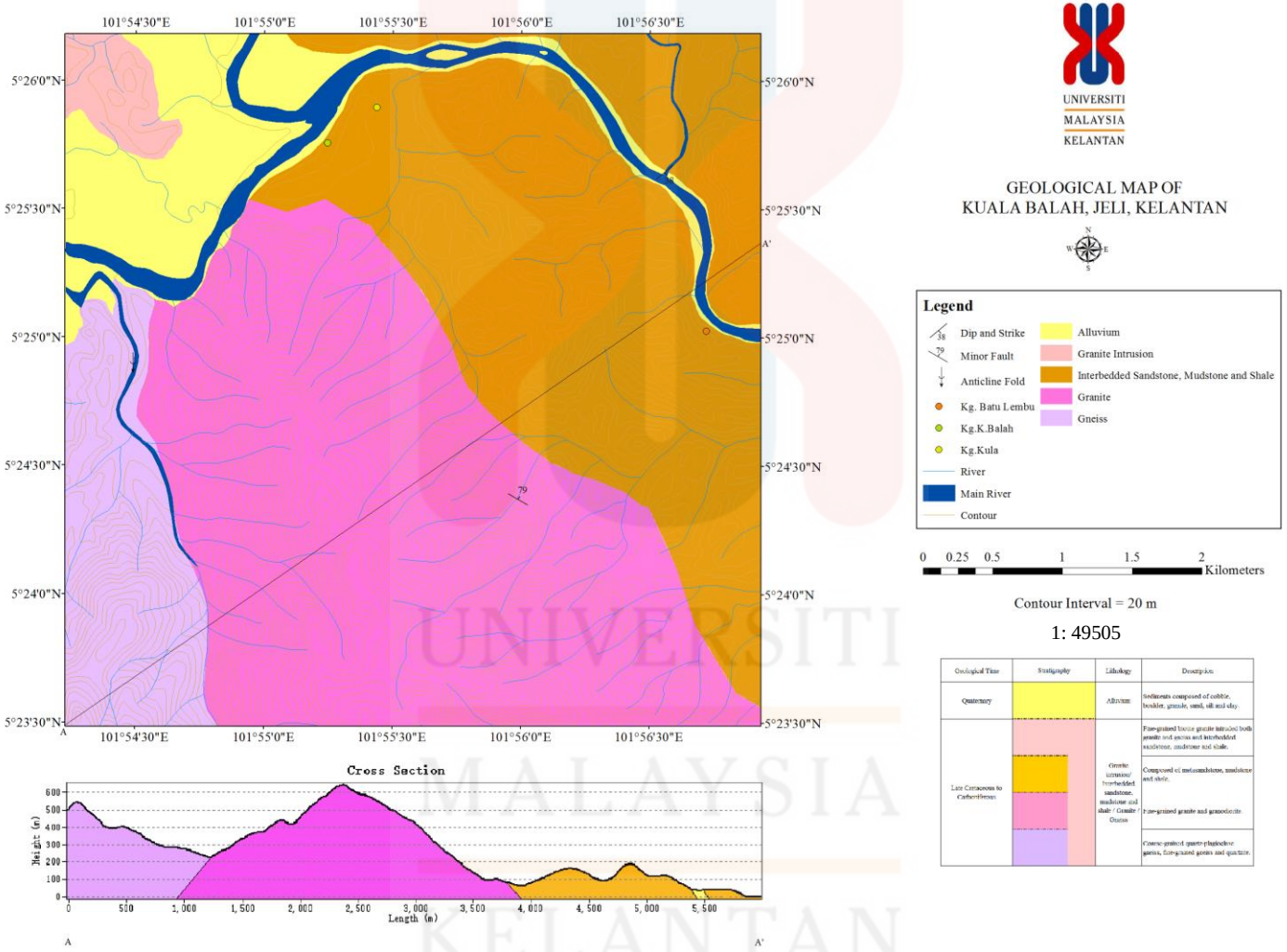

Figure 4.20: Geological map of Kuala Balah, Jeli, Kelantan with cross section.

and granodiorite, sedimentary rocks and the youngest granite intrusion. There are several sample of lithology is taken as hand specimen and also interpretation of petrography.

4.3.1 Gneiss

Coarse-Grained Quartz-Plagioclase Gneiss

It is identified as gneiss based on the hand specimen because it is coarse- grained and foliated. There is segregation of light-colour minerals and dark-colour minerals to show the banding structure. The minerals observed are quartz, feldspar and biotite on the hand specimen. This gneiss is Permo-Carboniferous or Triassic in age (Singh *et al.*, 1984). Figure 4.21 and Figure 4.22 illustrated hand specimen and foliation of gneiss.

Figure 4.21: Hand specimen of coarse-grained quartz-plagioclase gneiss.

Figure 4.22: Foliation of coarse-grained quartz-plagioclase gneiss.

Based on the observation of thin section, the major minerals such as quartz, alkali feldspar and plagioclase are observed. The minor mineral in this rock include biotite, hornblende, orthopyroxene and clinopyroxene. Hornblende and orthopyroxene have moderate relief while clinopyroxene has high relief. Biotite, hornblende, orthopyroxene and clinopyroxene aligned due to metamorphism. Orthopyroxene has parallel extinction while clinopyroxene has incline extinction. The characteristic of hornblende is the angle between cleavages are 56° and 124°. As a result from the observation of hand specimen and thin section, this rock is identified as coarse-grained quartz-plagioclase gneiss. The microscopic image of coarse-grained quartz-plagioclase gneiss under XPL is presented in Figure 4.23 while microscopic image of coarse-grained quartz-plagioclase gneiss under PPL showed in Figure 4.24. Table 4.1 presented the mineral composition of fine-grained gneiss.

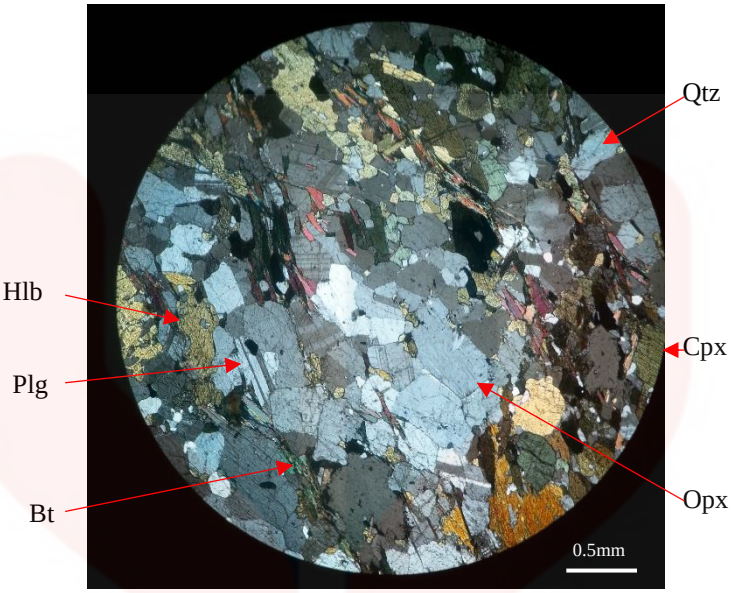

Figure 4.23: Microscopic image of coarse-grained quartz-plagioclase gneiss under XPL (4x).

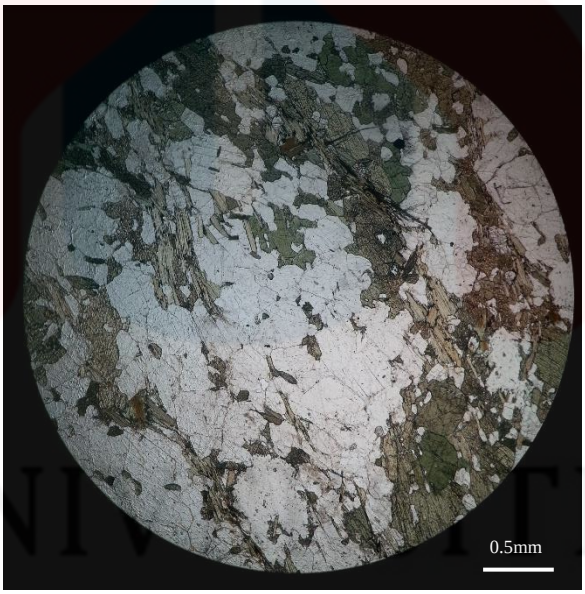

Figure 4.24: Microscopic image of coarse-grained quartz-plagioclase gneiss under PPL (4x).

Table 4.1: Mineral composition of coarse-grained quartz-plagioclase gneiss.

Composition of mineral	Percentage (%)
Quartz	28
Alkali feldspar	4
Plagioclase	28
Biotite	2
Hornblende	2
Orthopyroxene	18
Clinopyroxene	20

Fine-Grained Gneiss

Gneiss is the high grade foliated metamorphic rock that formed in condition of higher temperature and pressure compared to other metamorphic rocks. It is easily to recognized due to the foliation. The minerals can be identified by unaided eyes are biotite, quartz and alkali feldspar. It usually formed during the mountain building which the country rocks such as granite and sedimentary rocks subjected to high temperature and pressure. The age of this gneiss is Permo-Carboniferous or Triassic (Singh *et al*., 1984).

Based on the thin section of fine-grained gneiss, the gneissose texture is obvious under PPL because of the alignment of the dark minerals. These dark minerals are biotite, orthopyroxene and clinopyroxene. All of the minerals are interlocking to each other and elongated.

The contact between two types of metamorphic rock is found at N 05° 24’ 49.9”, E 101° 54’ 28.8” and showed in Figure 4.25. From the cut section, the gneissose texture is clearly observed. The hand specimen and cut section of fine-grained gneiss found is presented in Figure 4.26 and Figure 4.27. Figure 4.28 and Figure 4.29 showed the microscopic image of fine-grained gneiss under XPL and PPL. Table 4.2 showed the mineral composition of fine-grained gneiss.

Figure 4.25: Coarse-grained quartz-plagioclase gneiss and fine-grained gneiss. (Coordinate: N 05° 24' 49.9", E 101° 54' 28.8")

Figure 4.26: Hand specimen of fine-grained gneiss.

Figure 4.27: Cut section of fine-grained gneiss.

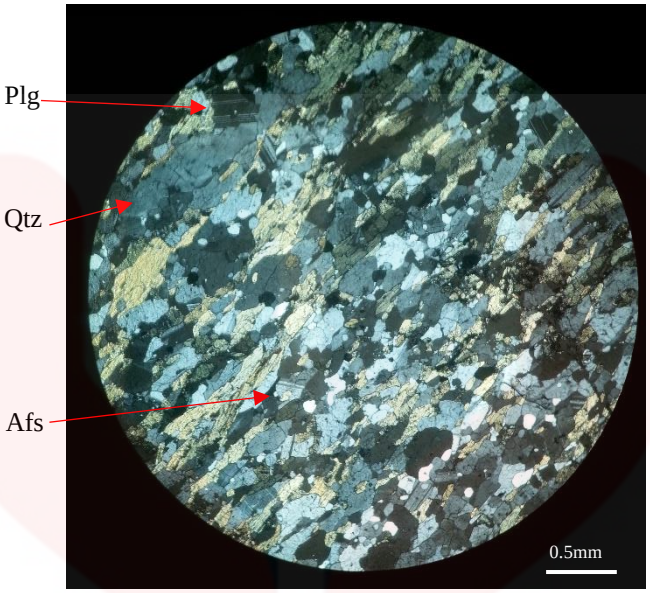

Figure 4.28: Microscopic image of fine-grained gneiss under XPL (4x).

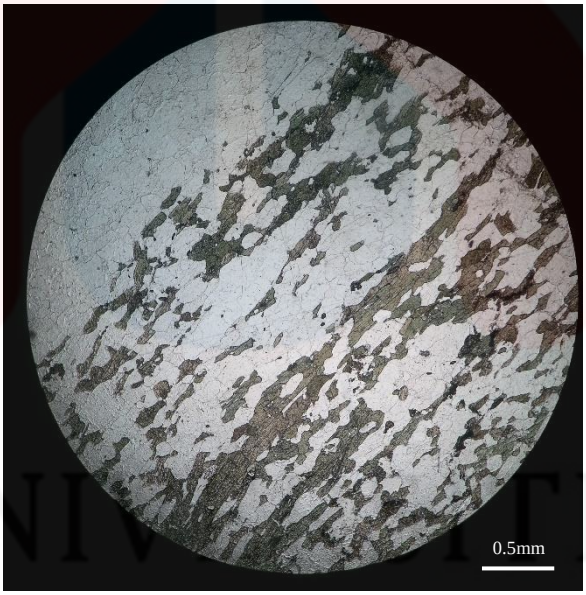

Figure 4.29: Microscopic image of fine-grained gneiss under PPL (4x).

Table 4.2: Mineral composition of fine-grained gneiss.

Composition of mineral	Percentage (%)
Quartz	20
Alkali feldspar	5
Plagioclase	20
Biotite	1
Orthopyroxene	27
Clinopyroxene	27

Quartzite

Quartzite is one of the non-foliated metamorphic rock which composed dominantly quartz minerals. The quartzite is found at N 05° 24’ 53.5” and E 101° 54’ 29.4” which is located in Sungai Chenor, Kuala Balah. It is grey in colour and medium-grained. The quartz minerals can be observed by unaided eyes. The age of quartzite is Permo-Carboniferous or Triassic (Singh *et al*,. 1984). Figure 4.30 showed the outcrop of the quartzite and Figure 4.31 presented the hand specimen of quartzite.

Figure 4.30: Outcrop of quartzite. (Coordinate: N 05° 24' 53.5", E 101° 54' 29.4")

Figure 4.31: Hand specimen of quartzite.

Based on the observation of thin section, the quartzite composed 90% of quartz and the quartz minerals are interlocking with each other. This is due to during the formation of quartzite, the original rock had went through

condition of high temperature and pressure that compacted the rock and forced the mineral to interlocked each other. Some of the minerals are elongated due to the compaction. Figure 4.32 and Figure 4.33 showed the microscopic image of quartzite under XPL and PPL respectively. Mineral composition of quartzite is tabulated in Table 4.3.

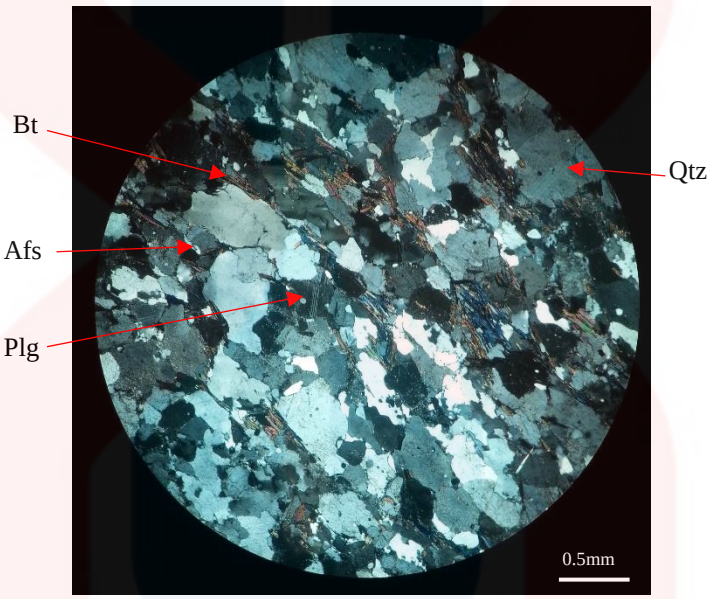

Figure 4.32: Microscopic image of quartzite under XPL (4x).

Figure 4.33: Microscopic image of quartzite under PPL (4x).

Table 4.3: Mineral composition of quartzite.

Composition of mineral	Percentage (%)
Quartz	90
Alkali feldspar	1
Plagioclase	4
Biotite	5

4.3.2 Granite

Fine-grained Granite

The granite is found in the rubber plantation area at N 05° 24’ 23.4” and E 101° 56’ 00.9” which is fresh in conditions. The size of outcrop is approximately 1m in length and 0.7m in height. The vegetation around the outcrop is rubber tree and there is a small river near to the outcrop. This granite is phaneritic and medium-grained. The rock is made up of wholly crystals. The fabric of this granite is inequigranular. The grain size of the minerals are not similar to each other’s. This specimen contains high proportion of quartz and alkali feldspar and biotite as the minor mineral. Based on the hand specimen, the content of biotite is less than fine-grained biotite granite. It is lighter in colour. The age of this granite is range in Carboniferous to Triassic (Singh *et al*., 1984). The hand specimen of fine-grained granite is showed in Figure 4.34 and cut section of fine-grained granite is presented in Figure 4.35.

Figure 4.34: Hand specimen of fine-grained granite.

Figure 4.35: Cut section of fine-grained granite.

According to the observation of thin section. The mineral contents are quartz, alkali feldspar, plagioclase and biotite. All the minerals are anhedral in shape. Quartz, alkali feldspar and plagioclase are low relief while the biotite

has medium relief. Quartz, alkali feldspar and plagioclase are colourless in true colour. Alkali feldspar has zebra strip and plagioclase has twinning. The interference colour of biotite is brown and dark brown in true colour. Figure 4.36 showed the microscopic image of fine-grained granite under XPL and Figure 4.37 presented microscopic image of fine-grained granite under PPL. Mineral composition of fine-grained granite is tabulated in Table 4.4. The QAP diagram of fine-grained granite illustrated in Figure 4.38.

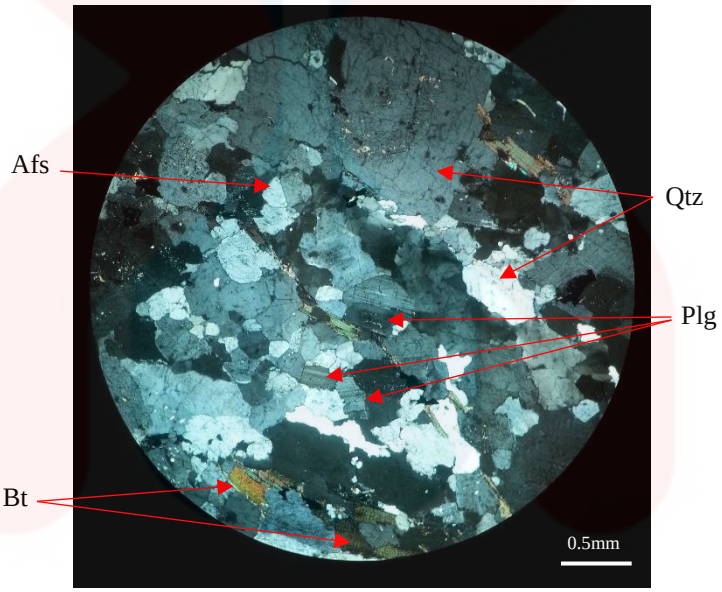

Figure 4.36: Microscopic image of fine-grained granite under XPL (4x).

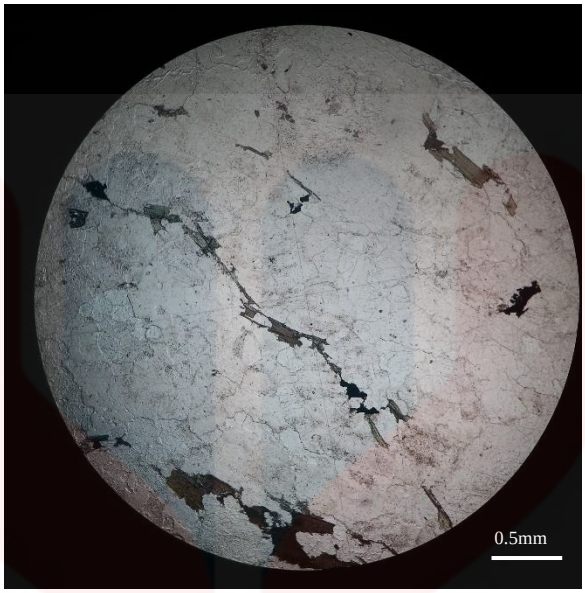

Figure 4.37: Microscopic image of fine-grained granite under PPL (4x).

Table 4.4: Mineral composition of fine-grained granite.

Composition of mineral	Percentage (%)
Quartz	40
Alkali feldspar	30
Plagioclase	25
Biotite	5

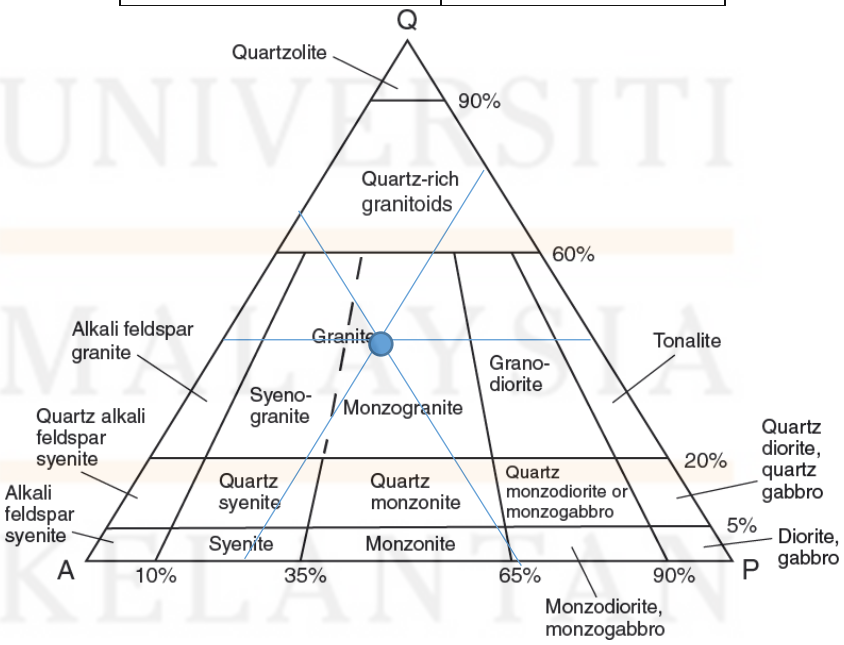

Figure 4.38: QAP diagram of fine-grained granite.

Granodiorite

This outcrop of granodiorite is found on the waterfall at N 05° 24’ 22.6” and E 101° 55’ 59.5”. The outcrop is 1.5m in length and 0.8m in height. This granodiorite has same mineral contents as the previous granite but different in percentage. The rock texture is phaneritic and fine-grained. There are two types of texture and colour observed on the same outcrop. It is because of the accumulation of magma in the magma chamber. They are both from the same magma but different distribution of minerals. The granodiorite has an age of Carboniferous to Triassic (Singh *et al*., 1984). Figure 4.39 presented the outcrop of granodiorite. The cut section of granodiorite is showed in Figure 4.40.

Figure 4.39: Outcrop of granodiorite. (Coordinate: N 05° 24' 22.6", E 101° 55' 59.5")

Figure 4.40: Cut section of granodiorite.

Based on the thin section observation, the minerals contain are quartz, alkali feldspar and plagioclase as major minerals. Biotite and garnet also observed in this particular thin section. Quartz, alkali feldspar and plagioclase has low relief, biotite has medium relief and garnet has high relief. Quartz, alkali feldspar and plagioclase are colourless under PPL. Biotite is brown in colour under XPL and pale brown under PPL. Quartz. Garnet is hexagonal in shape and black in colour under PPL. The microscopic image of granodiorite under XPL showed in Figure 4.41. Figure 4.42 illustrated microscopic image of granodiorite under PPL. Table 4.5 presented mineral composition of granodiorite. QAP diagram of granodiorite is showed in Figure 4.43.

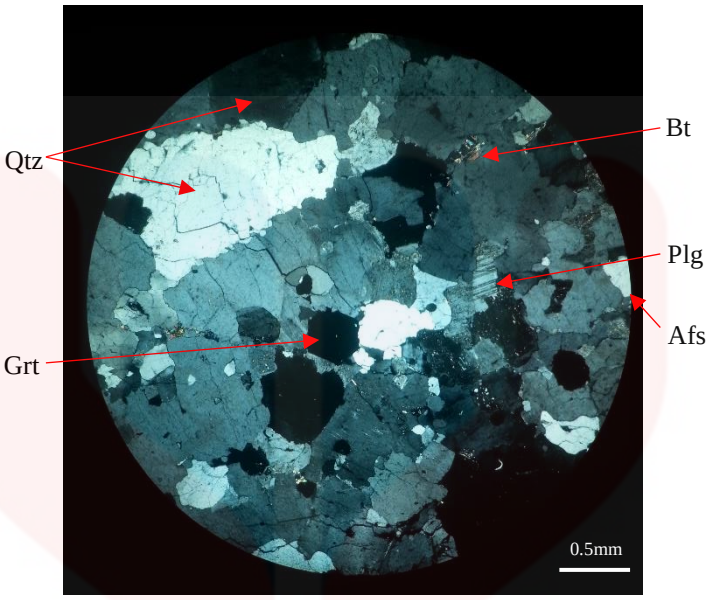

Figure 4.41: Microscopic image of granodiorite under XPL (1) (4x).

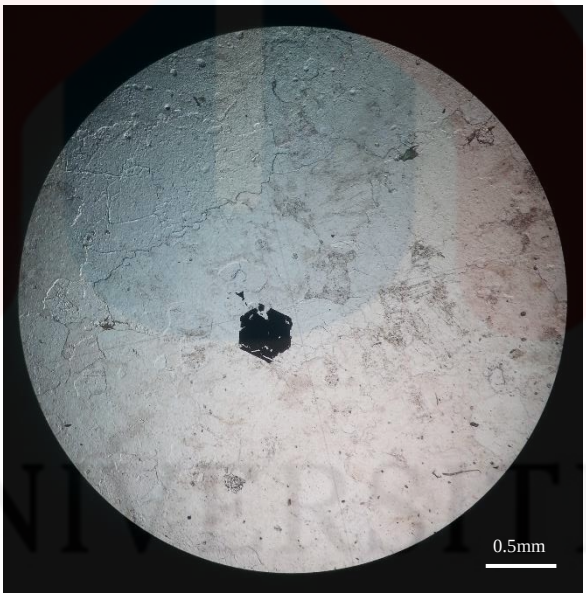

Figure 4.42: Microscopic image of granodiorite under PPL (1) (4x).

Table 4.5: Mineral composition of granodiorite (1).

Composition of mineral	Percentage (%)
Quartz	46
Alkali feldspar	15
Plagioclase	35
Biotite	3
Garnet	1

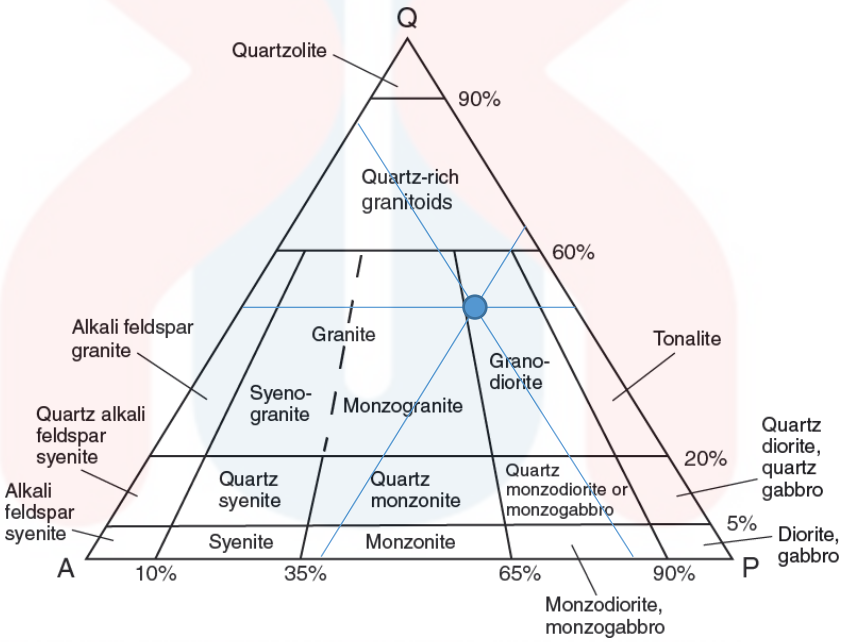

Figure 4.43: QAP diagram of granodiorite (1).

From the observation of hand specimen, it consists of pinkish alkali feldspar, quartz, plagioclase and small portion of biotite. It is phaneritic and fine- grained. It is holocrystalline and equigranular. The hand specimen of granodiorite is presented in Figure 4.44 and Figure 4.45 showed the cut section of accumulation part of the granodiorite.

Figure 4.44: Hand specimen of granodiorite.

Figure 4.45: Cut section of mineral accumulation of granodiorite.

According to thin section observation, the minerals identified are quartz, alkali feldspar, plagioclase and biotite and the size is smaller. The plagioclase is dominant after quartz in this part. Biotite is covered small portion and it has

medium relief. Quartz, alkali feldspar and plagioclase are euhedral in shape while biotite is subhedral in shape. Figure 4.46 and Figure 4.47 presented the microscopic image of granodiorite under XPL and PPL individually. Table 4.6 showed the mineral composition of granodiorite. Figure 4.48 illustrated the QAP diagram for granodiorite.

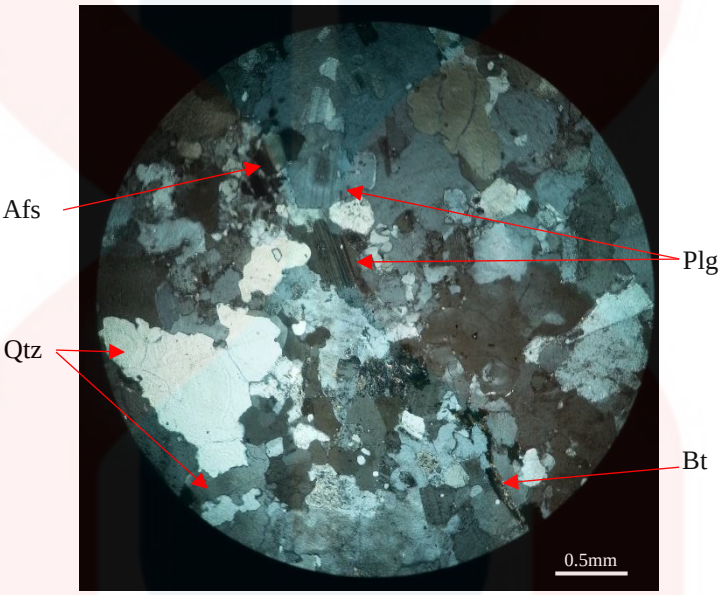

Figure 4.46: Microscopic image of granodiorite under XPL (2) (4x).

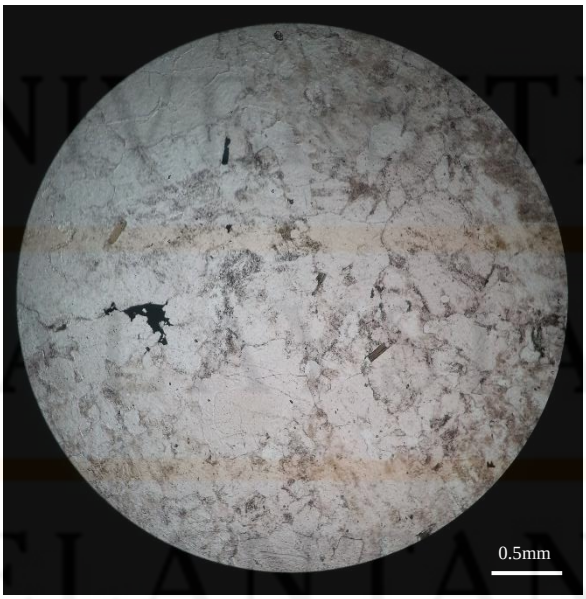

Figure 4.47: Microscopic image of granodiorite under PPL (2) (4x).

Table 4.6: Mineral composition of granodiorite (2).

Composition of mineral	Percentage (%)
Quartz	48
Alkali feldspar	10
Plagioclase	40
Biotite	2

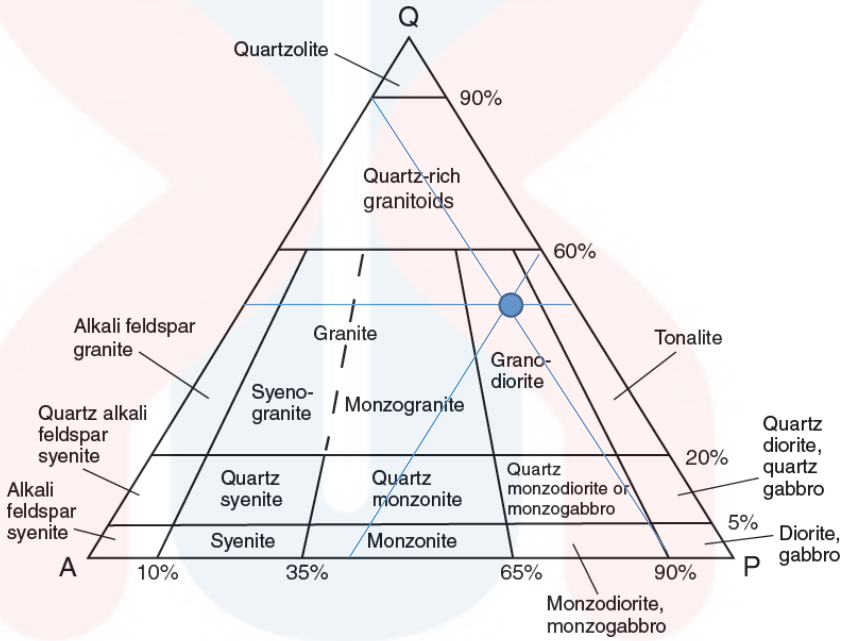

Figure 4.48: QAP diagram of granodiorite (2).

Quartz is the most resistant mineral among the numerous minerals. Quartz is usually found even other minerals had been weathered and decomposed. The quartz is found at N 05° 24’ 23.4” and E 101° 56’ 00.9. It identified as quartz vein intruded to the granodiorite. The size of the quartz is 1.9m in length and 1.0 m in height. It is very hard and difficult to break up. From the observation of thin section, it composed 100% of quartz mineral. The size of quartz minerals range from 0.004mm to 0.2mm. Quartz is low relief and colourless under PPL. The quartz is euhedral in shape. They filled in the pore

space randomly when in liquid state and crystallized later. Figure 4.49 and 4.50 presented the outcrop and hand specimen of quartz respectively. The microscopic image of quartz under XPL and PPL are presented in Figure 4.51 and Figure 4.52 respectively. Table 4.7 showed the mineral composition of quartz.

Figure 4.49: Quartz at N 05° 24’ 23.4”, E 101° 56’ 00.9”.

Figure 4.50: Hand specimen of quartz.

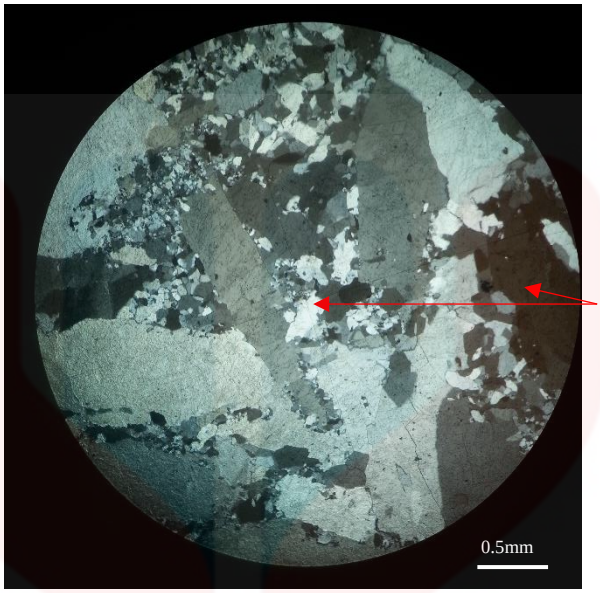

Figure 4.51: Microscopic image of quartz under XPL (4x).

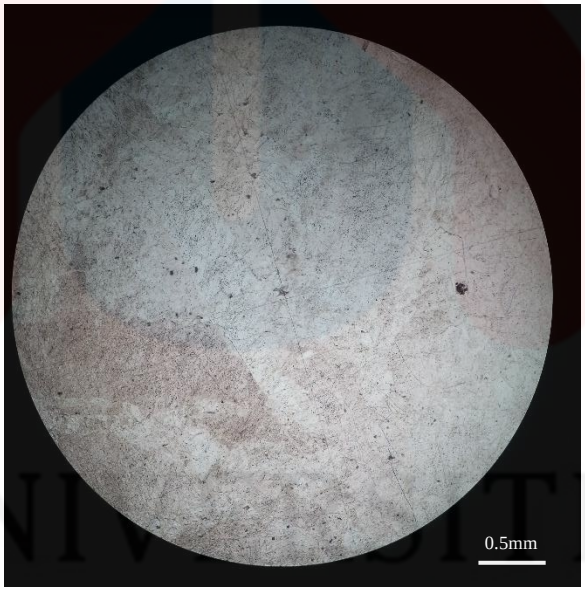

Figure 4.52: Microscopic image of quartz under PPL (4x).

Table 4.7: Mineral composition of quartz.

Composition of mineral	Percentage (%)
Quartz	100

4.3.3 Interbedded Sandstone, Mudstone and Shale

Shale

There are total two sample of shale is taken from the study area. The characteristics of shale is the lamination within the lithology. The coordinate of one of the shale is N 05° 26’ 04.3”, E 101° 56’ 08.9” located at the side of Sungai Balah, Jeli, Kelantan. The outcrop is covered by vegetation. The size of the outcrop is approximately 5m in length. This shale is grey in colour and fine-grained. The lamination is observed from the hand specimen. The shale is Triassic in age according to geological map of Kelantan. Figure 4.53, Figure 4.54 and Figure 4.55 showed the outcrop, hand specimen and lamination of shale at N 05° 26’ 04.3”, E 101° 56’ 08.9”.

Figure 4.53: Outcrop of shale. (Coordinate: N 05° 26' 04.3", E 101° 56' 08.9")

Figure 4.54: Hand specimen of shale.

Figure 4.55: Lamination of shale (1).

Another shale sample is found at N 05° 25’ 18.2”, E 101° 55’ 47.1”. The outcrop is located at the excavated slope. The shale is weathered. The fresh outcrop unable to obtain hence the hand specimen is weathered shale. This shale is brown in colour and fine-grained. It identified as shale due to the lamination structure observed. This shale also believed has an age of Triassic based on geological map of Kelantan. The outcrop, hand specimen and lamination of this shale are presented in Figure 4.56, Figure 4.57 and Figure 4.58 respectively.

Figure 4.56: Outcrop at N 05° 25’ 18.2”, E 101° 55’ 47.1.

Figure 4.57: Hand specimen of shale at N 05° 25’ 18.2”, E 101° 55’ 47.1.

Figure 4.58: Lamination of shale (2).

Mudstone

Mudstone is found at N 05° 25’ 09.2”, E 101° 54’ 45.0”. It is located beside the Sungai Balah and weathered by vegetation. It is fine-grained and light grey in colour. It is composed of mud and the lamination structure is absent. At this location, it also a baking zone between mudstone and acid intrusion. From the geological map, the age of the mudstone is Triassic. Figure 4.59 and Figure 4.60 showed the mudstone outcrop and hand specimen respectively.

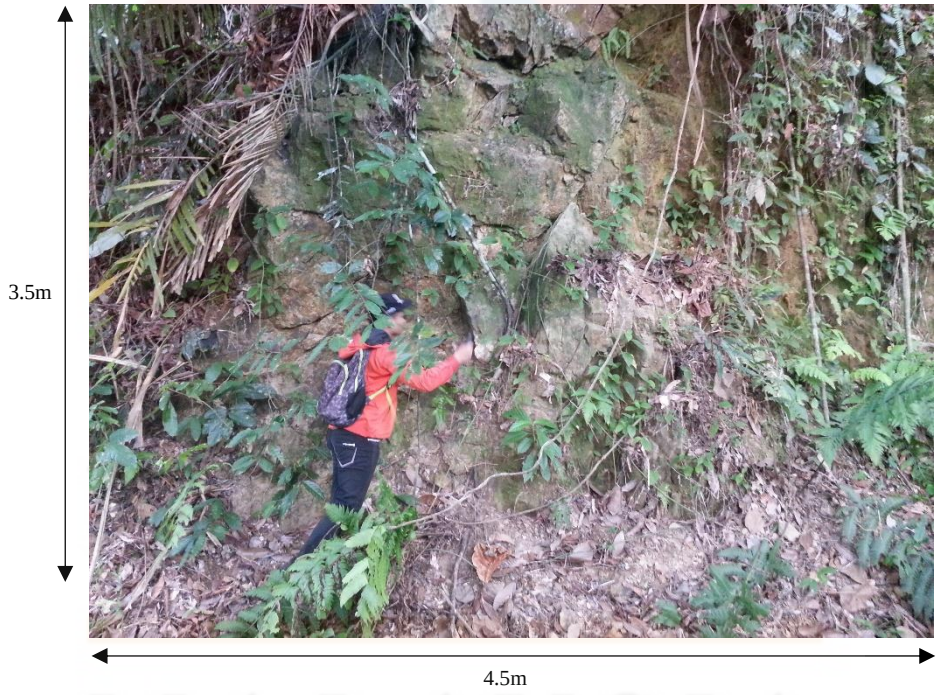

Figure 4.59: Mudstone outcrop at N 05° 25’ 09.2”, E 101° 54’ 45.0”.

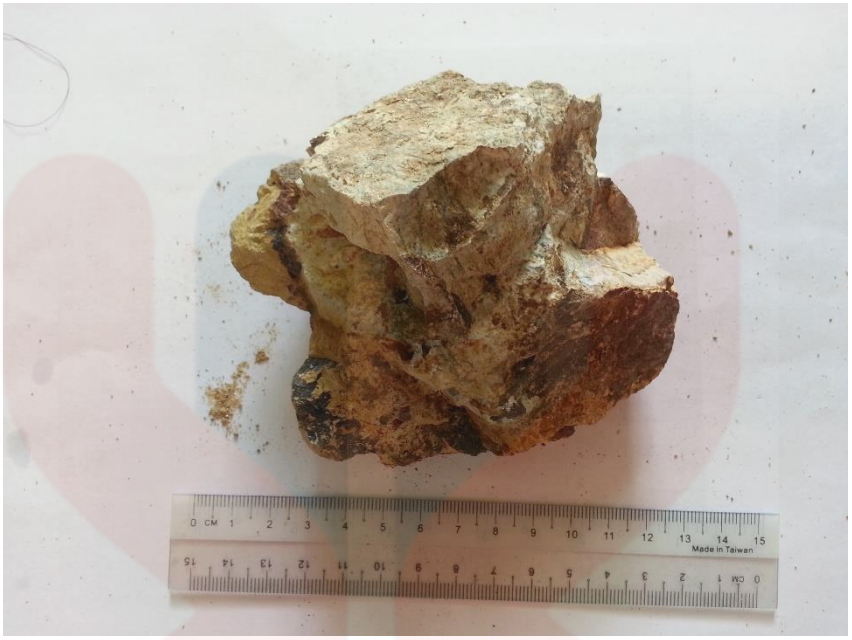

Figure 4.60: Hand specimen of mudstone.

Metasandstone

The metasandstone is found in the middle of Sungai Balah with the coordinate of N 05° 25’ 35.9” and E 101° 56’ 30.8”. From the observation of hand specimen, it is fine grained and grey in colour. The crystalline structure of minerals are observed from the hand specimen. This rock is hard and difficult to break. This metasandstone is Triassic in age. The dominant mineral sandstone observed under microscope is quartz. Other minerals like alkali feldspar, plagioclase and biotite also observed. Besides the minerals, matrix and cement are observed around the grain of minerals. The outcrop of metasandstone is presented in Figure 4.61 and the hand specimen is illustrated in Figure 4.62. Figure 4.63 and Figure 4.64 showed microscopic image of

metasandstone under XPL and PPL. The mineral composition of metasandstone is tabulated in Table 4.8.

Figure 4.61: Outrop of metasandstone in Sungai Balah. (Coordinate: N 05° 25' 35.9", E 101° 56' 30.8")

Figure 4.62: Hand specimen of metasandstone.

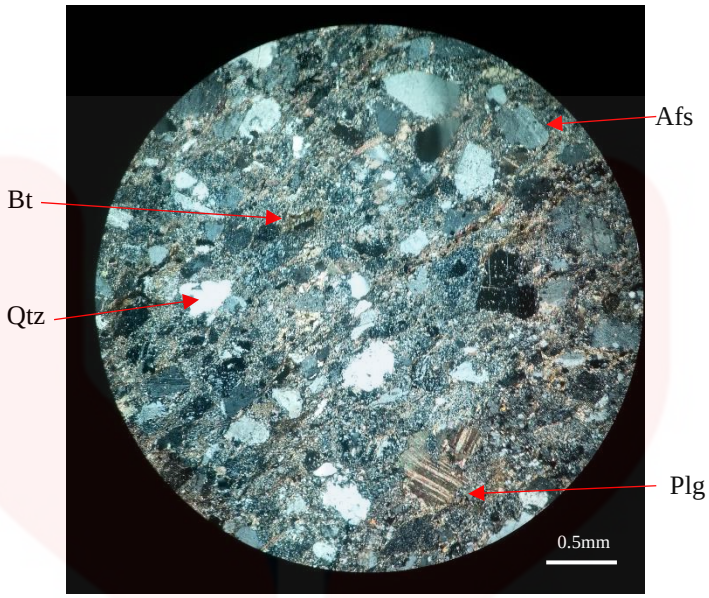

Figure 4.63: Microscopic image of metasandstone under XPL (4x).

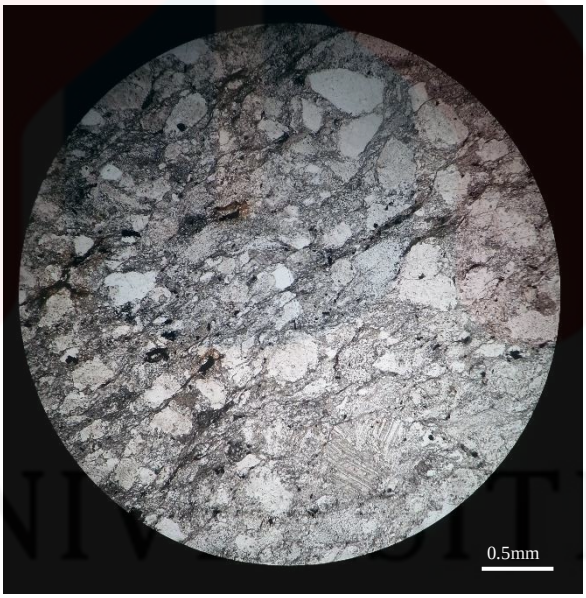

Figure 4.64: Microscopic image of metasandstone under PPL (4x).

Table 4.8: Mineral composition of metasandstone.

Composition of mineral	Percentage (%)
Quartz	60
Alkali feldspar	10
Plagioclase	38
Biotite	2

4.3.4 Granite Intrusion

Fine-Grained Biotite Granite

The fine-grained biotite granite has been went through weathering process caused it leave little part of the outcrop in the excavated slope. The coordinate of this granite is N 05° 25’ 54.2”, E 101° 54’ 29.4”. The surrounding of the outcrop is totally weathered to residual soil. The size of fine-grained granite is 3m in length and 1m in height. This fine-grained biotite granite has an age between Triassic to Late Cretaceous according to Singh *et al*., 1984. It is possibly younger than granite and gneiss and the interbedded sandstone, mudstone and shale. It is belongs to part of the Noring Granite which is the younger lithology of Stong Migmatite Complex.

From the observation of the hand specimen, it is phaneritic in texture and it indicated that this type of rock is an intrusive igneous rock that undergoes slowly cooling process. This rock also composed wholly crystals. The fabric is equigranular although the grain size is almost the same but the grain size of each minerals are slightly different. It is identified as fine grained granite. This outcrop is weathered but it can be observed that it consists of many biotite that black in colour. Other than biotite, quartz, alkali feldspar and plagioclase also observed. The picture of the outcrop is showed in Figure 4.65 and the hand specimen is presented in Figure 4.66.

Figure 4.65: Outcrop of fine-grained biotite granite. (Coordinate: N 05° 25' 24.2", E 101° 54' 29.4")

Figure 4.66: Hand specimen of fine-grained biotite granite.

From the observation of thin section under microscope, the minerals observed are quartz, alkali feldspar and plagioclase. Except the major minerals of granite which are quartz, alkali feldspar and plagioclase. The minor mineral

is biotite that consists around 10% of the total proportion of this type of granite. The biotite is medium relief and brown in colour in both XPL and PPL. All the minerals are euhedral in shape. Quartz, alkali feldspar and plagioclase are colourless under PPL. Figure 4.67 showed the microscopic image of fine-grained biotite granite with labels under XPL and Figure 4.68 presented the microscopic image of fine-grained biotite granite with labels under PPL. Table 4.9 showed the mineral composition of fine-grained biotite granite. The QAP diagram for fine-grained biotite granite is illustrated in Figure 4.69.

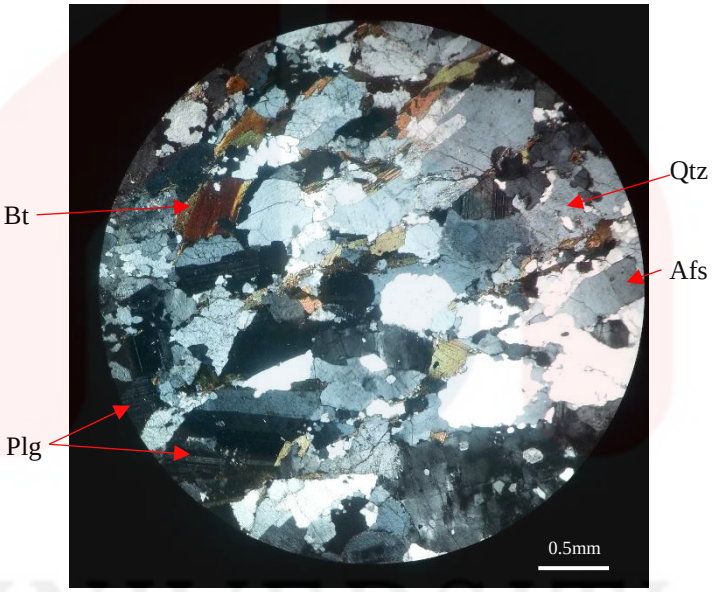

Figure 4.67: Microscopic image of fine-grained biotite granite under XPL (4x).

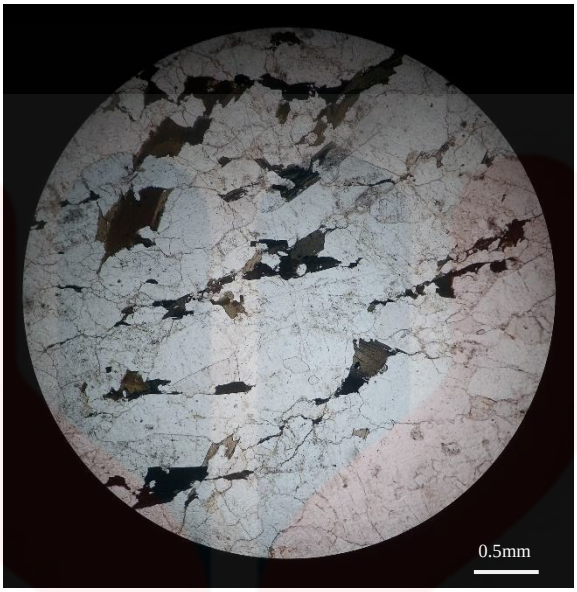

Figure 4.68: Microscopic image of fine-grained biotite granite under PPL (4x).

Table 4.9: Mineral composition of fine-grained biotite granite.

Composition of mineral	Percentage (%)
Quartz	45
Alkali feldspar	25
Plagioclase	20
Biotite	10

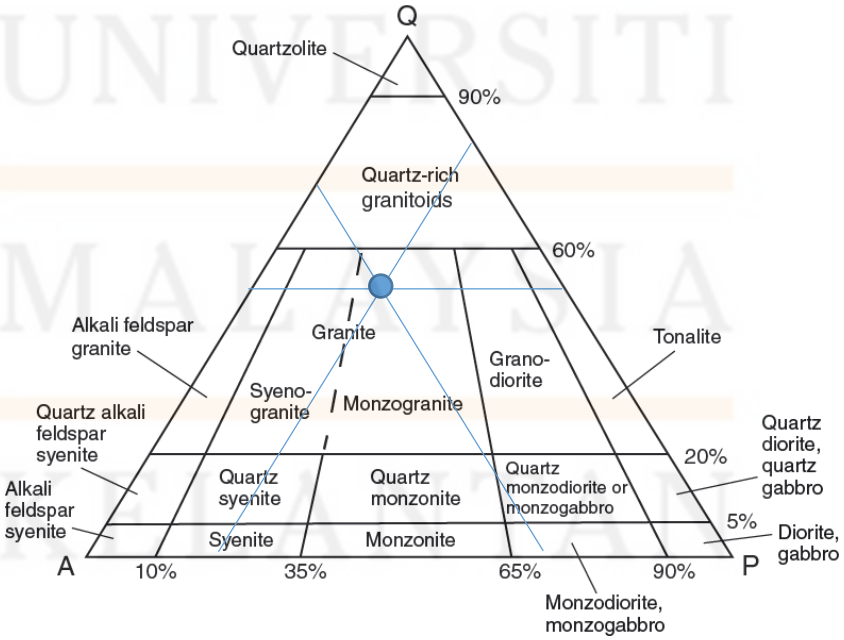

Figure 4.69: QAP diagram for fine-grained biotite granite.

4.3.5 Alluvium

The alluvium is cover the area of Sungai Balah and the area without contour. This indicated this area has no any lithology exist. Within the alluvium area, there is only sediments with variety grain size found. The grain size of the sediments are range from clay to boulders. The boulders are transported from the upstream which composed of igneous and metamorphic rocks. The cloudiness of the river water at the downstream of Sungai Balah indicated it consists of high percentage of fine-grained sediments like silt and clay. Figure 4.70 showed the alluvium area with boulders.

Figure 4.70: Alluvium area with boulders. (Coordinate: N 05° 24' 47.2", E 101° 54' 27.5")

4.3.6 Lithostratigraphy

The plutonic and metamorphic rock are found in one area and the boundary is determined approximately based on the contour pattern. For plutonic rock, the types found are fine-grained biotite granite, fine-grained granite and granodiorite. Sedimentary rocks found are shale and mudstone while metamorphic rocks found are quartzite, coarse-grained quartz-plagioclase gneiss and fine-grained gneiss. Metasedimentary rock also found in the area of sedimentary rock but the quantity is not map able. Therefore there is no metasedimentary rock mapped in geological map. The metasedimentary rock is metasandstone. Besides that, alluvium also categorized due to it covers the area without contour and Sungai Balah.

The fine-grained granite and granodiorite are lie at the zone of Kenerong Leucogranite and fine-grained biotite granite is one part of Noring Granite. Hence, fine-grained granite and granodiorite possibly are older than fine-grained biotite granite. The metamorphic rocks such as quartzite, fine-grained gneiss and coarse-grained quartz-plagioclase gneiss are older than fine-grained granite and granodiorite. The metamorphic rocks are believed have an age of Permo-Carboniferous or Triassic. The fine-grained granite and granodiorite have lower limit age of Carboniferous to Triassic. The metasandstone, shale and mudstone are Triassic in age. The fine-grained biotite granite is a granite intrusion to granite and gneiss and sedimentary rocks in the study area. The latest granite intrusion is range in Triassic to Late Cretaceous. Alluvium is the younger part which is Quaternary in age. All the contacts between the lithologic units are unconformity.

The depositional environment for shale and mudstone are located at deep and calm water due to it is made up if very fine particles that must be deposited in very calm water. The sandstone is formed at the beach or shallow water that has high energy that the environment of shale and mudstone. The sand particles can be deposited in the shallow water due to their grain size and density. Both of these sedimentary rocks are then went through lithification process included cementation and compaction to formed shale, mudstone and sandstone. The stratigraphy column has constructed and showed in Figure 4.71.

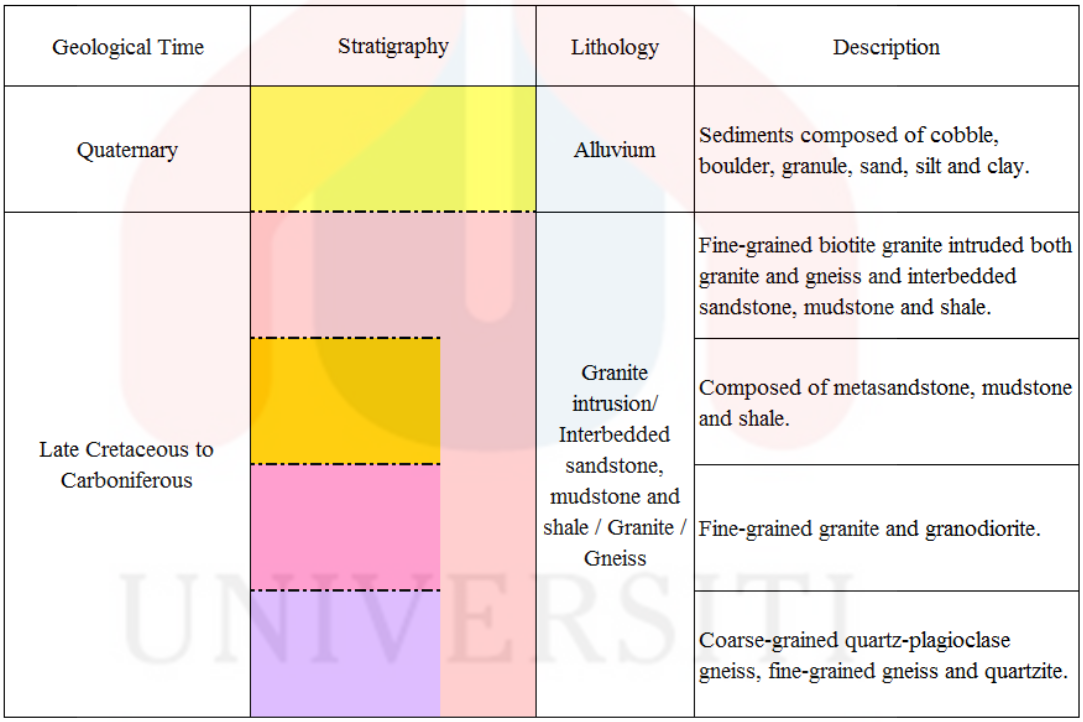

Figure 4.71: Stratigraphy column of Kuala Balah, Jeli, Kelantan.

4.4 Structural Geology

Lineament, fold, fault and joint analysis are discussed in this part. The information is based on the outcrop observed in the field during geological

mapping. The information is analysed by using GeoRose software and Stereonet software.

4.4.1 Lineament Analysis

Caran et al. (1981) defined lineament as a pattern in a photograph, map or model of earth's surface or subsurface of earth which is stratigraphically, structurally or geophysically defined that must be linear, continuous, well expressed and related to features of the solid earth. Fault zones, igneous intrusions, shear zones, valley, fault or fold-aligned hills, streams and coastlines contributed to lineaments.

Lineament can be observed from the aerial photograph, satellite image, terrain map and geological map. Lineament is categorized into two types which are positive lineament and negative lineament. According to Mohd Hashim and Akhir (2010), ridge and range present the positive lineament while negative lineament represent by streams, faults and valleys. The terrain map with label of study area is presented in Figure 4.72 and Figure 4.73 showed lineament in the study area.

The values of the orientation of the lineaments are measured on the terrain map in regional scale. Around 80 readings of lineament have been measured and the orientation of the force that created the lineament are determined based on the rose diagram plotted by GeoRose software. The major orientation of lineament is N 10°W and S 10°E which indicated the main force that deformed this area is from the particular direction. The tension is range

between N 80°E and S 80°W. Figure 4.74 illustrated the orientation of the lineament on the rose diagram with label of forces.

4.4.2 Fold Analysis

Fold is one the geologic structure formed by the deformation. It is results when flat-lying or other undeformed surface is wrapped or deformed into an undulating geologic structure. When two tectonic plates are collide, fold is created on the Earth's crust. Normally folding occurs beneath the Erath where rocks are ductile than at the shallow depths or at the surface. The type of fold included anticline, syncline, monocline, chevron, recumbent and plunging fold.

There only one type of fold observed in the study area. The coordinate of the fold found is N 05° 24' 53.5", E 101° 54' 29.4" and elevation of 85m. The fold observed is anticline fold. Anticline fold is that concave towards older rocks in its centre like an arch. The strike and dip of the two limbs of the fold are 150°/87° and 212°/66° separately. The anticline fold with labels of strike and dip is presented in Figure 4.75.

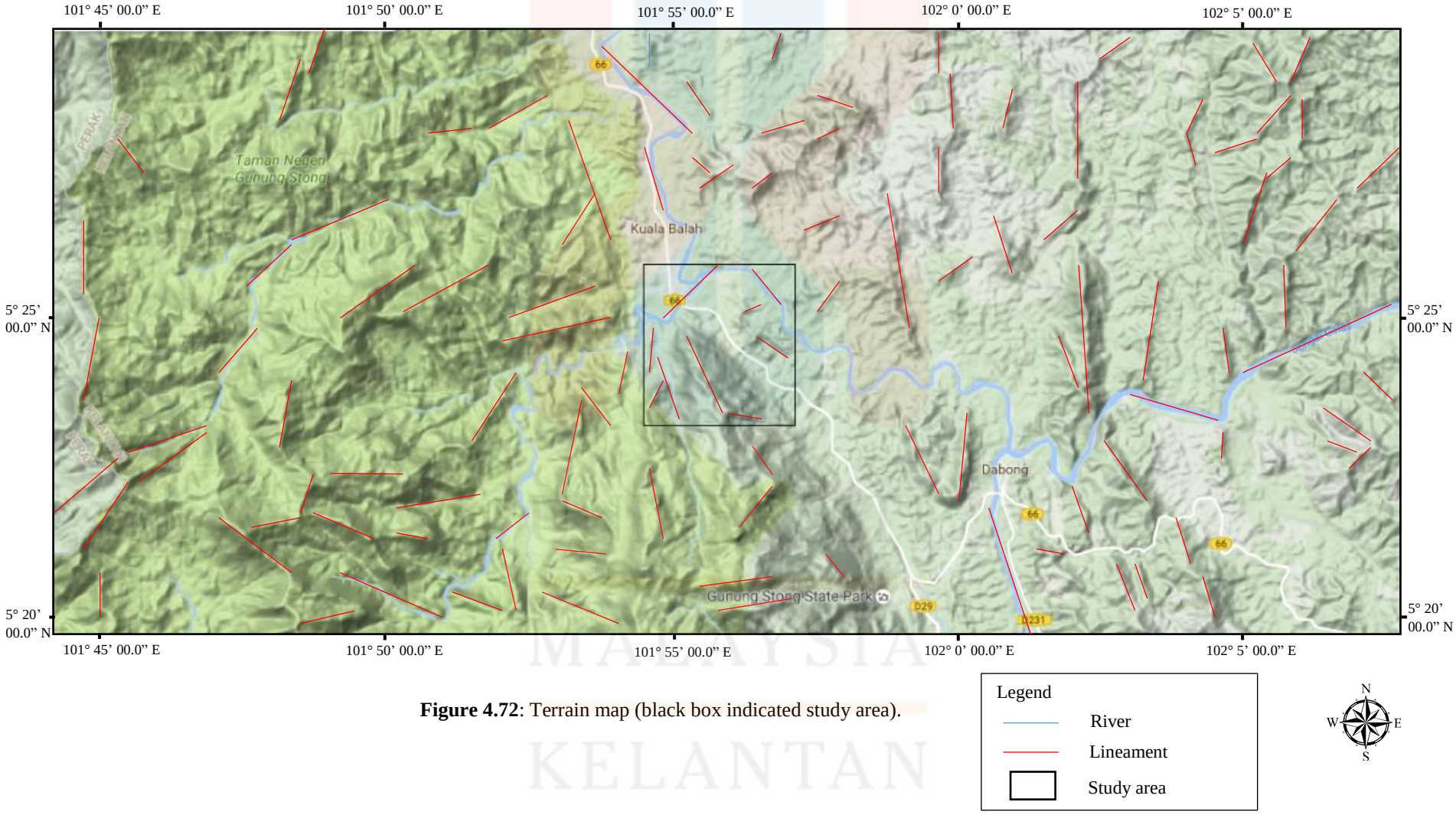

Figure 4.72: Terrain map (black box indicated study area).

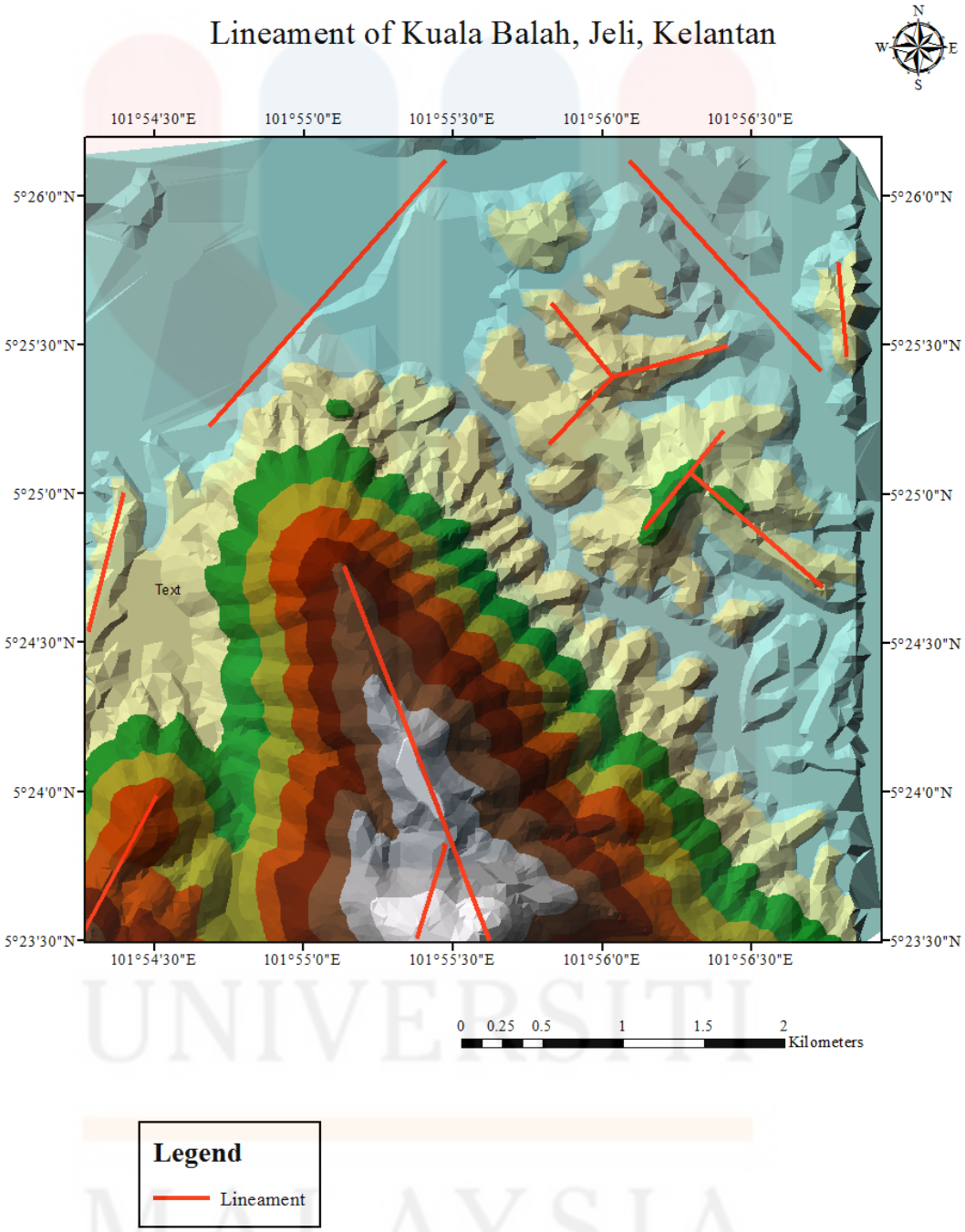

Figure 4.73: Lineament of Kuala Balah, Jeli, Kelantan.

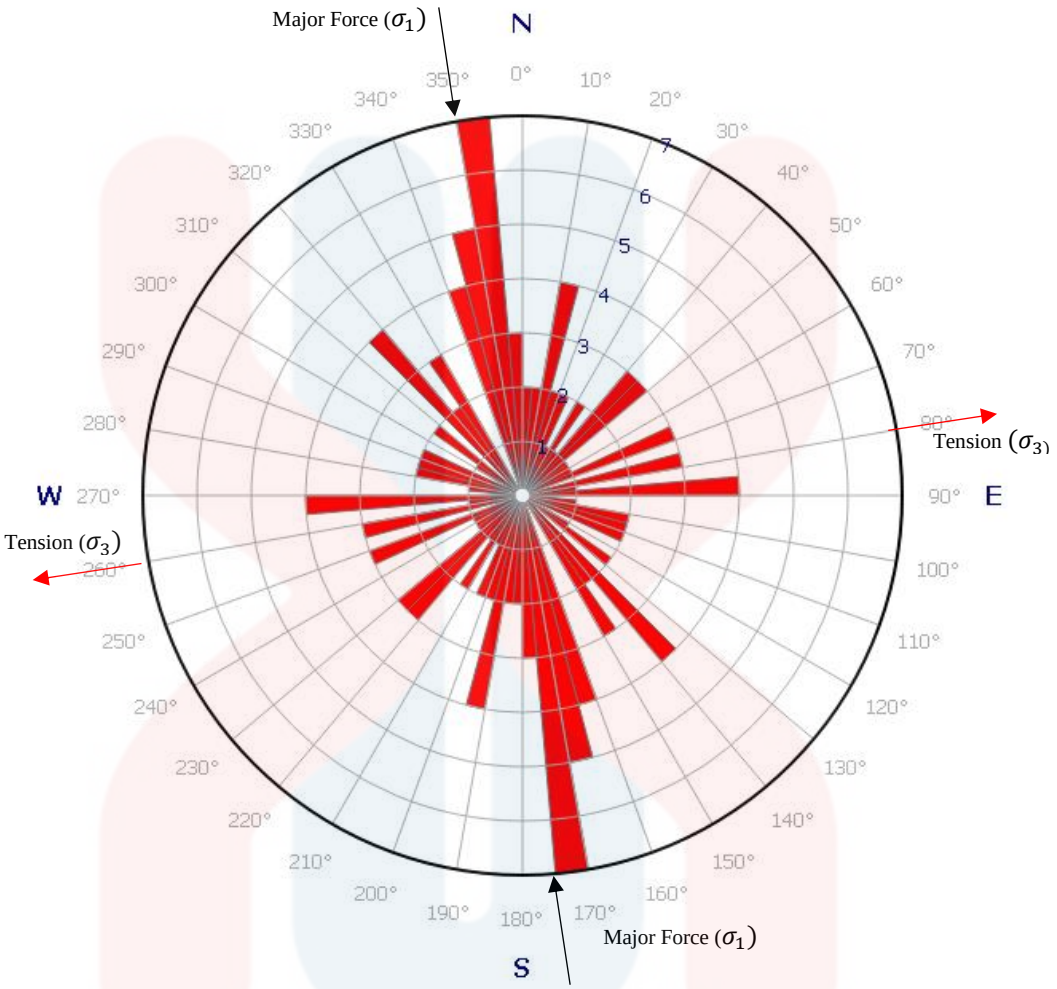

Figure 4.74: Orientation of lineament.

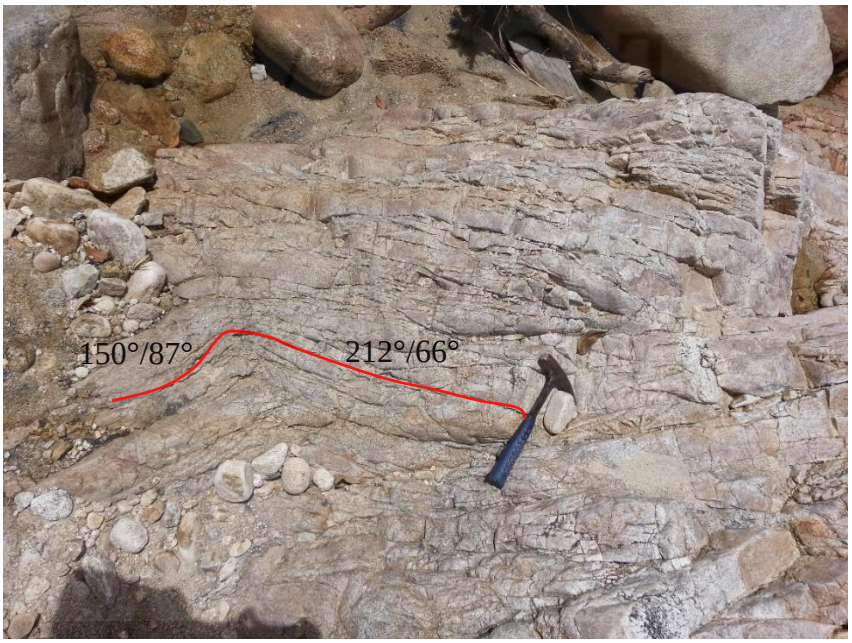

Figure 4.75: Anticline fold. (Coordinate: N 05° 24' 53.5", E 101° 54' 29.4")

From the plot of two planes of the limbs of fold which are 150°/87° and 212°/66°, the intersection point is 322°/64°. The intersection point also known as σ_2. A fold axis passed through the centre pint of the stereonet and the There is two σ_1 for fold which is two direction of forces to deformed the rocks and intersection point between two planes of fold is drawn to determine the minor force created fold which is σ_3. The major forces to create the fold are the edges of two poles of planes of limbs. Directions of σ_1 are 052° and 232° while σ_3 is 142°/26°. Figure 4.76 showed the planes of fold with the labels of σ_1, σ_2 and σ_3.

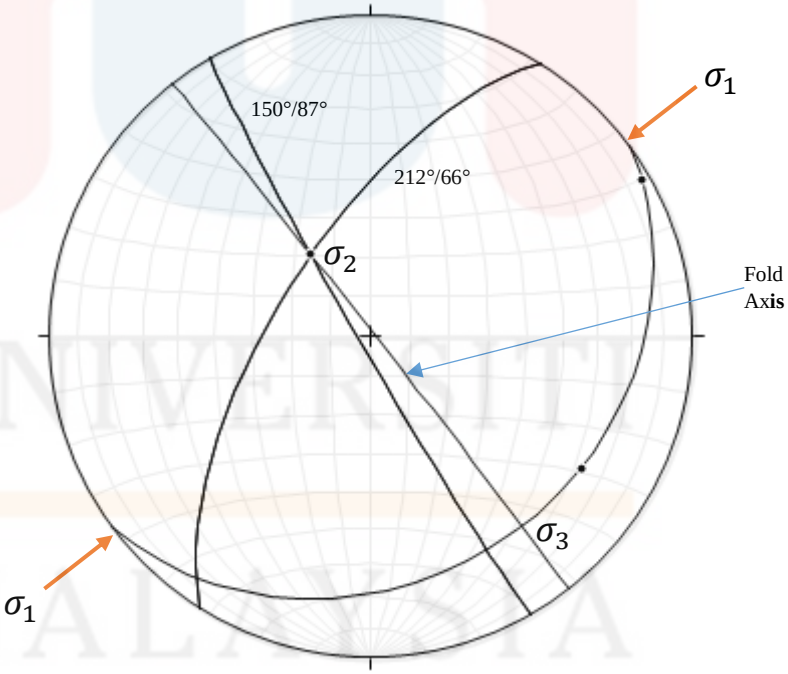

Figure 4.76: Planes of fold.

4.4.3 Fault Analysis

Fault is defined as the fracture zone between the rocks. Fault is classified into several types included dip-slip fault, strike-slip fault, oblique-slip fault, normal fault, reverse fault, and thrust fault. Fault can be formed at all types of rocks due to the deformation. There is only normal fault found in the study area. The strike and dip of the fault is taken.

Normal fault occurred when there is a tension applied and pull apart the rock. The hanging wall moved downward relative to the footwall. The normal faults is found at N 05° 24’ 22.6”, E 101° 55’ 59.5” with elevation of 112m.The Figure 4.77 represented the two normal faults found with label of direction. The strike and dip for normal fault 1 is 330°/79° and 275°/ 70° for the normal fault 2.

Figure 4.77: Normal faults. (Coordinate: N 05° 24' 22.6", E 101° 54' 59.5")

The fault planes of the two normal fault is plotted and the direction of forces are determined based on the stereonet drawn. For fault 1, σ_1, σ_2 and σ_3 are 240°/ 72°, 150°/ 79° and 060°/ 28° respectively. It indicated the major direction of force from 240°/ 72° and it rock extended in the direction of 060°/ 28°. The major force of fault 2 from 185°/ 80° and the tension is 005°/ 10°. The σ_1 is 185°/ 80°, σ_2 is 095°/ 70° and σ_3 is 005°/ 10°. Figure 4.78 and Figure 4.79 presented the plane of normal faults.

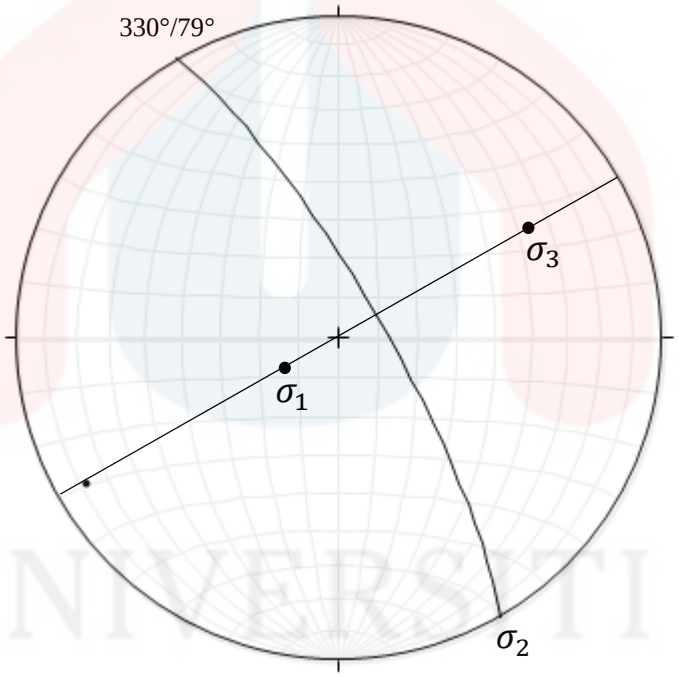

Figure 4.78: Plane of fault 1.

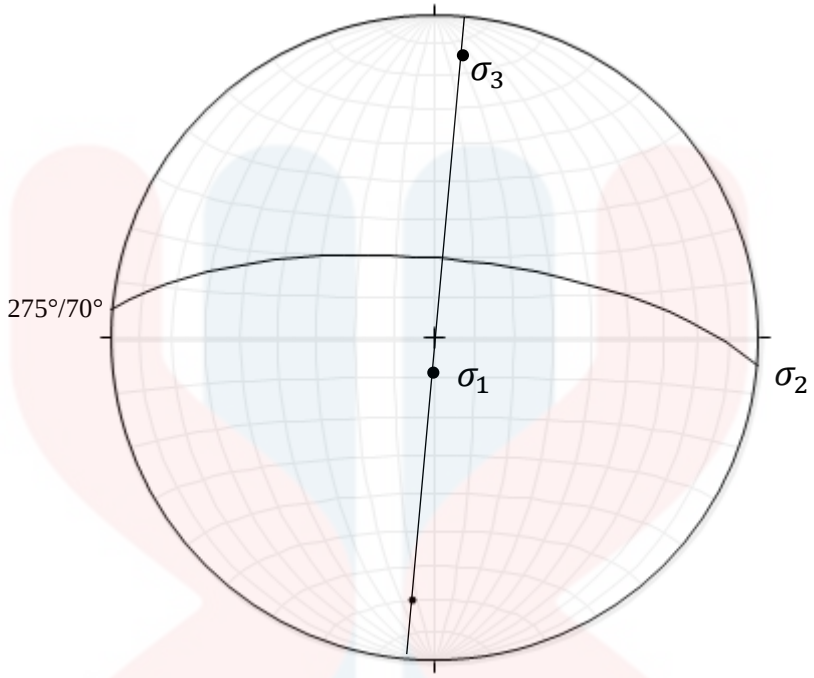

Figure 4.79: Plane of fault 2.

4.4.4 Joint Analysis

Joint is the fracture that shown on the surface of the rock. Joint can be formed on all type of rocks included igneous rock, sedimentary rock and metamorphic rock. In this study area, it is mostly made up of intrusive rock and metamorphic rock which is granite and gneiss. Due to this reason, the joints are abundant on the outcrops found. The joints are belong to non-systematic joints which defined as irregular form, orientation and spacing joints.

The 100 joint readings are taken for each outcrops for the joint analysis by plotting the rose diagram to determine the direction of the force applied on the outcrops. The location map of joint is showed in Figure 4.80.

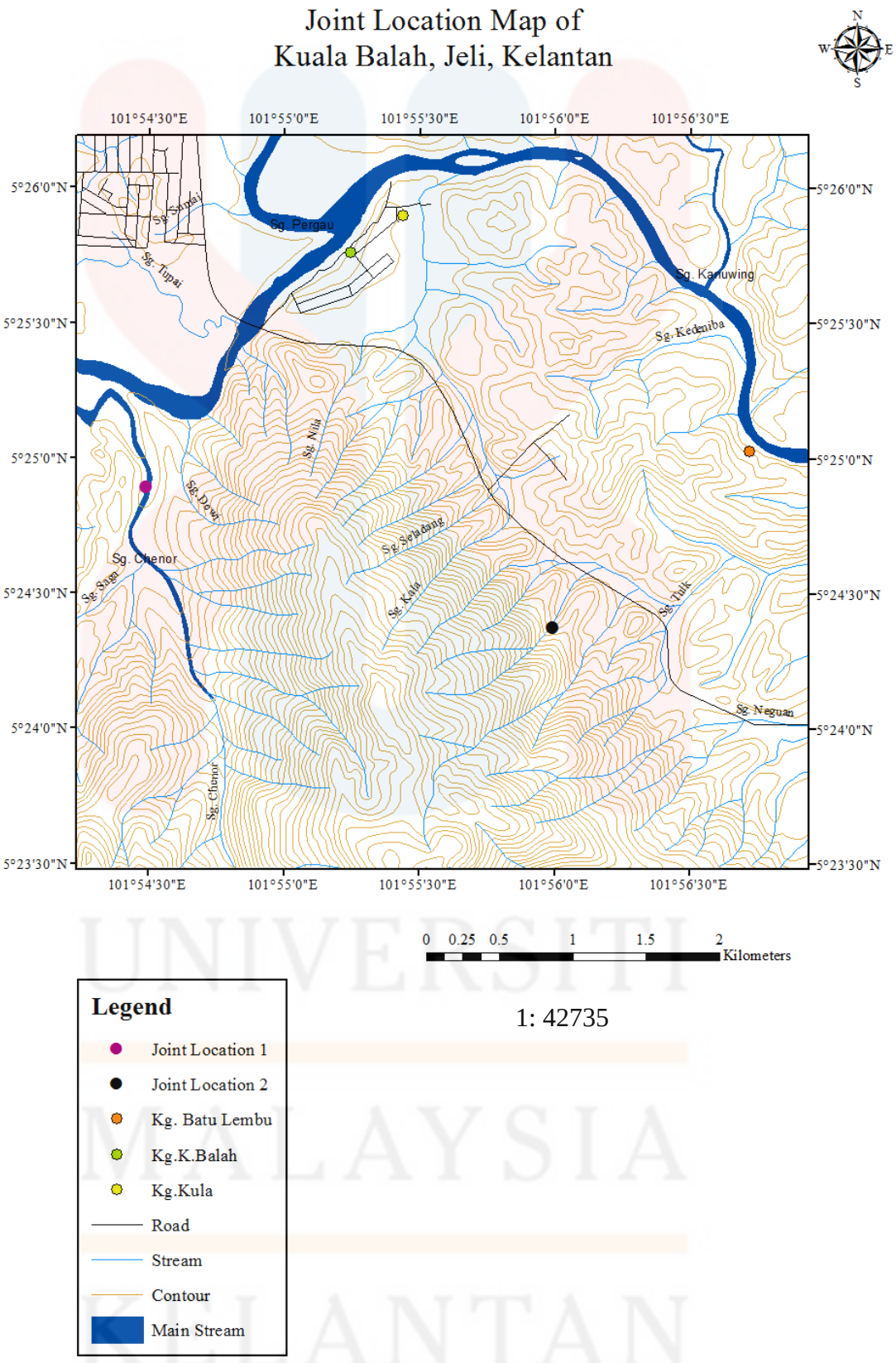

Figure 4.80: Joint location map of Kuala Balah, Jeli, Kelantan.

Outcrop 1

The location of outcrop 1 found with the coordinate N 05° 24’ 53.5”, E 101° 54’ 29.4” and elevation of 85m. It is located in the river named Sungai Balah. From the readings collected, there are total 17 readings in the range of N 20° E to N 25°E. The second most readings collected are N 15° E to N 20° E, N 25° E to N 30° E and N 30° E to N 35° E. For this case, it indicated that the major force to create the joints is from the direction of N 27.5° E and its opposite direction which is S 27.5° W. These two directions also known as σ_1 which is the main direction of force to create the joints. The pictures of outcrops are shown in Figure 4.81 and 4.82. The 100 readings of joints are tabulated in Table 4.10. The interpretation done by GeoRose Software in form of rose diagram with σ_1 is presented in Figure 4.83.

Figure 4.81: Outcrop 1 for joint analysis (1). (Coordinate: N 05° 24' 53.5", E 101° 54' 29.5")

Figure 4.82: Outcrop 1 for joint analysis (2). (Coordinate: N 05° 24' 53.5", E 101° 54' 29.5")

Table 4.10: 100 readings of joints of outcrop 1.

200°	110°	345°	184°	214°	197°	182°	215°	215°	210°
215°	88°	203°	208°	203°	200°	208°	214°	198°	208°
203°	290°	201°	174°	204°	220°	195°	245°	224°	156°
202°	20°	200°	200°	211°	180°	235°	200°	197°	178°
295°	170°	210°	178°	187°	229°	225°	205°	202°	175°
272°	178°	190°	194°	230°	224°	214°	244°	198°	155°
165°	168°	184°	200°	175°	200°	215°	209°	188°	185°
152°	168°	209°	202°	174°	203°	215°	205°	208°	199°
163°	152°	214°	195°	160°	193°	220°	250°	185°	154°
173°	195°	209°	199°	192°	212°	213°	220°	193°	170°

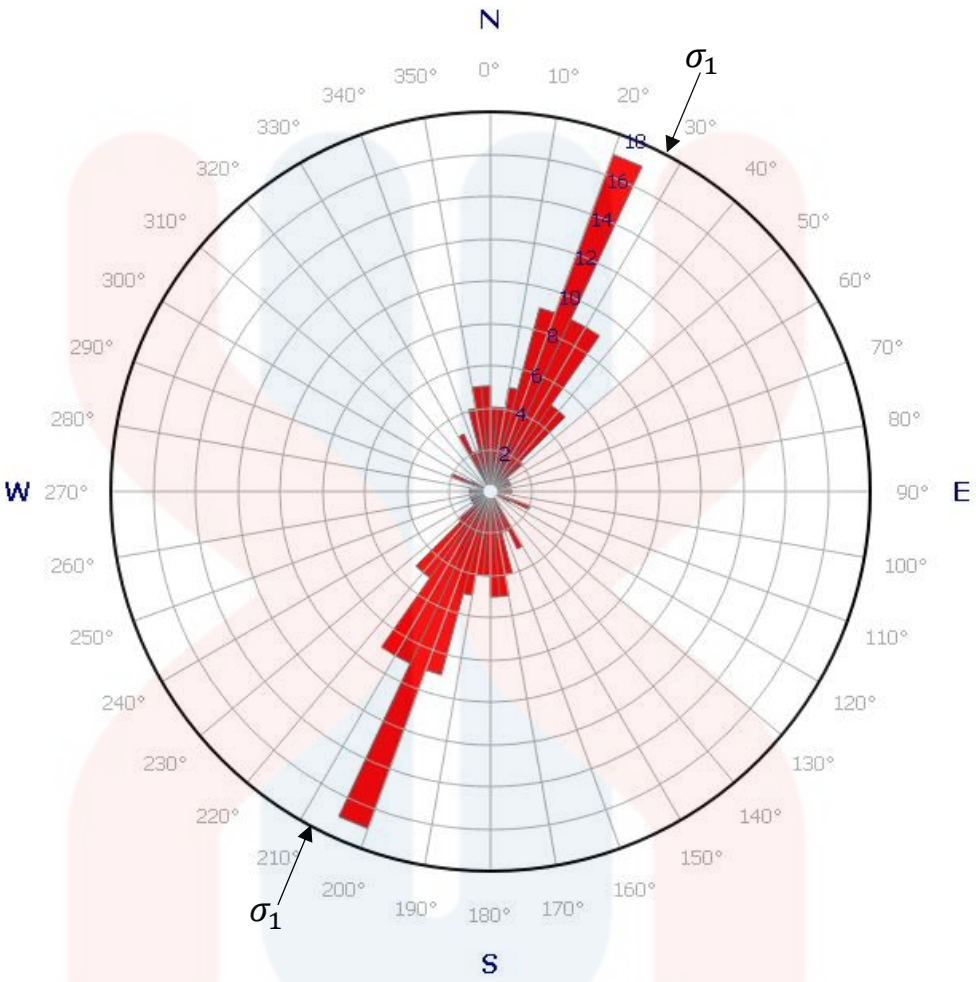

Figure 4.83: Rose diagram for outcrop 1.

Outcrop 2

Outcrop 2 is found at N 05° 24’ 22.6”, E 101° 55’ 59.5” and elevation of 112m. It is located in the rubber plantation area. This outcrop formed a waterfall but with less water. From the reading, there are 12 readings in the range of N 60° E to N 65° E while there are 2 ranges contain 7 readings which are N 75° W to N 80° W and N 75° E to N 80° E. From the two range, N 75° W to N 80° W is not use in the joint analysis because it is excess 90° than the

highest range of readings. The middle point of N 75° E to N 80° E is N 77.5° E is use for the analysis with the highest range of readings. Based on the interpretation for joint analysis of outcrop 2, the force is from N 70° E and its opposite direction S 70° W. N 70° E and S 70° W are the major force direction of deformation which is σ_1. The Figure 4.84 shows the outcrop 2 which composed of granodiorite. The reading of joints are tabulated in Table 4.11 and the Figure 4.85 showed the rose diagram for outcrop 2 with label of σ_1.

Figure 4.84: Outcrop 2 for joint analysis. (Coordinate: N 05° 24' 22.6", E 101° 55' 59.5")

Table 4.11: 100 readings of joints for outcrop 2.

222°	256°	215°	283°	293°	34°	289°	69°	261°	155°
217°	255°	226°	279°	311°	8°	261°	254°	243°	117°
202°	253°	219°	279°	334°	86°	248°	252°	230°	121°
228°	206°	214°	239°	109°	278°	288°	285°	237°	120°
244°	204°	237°	154°	372°	257°	109°	106°	275°	200°
248°	254°	235°	161°	117°	63°	267°	52°	267°	261°
251°	258°	280°	253°	243°	42°	244°	234°	244°	203°
249°	260°	295°	208°	328°	288°	243°	237°	243°	236°
249°	247°	211°	200°	221°	240°	240°	231°	240°	87°
259°	214°	284°	146°	352°	243°	256°	270°	256°	56°

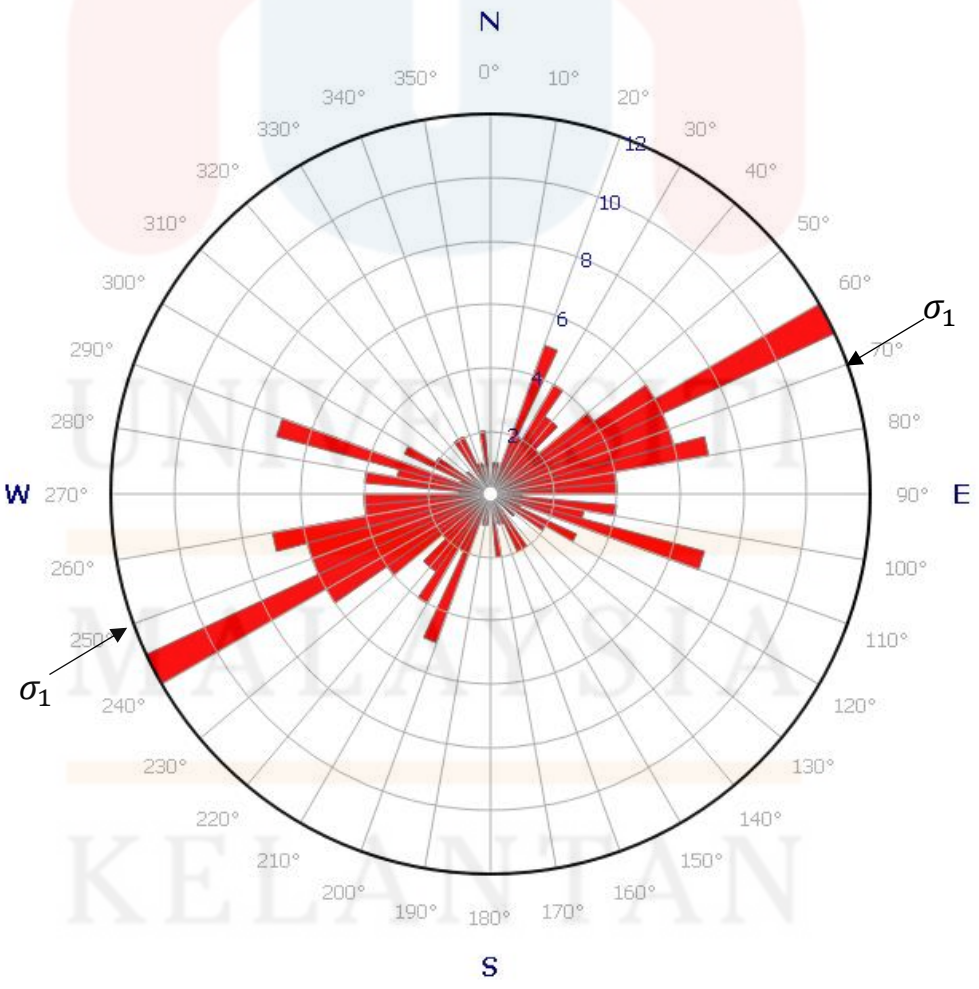

Figure 4.85: Rose diagram for outcrop 2.

4.4.5 Structural Mechanism

From all the orientation of forces that created the lineaments, folds, faults, and joints, the direction of force that formed these structures is determined. The major forces for lineaments are from N 10°W and S 10°E while the major forces for fold are N 52°E and S 52°W. The faults has the major forces from N 60°E, S 60°W, N 5°E and S 5°W. For the joints, the major force are from directions of N 25°E, S 25°W, N 65°E and S 65°W.

Based on all the major direction of forces, the direction of the forces for the deformation are range in N 5°E to N 65°E and S 5°W and S 65°W. With the rose diagram of all the strike readings of lineaments, fold, faults and joints, the major forces of the structural deformation are N 27.5°E and S 27.5°W. The major forces is the compression force to the deformation. The tensions are toward the direction of N 62.5°W and S 62.5°E. These are the minor forces where the geologic material or structure extend towards these directions. Figure 4.86 illustrated the major forces and tension of the structural deformations in Kuala Balah, Jeli, Kelantan.

4.5 Historical Geology

Historical geology included the origin and formation of the geological features and Earth. In the study area, the metamorphic rocks such as quartzite, fine-grained gneiss and coarse-grained quartz-plagioclase gneiss are formed due to the metamorphism are the oldest rocks. It followed by granite and granodiorite which intruded to the Earth's surface and formed the mountain

after long period of intrusion. After the intrusion, the granite and granodiorite went through several deformation processes which formed the geological structures such as fault, fold and joints. The sedimentary rocks are formed during the uplift and intrusion of granite and granodiorite. The later granite intrusion intruded both gneiss, quartzite, granite, granodiorite and sedimentary rocks such as sandstone, mudstone and shale. Sandstone had been went through metamorphism process which has not complete and formed metasandstone. After a long period, the rocks are weathered and become sediments and hence formed an alluvium area.

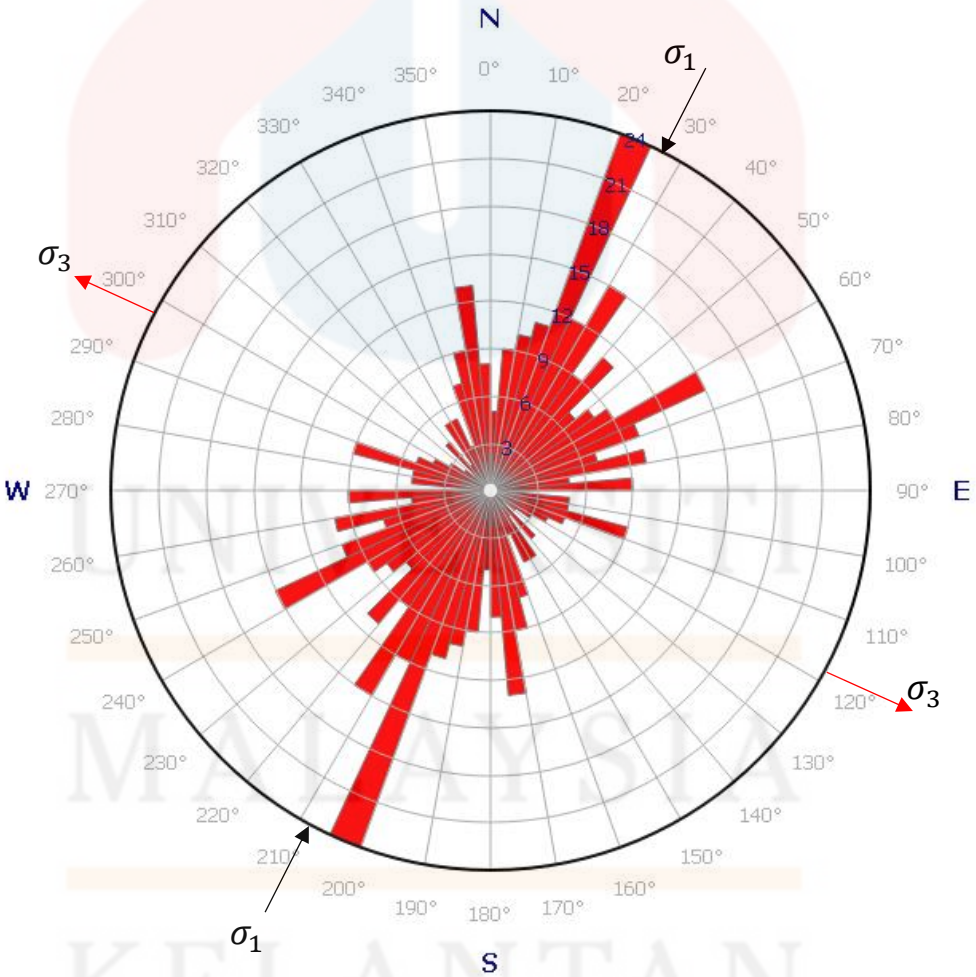

Figure 4.86: Forces of structural deformation in Kuala Balah, Jeli, Kelantan.

Chapter 5

SOIL CUT-SLOPE ASSESSMENT

5.1 Introduction

In Chapter 5, it discussed about the specification of this research which is soil cut-slope assessment. It divided into two parts, slope failure inventory and soil cut-slope stability analysis.

Slope failure inventory is the summary of several parameters measured and observed for the cut-slope failure available within 25 km^2 of the study area. The parameters included slope geometry, mode / type of failure, failure geometry, weathering grade, origin of soil / rock, causes of failure, type of slope stabilization protection available and the vegetation cover.

For the soil cut-slope stability analysis, the properties of soil selected slope such as moisture content, liquid and plastic limit, particle size distribution and soil strength are done by laboratory tests. The classification of the soil is carried out based on the properties of soil. Factor of safety of the selected slope is calculated by using Slope/W software with Morgenstern-Price method. The unit weight of soil is calculated from the soil sample and the cohesion is determined by soil strength test.

5.2 Slope Failure Inventory

Slope failure inventory is a table that recorded various parameters of the slope failure characteristics. The basic parameters included slope geometry, mode / type of failure, failure geometry, weathering grade, cause of failure and type of stabilization protection. The additional parameters such as origin of rock / soil and vegetation cover is added to the inventory constructed.

Slope geometry is the physical measurement of the slope included height, length and angle of slope. There are up to fifteen types of slope failure available. In the study area, the slope failure is dominantly made up of soil and predominantly fine soil. The failure geometry measured are height and length.

There are total six weathering grade range from fresh rock to residual soil with number one to six. Slope failure is caused by numerous factors such as geological condition, morphological causes and human causes. Slope failure in the study area is mostly caused by high water content within soil particles from rainfall.

Some of the slope had been protected with stabilization protection because of the previous failure. The slope still failed after the stabilization protection is done. The origin or rock or soil is determined according to the gravel found in the soil. It is important to relate the reason of failure with the type of rock. The vegetation cover is the vegetation that grew on the slope as protection or natural growth.

There are total eight slope failure observed in the study area. The characteristics is taken for each slope. The length of slopes are range between

11m to 186m and 10m to 20m in height. The angle of slopes are around 35° to 46°. The type of failures are mostly rotational slide of soil. The other types of failure are included slump and earth slide.

The failure geometry of slopes are various in length and height. The length of failure is between 8.2m to 29.5m and 3m to 16m in height. This indicated the size of failures are small to large but the depth of the failures are not measured. The dominant weathering grade is five and only one of the slope has weathering grade of four.

The origin of soil are mostly shale and the soil of a slope is decomposed from granite. This can be observed from the remaining rock in the slopes. The triggering factors that caused the slope failure in this area are rainfall and weathering. All the slopes are protected by vegetation and some of the slopes have Gabion retaining wall as stabilization protection at the bottom of slopes. Almost all the slopes are covered by different type vegetation. The vegetation cover percentage is high for these slopes.

The summary of the slope failure characteristics is tabulated and showed in Table 5.1 and 5.2 as slope failure inventory. The location of soil cut-slope failures is presented in Figure 5.1. Figures of cut-slope failure are attached in APPENDIX-E.

Table 5.1: Slope failure inventory in Kuala Balah, Jeli, Kelantan.

Slope number, coordinate & elevation	Slope geometry	Mode / type of failure	Failure geometry	Weathering grade	Origin of soil / rock	Causes of failure	Type of slope stabilization protection	Vegetation cover of failure
1. N 05° 24' 44.0" E 101° 55' 54.2" 71m	L = 34m H = 10m ∡ = 46°	Rotational Slide	L = 29.5m H = 8m	4	Shale	Rainfall	Vegetation	90%
2. N 05° 24' 41.9" E 101° 55' 55.1" 77m	L = 99.5m H =15 m ∡ = 40°	Rotational Slide	L = 10m H = 12m	5	Shale	Weathering & Rainfall	Vegetation & Gabion retaining wall	20%
3. N 05° 24' 41.9" E 101° 55' 55.1" 77m	L = 99.5m H = 15m ∡ = 40°	Rotational Slide	L = 30m H = 10m	5	Shale	Weathering & Rainfall	Vegetation & Gabion retaining wall	30%
4. N 05° 24' 33.1" E 101° 56' 07.3" 61m	L = 11m H = 24m ∡ = 45°	Rotational Slide	L = 10m H = 16m	5	Shale	Weathering & Rainfall	Vegetation & Gabion retaining wall	50%
5. N 05° 24' 09.3" E 101° 56' 26.5" 70m	L = 14m H = 10m ∡ = 40°	Rotational Slide	L = 8.2m H =3m	5	Shale	Weathering & Rainfall	Vegetation	30%
6. N 05° 24' 00.6" E 101° 56' 45.0" 59m	L = 186m H = 20m ∡ = 35°	Rotational Slide	L = 25.7m H = 16m	5	Shale	Weathering & Rainfall	Vegetation	30%
7. N 05° 24' 25.3" E 101° 56' 22.1" 56m	L = 68.5m H = 31m ∡ = 40°	Rotational Slide	L = 26.8m H = 20m	5	Granite	Weathering & Rainfall	Vegetation	70%
8. N 05° 24' 25.5" E 101° 56' 20.9" 62m	L = 50m H = 23m ∡ = 40°	Rotational Slide	L = 15.6m H = 15m	5	Shale	Weathering & Rainfall	Vegetation	80%

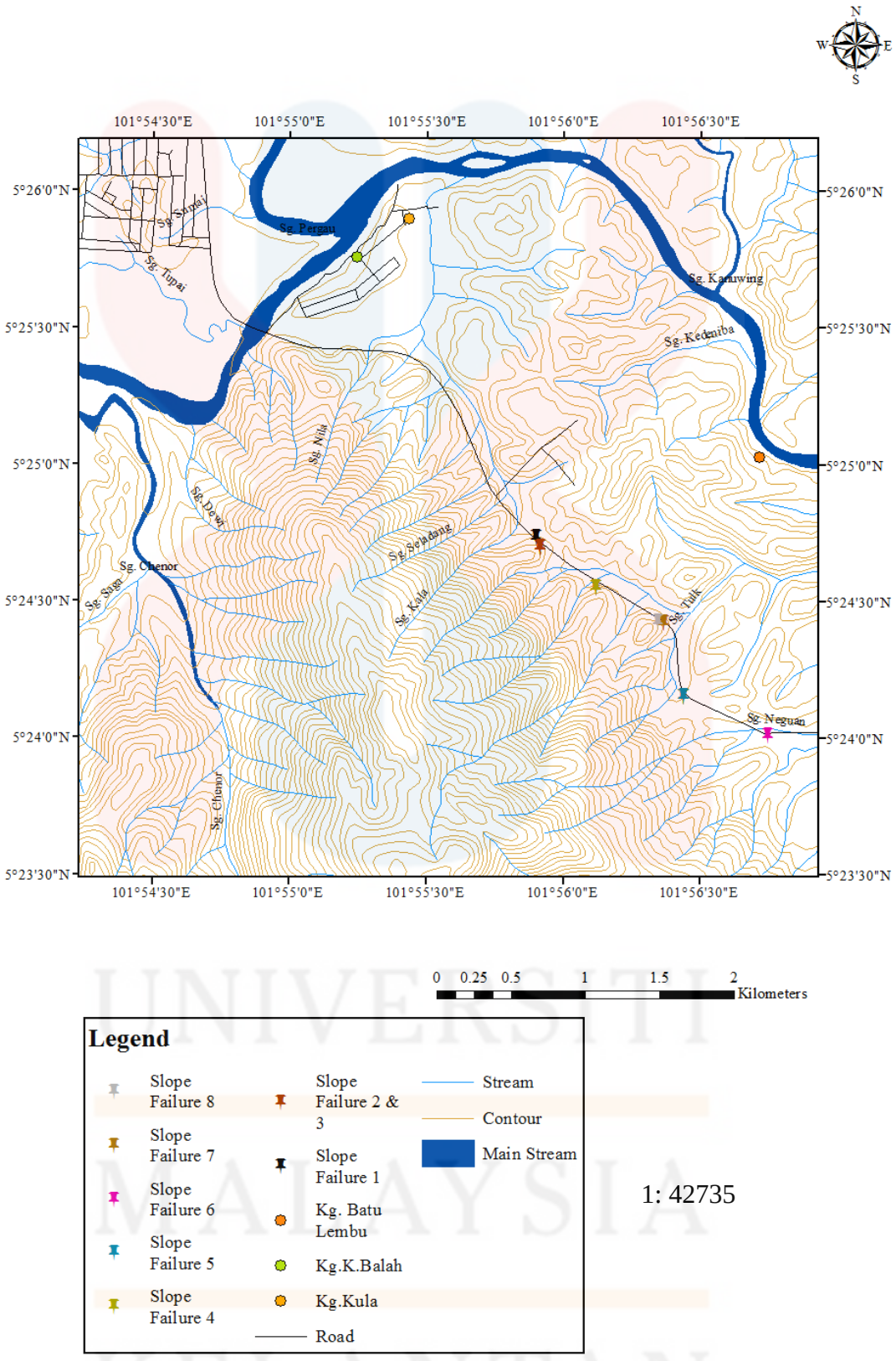

Figure 5.1: Location of soil cut-slope failure in Kuala Balah, Jeli, Kelantan.

5.3 Soil Cut-Slope Stability Analysis

The moisture content, liquid and plastic limits, particle size distribution and soil strength of soil is determined by laboratory test. Particle size distribution of soil is carried out by sedimentation by pipette analysis method. Laboratory vane shear strength test is done by determined the undrained shear strength of soil. These tests are significant for the classification of soil for the slope stability analysis. The factor of safety of stable slope is more than 1.0.

There are only total of four slopes are selected for the determination of slope stability analysis. The soil samples are took from both stable slope and fail slope. The fail slope is the failure area of the slope while the stable slope is the area without failure. The stable slope included the top of the slope and the surrounding area of the failure slope.

The map of selected slopes is showed in Figure 5.2. The details of the soil samples took from the selected slopes are tabulated in Table 5.2. In APPENDIX-F, the pictures of the laboratory tests are enumerated.

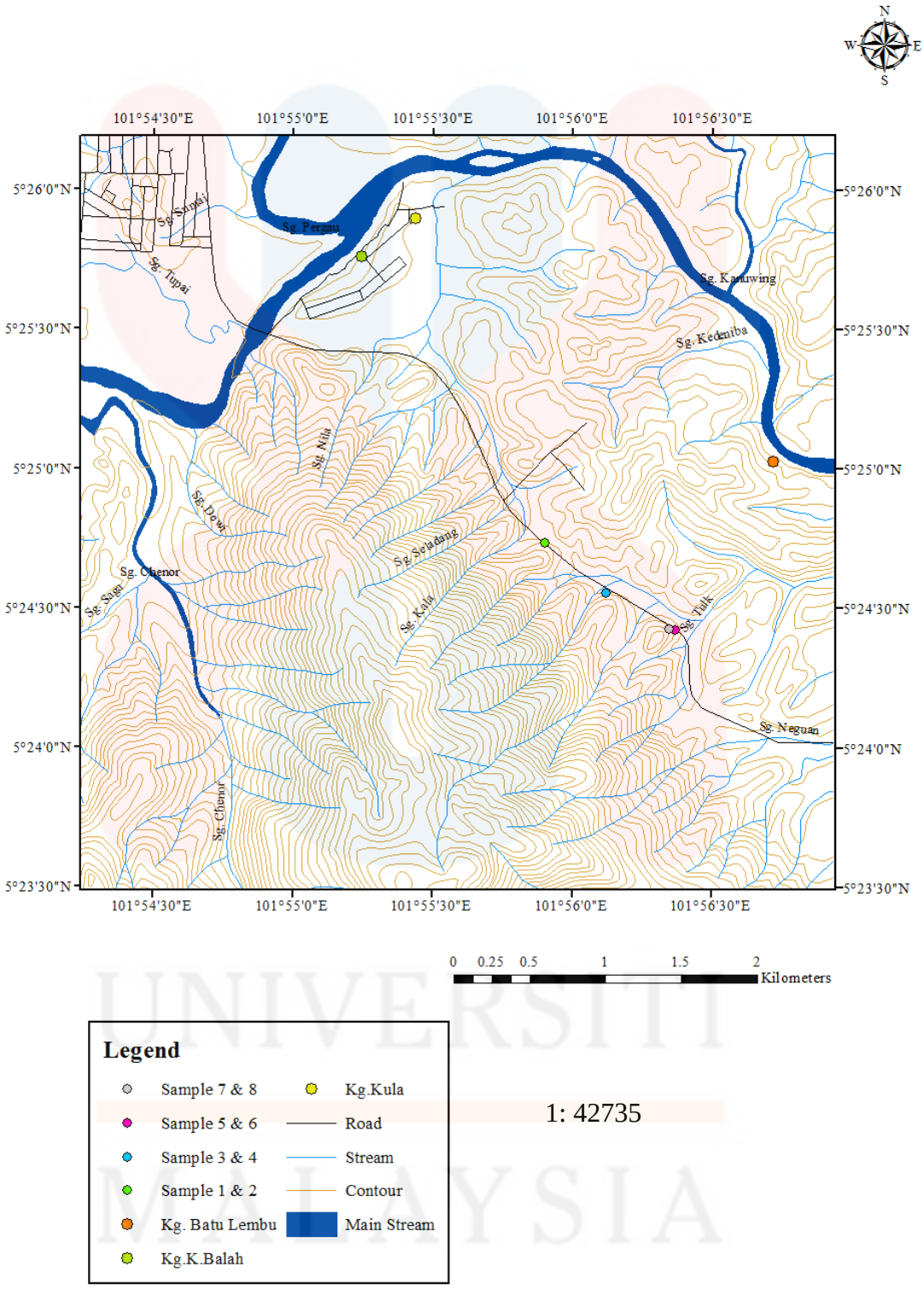

Figure 5.2: Soil sample location of soil at Kuala Balah, Jeli, Kelantan.

Table 5.2: List of soil sample.

No. of sample	Coordinate & Elevation	Description
1	N 05° 24'44.0" E 101° 55' 54.2" 71m	Stable Slope
2	N 05° 24'44.0" E 101° 55' 54.2" 71m	Fail Slope
3	N 05° 24' 33.1" E 101°56' 07.3" 85m	Stable Slope
4	N 05° 24' 33.1" E 101°56' 07.3" 61m	Fail Slope
5	N 05° 24' 25.3" E 101°56' 22.1" 87m	Stable Slope
6	N 05° 24' 25.3" E 101°56' 22.1" 56m	Fail Slope
7	N 05° 24' 25.5" E 101°56' 20.9" 85m	Stable Slope
8	N 05° 24' 25.5" E 101°56' 20.9" 62m	Fail Slope

5.3.1 Moisture Content

In the stable slope, the moisture content is higher than in the failure slope. The sample took from the top of stable slope or the inclined stable slope while the sample of failure slope is took from the failure plane. The water seep into the soil is more effectively at horizontal location compared to the incline plane.

Due to this reason, the moisture content in the stable slopes are higher and they may fail once excess the limit of the water they can effort. In the results, three slopes has higher moisture content at stable location than at failure plane. One of the slope has high moisture content at failure plane than

stable plane is because two of the sample is took from the incline plane of slope. Logically, the water content must be higher in failure plane than stable plane if the sample are both took at inclined plane.

Other than that, at slope location of soil sample 1 and 2 the weathering grade is lower than other slopes. This reduced the porosity and permeability of the soil and bedrock. From the comparison of the moisture content for eight soil samples took from 4 slopes. Location of soil sample 5 and 6 is underlain by granitic rock which then decomposed to soil. The granitic material has higher porosity and permeability compared to sedimentary material.

According to the results, the moisture content of soils are range from 23.38% to 41.69%. Sample 3, 5 and 7 are took from the stable slope have higher moisture content which is 41.45%, 41.69% and 41.13%.

The results of moisture content of the selected soil samples are tabulated in Table 5.3.

Table 5.3: Result of moisture content from laboratory test.

No. of sample	Mass of container, W1 (g)	Mass of wet soil & container, W2 (g)	Mass of dry soil & container, W3 (g)	Mass of dry soil, W3-W1 (g)	Mass of water loss, W2-W3 (g)	Moisture content (%)
1	6.594	327.400	266.671	259.717	60.729	23.38
2	6.614	319.278	252.515	245.901	66.763	27.15
3	6.314	318.188	226.805	220.491	91.383	41.45
4	6.659	324.962	239.690	233.031	85.272	36.59
5	7.038	352.840	251.087	244.049	101.753	41.69
6	7.634	309.323	232.553	224.919	76.770	34.13
7	7.302	343.979	245.859	238.557	98.120	41.13
8	6.915	348.350	250.024	250.024	91.411	36.56

5.3.2 Plastic and Liquid Limits

Plastic limit and liquid limit is used to measure the plasticity index of fine-grained soil with the moisture content in the soil. Negative value to zero of plasticity index indicated the soil is non-plastic, less than seven is low plastic soil, seven to seventeen indicated moderate plastic and more than seventeen showed the soil is highly plastic.

From the results of plastic limit from laboratory test, the plastic limit of all soil samples are range from 34.5 to 51.5. The liquid limit is 41.2 to 74.7. By calculation of plasticity index, it range from 5.1 to 35.4.

The results of plasticity index showed the soils are low plastic to highly plastic. It is only one soil sample is low plastic while four of the soils are moderate plastic and three of them are highly plastic.

Plasticity index is significant in slope stability because it is linked to consistency and the soil strength. It acts as an indicator for potential slope instability problems. The higher plasticity index indicated the poor performing soils. The high plasticity index also showed the moisture content of soil is high and the soil strength is reduced and lead to the unstable conditions.

The results of plastic limit, liquid limit and plasticity index are tabulated in Table 5.4. The details results of plastic limit and liquid limit are attached in APPENDIX-G.

Table 5.4: Results of plastic limit, liquid limit and plasticity index.

No. of sample	Liquid limit	Plastic limit	Plasticity index
1	41.2	36.1	5.1
2	46.3	34.5	11.8
3	66.9	51.5	15.4
4	52.0	43.2	8.8
5	74.7	36.4	38.3
6	73.4	50.9	22.5
7	73.8	38.4	35.4
8	54.2	45.9	8.3

5.3.3 Particle Size Distribution

In the particle size distribution, it divided into six categories which are boulder, cobble, gravel, sand, silt and clay. It is significant to classify the type of soil instead for the slope stability stabilization and protection.

The pipette analysis if carried out for the sedimentation test for fine-grained soil which the soil particles can passed through No.200 sieve (75μm). Based on the Stokes Law, the velocity of the soil sedimentation is affected by the size, weight, shape of soil and viscosity of liquid.

According to the laboratory test carried out, all of the soils contained more than 50 % of silt and only small amount of clay. It can be observed that the fine sand content at the stable slope is higher than at the failure slope. The silt content is higher in failure slope compared to the stable slope.

Particle size distribution is correlated to the speed of the water or other fluid flows through the soil. For the soil has more sand, the water or fluid can moves faster because there is more pore space between the sand particles. The water can loss from the soil easily. In contrast, the higher content of silt or clay, the water or fluid moves slowly between the particles due to the silt and clay are compacted and there is less or no occupancy for the water or fluid. Once, the water is occupied the pore space, the water difficult to escape and cause the water content increase.

The summary of the particle size distribution of the soil is tabulated in Table 5.5. The graph of grain size against cumulative percentage is presented in Figure 5.3 and graphs of grain size against cumulative percentage for each sample are attached in APPENDIX-H.

Table 5.5: Summary of laboratory test of particle size distribution.

No. of sample	Fine sand (%)	Coarse silt (%)	Medium silt (%)	Fine silt (%)	Clay (%)
1	62.0	27.9	2.0	8.0	0.1
2	37.9	60.5	0.3	0.2	1.1
3	47.8	19.6	17.7	8.9	6.0
4	41.4	48.7	1.0	7.9	1.0
5	41.3	5.9	27.2	18.4	7.2
6	56.3	42.7	0.9	0	0.1
7	33.1	21.5	25.5	9.5	10.4
8	28.7	64.2	6.2	0.4	0.5

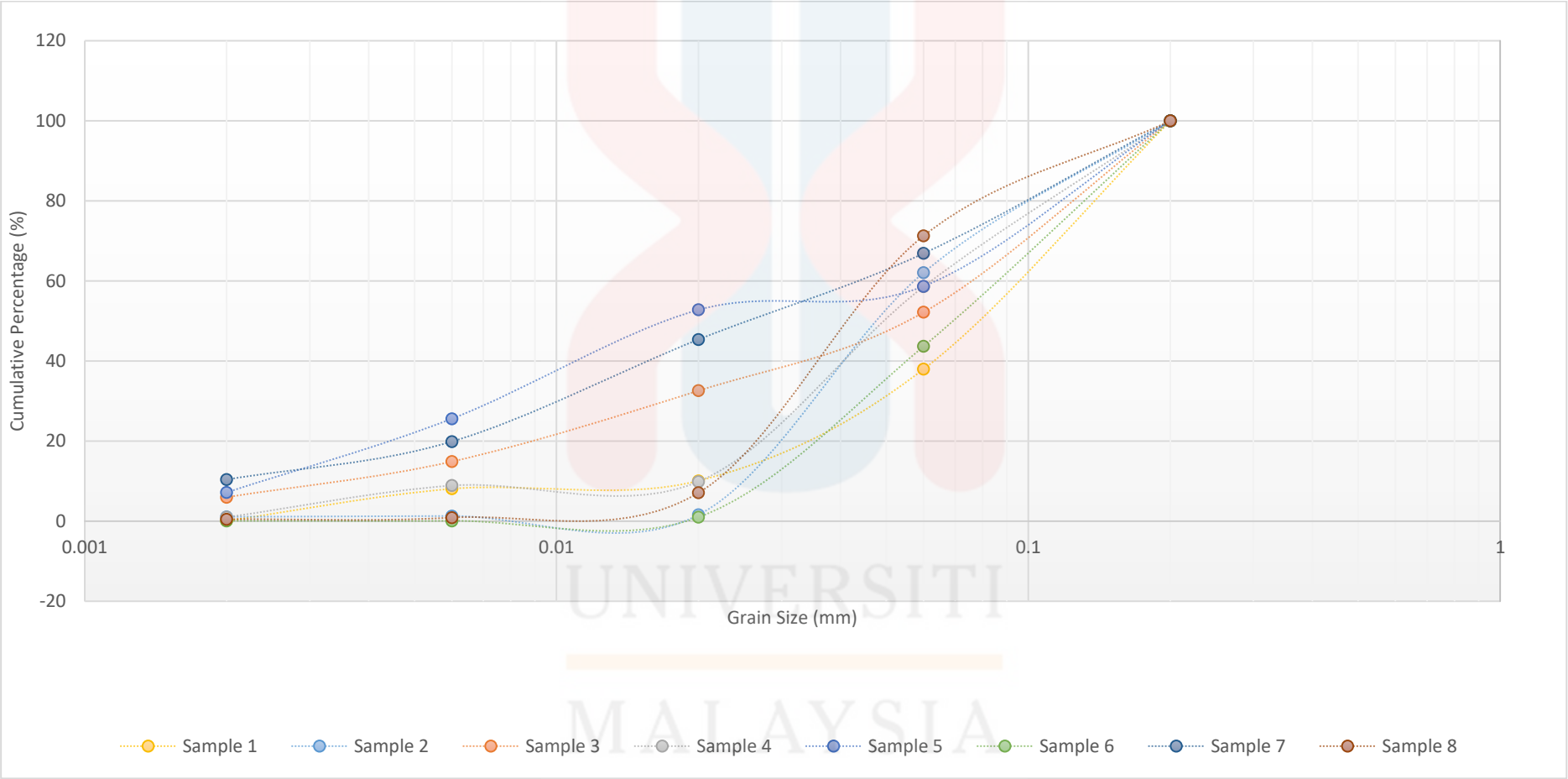

Figure 5.3: Graph of grain size against cumulative percentage.

5.3.4 Soil Strength

The soil strength is determined by obtain the average undrained shear strength in laboratory using laboratory vane shear strength test for this research. For undrained shear strength, the pore pressure changes are replace the volume changes, hence the effective strength is similar to the stress in the field.

This test cannot be conducted with the dry soil. Water is added to the soil to increase the moisture content to carry out the test. The size of vane blade used is 12mm in diameter and 24mm in height. Shear strength is used to measure the maximum stress that the soil can sustain. The undrained shear strength of soil is correlated to the moisture content of soil. The moisture content can lower the strength of soil by increase the pore water pressure in the soil. This can be proved by the sample 6 which has the moisture content of 83.2%, the average undrained shear strength is the lowest among all the samples which is 4.99 kPa. The average undrained shear strength is calculated by using the formula and the torque is obtained based on the graph of spring calibration. The results of average undrained shear strength and moisture content are tabulated in Table 5.6.

Results of laboratory vane shear strength and graph of spring calibration are attached in APPENDIX-I.

Table 5.6: Average undrained shear strength and moisture content.

No. of sample	Average undrained shear strength, C_u (kPa)	Moisture content (%)
1	46.84	44.6
2	6.65	42.3
3	26.06	43.5
4	31.04	85.6
5	15.24	49.4
6	4.99	83.2
7	18.01	42.9
8	17.74	62.2

5.3.5 Classification of Soil

The soils are classified based on the particle size distribution, liquid limit and plasticity index. Classification of soil is important in the foundation of slope stability. Some soil is not suitable for the construction due to poor performing characteristics.

Based on the particle size distribution, all the soil samples are contain high percentage of silt. Most of the soil has little composition of clay. All of the soil samples are grouped into fine-grained soils due to there is more than 50% of the particles passed through No.200 (75μm) sieve.

From the classification according to ASTM Standards flow chart, these soils are grouped into three different types which are sandy silty clay, sandy lean clay and sandy fat clay. The fat clay indicated the soil is high in plasticity.

From the classification of soil by plasticity chart, these soils are categorized into three types. The types of soil are silt, clay of high plasticity (fat clay), and silt of high plasticity (elastic silt). There is slightly different between two classifications. According to the classifications, the angle of friction of soil can be determined depend on the typical value of different types of soil. Table 5.7 showed the summary of classification of soil.

5.3.6 Factor of Safety by Morgenstern- Price Method

Before calculated the factor of safety, the characteristics of soil such as unit weight, cohesion and angle of friction must be obtained. For calculation of factor of safety, only the stable slopes are selected. The unit weight is obtained by ratio of the mass of soil to the volume of soil that get from the field. The in-situ unit weight is calculated as fast as possible after the sample is took in the laboratory. The cohesion of soil is obtained from the laboratory vane shear strength test. From the test, undrained shear strength is calculated and used as the cohesion of soil. The angle of friction is considered as zero for the undrained shear strength criterion. Table 5.8 presented the characteristics of selected slopes.

Table 5.7: Summary of classification of soil.

No. of sample	Fine sand (%)	Silt (%)	Clay (%)	Plasticity index, PI	Liquid Limit (%)	Type of soil (ASTM Standards)	Type of soil based on plasticity chart
1	62.0	37.9	0.1	5.1	41.2	Sandy Silty Clay	ML
2	37.9	61	1.1	11.8	46.3	Sandy Lean Clay	ML
3	47.8	46.2	6.0	15.4	66.9	Sandy Fat Clay	MH
4	41.4	57.6	1.0	8.8	52.0	Sandy Fat Clay	MH
5	41.3	51.5	7.2	38.3	74.7	Sandy Fat Clay	CH
6	56.3	43.6	0.1	22.5	73.4	Sandy Fat Clay	MH
7	33.1	56.5	10.4	35.4	73.8	Sandy Fat Clay	CH
8	28.7	70.8	0.5	8.3	54.2	Sandy Fat Clay	MH

Table 5.8: Characteristics of selected slopes.

Slope number, coordinate & elevation	Unit weight, γ (kN/m^3)	Cohesion, c (kPa)	Angle of friction, φ (°)
1 N 05° 24'44.0" E 101° 55' 54.2" 71m	14.95	46.84	0
2 N 05° 24' 33.1" E 101°56' 07.3" 85m	12.26	26.06	0
3 N 05° 24' 25.3" E 101°56' 22.1" 87m	17.15	15.24	0
4 N 05° 24' 25.5" E 101°56' 20.9" 85m	16.34	18.01	0

Slope 1

Slope 1 is 10m in height from the bottom of the slope. The slope angle is 46°, unit weight is 14.95 kN/m^3, undrained shear strength is 46.84 kPa and zero degree for angle of friction. This slope has been fail and covered by vegetation. The soil sample is took from the part of the slope with is stable. From the analysis, the lowest factor of safety is 2.548. It indicated the slope is stable and it might not fail if there is no disturbance. The factor of safety for stable slope beside the residential area should more than 1.4 which this area is safe for the residential. Figure 5.4 showed the slope model of slope 1 with the lowest factor of safety.

Slope 2

Slope 2 is 27m in height included the 3m depth below the surface of Earth. This slope is 45° of slope angle. The unit weight calculated is 12.26 kN/m^3 and the undrained shear strength from laboratory vane shear strength test is 26.06 kPa after the calculation. The angle of friction for the undrained shear conditions is equal to zero degree. Based on the analysis by Slope/ W, the lowest factor of safety for this slope is 0.620 which indicated this is a failure slope. The mitigation has been done for this slope but it still fail after heavy rainfall. The typical value of factor of safety for this slope is 1.2 due to it located at the roadside. The slope model with critical slip surface is illustrated in Figure 5.5.

Slope 3

This slope is 31m in height from the bottom edge of the slope. The angle of slope is 40 degree. It has 17.15 kN/m^3 of unite weight, undrained shear strength of 15.25 kPa and zero degree of angle of friction. The lowest factor of safety for this slope defined is 0.339 which is lower than lowest limit of the usual range of factor of safety. Slip surface is categorised as shallow slip surface due to it slip on the slope. The typical factor of safety for the slope along the roadside is 1.2. This slope is a failure slope located at the roadside on Malaysia Federal Route 66. Figure 5.6 showed the slope model 3 with factor of safety of 0.339.

Slope 4

This slope is located beside slope 3 but the height is slightly different. The height of this slope from the bottom edge of slope is 23m and 40 degree in angle of slope. Unit weight for the soil of this slope is 16.34 kN/m^3, 18.01 of undrained shear strength and zero degree of angle of friction. This slope has fail and located beside the major road. The factor of safety determined is 0.452 which is much lower than the typical value for the slope (1.2). Since this slope is far away from the main road, it does not affected the accessibility along the road. The slope model for slope 4 with critical slip surface is illustrated in Figure 5.7.

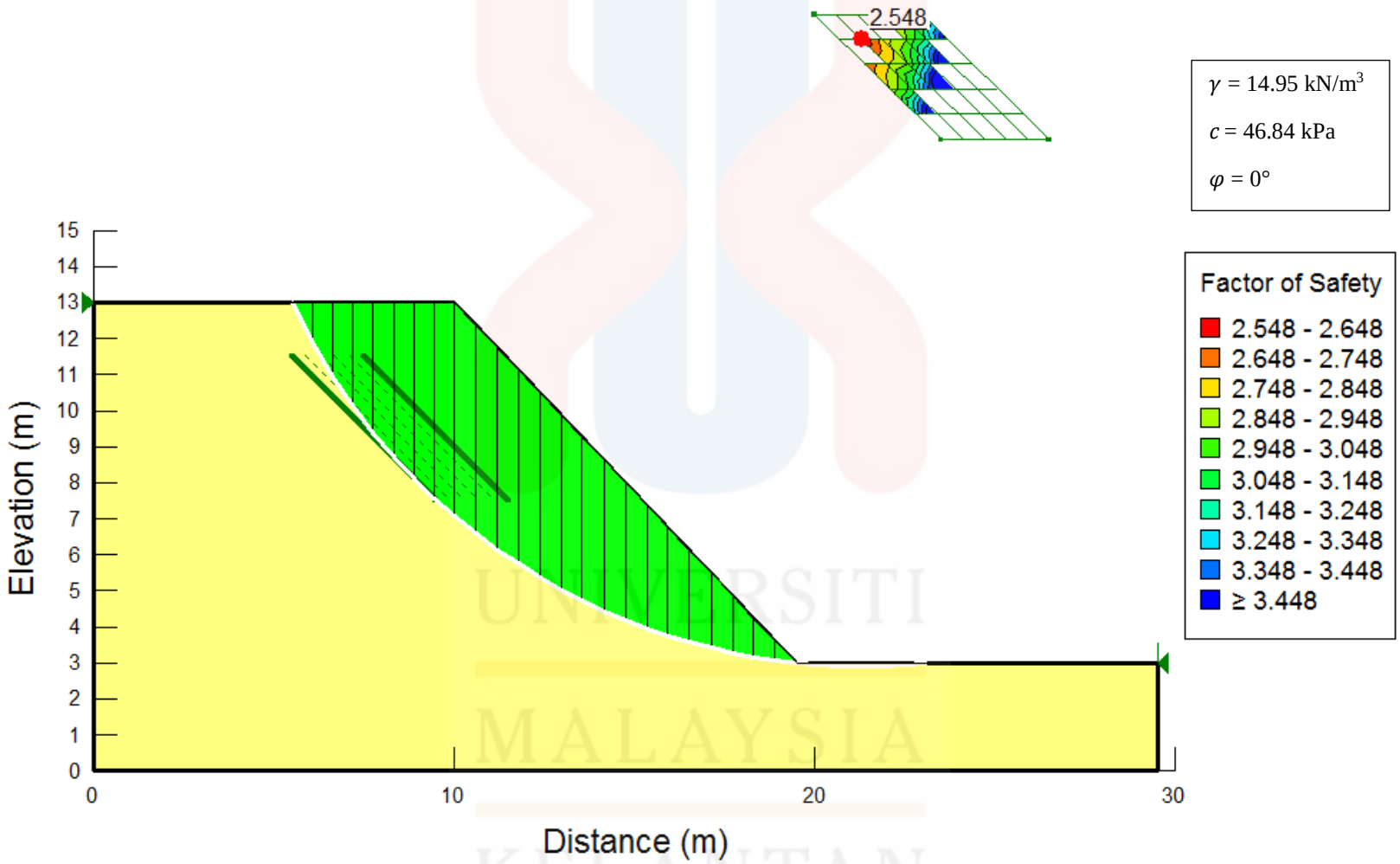

Figure 5.4: Slope 1 model with factor of safety of 2.548.

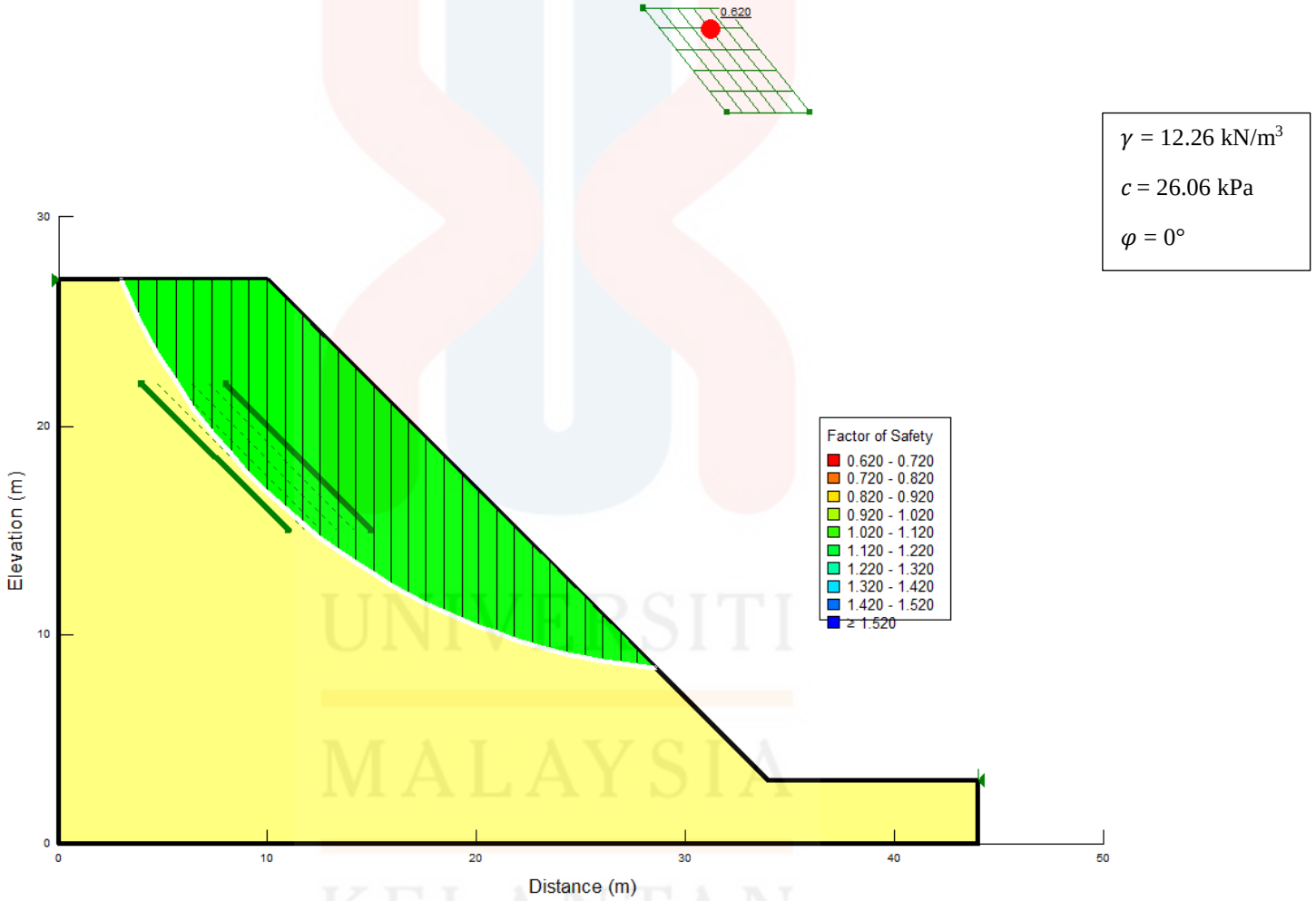

Figure 5.5: Slope model 2 with critical slip surface.

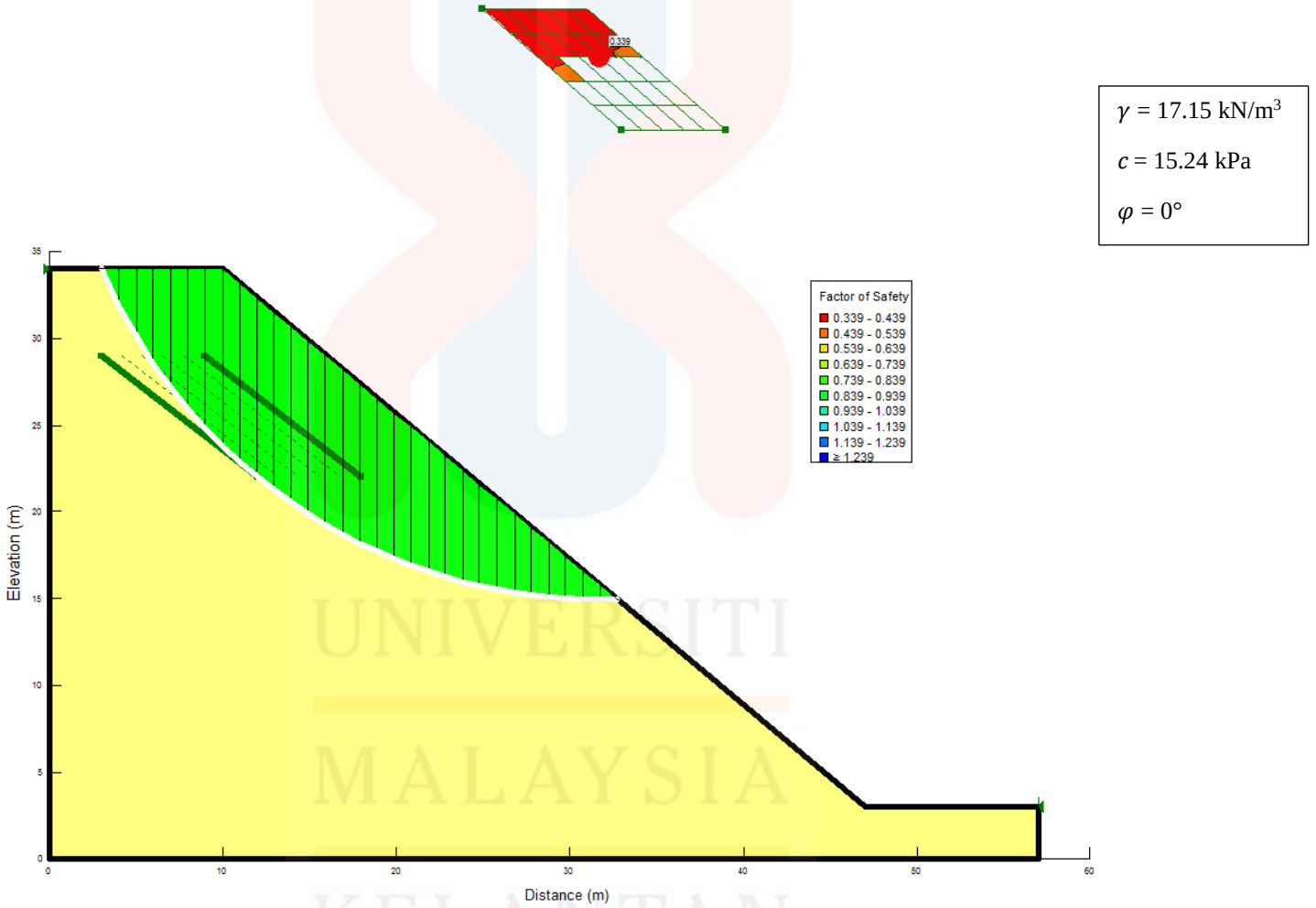

Figure 5.6: Slope model 3 with factor of safety of 0.339.

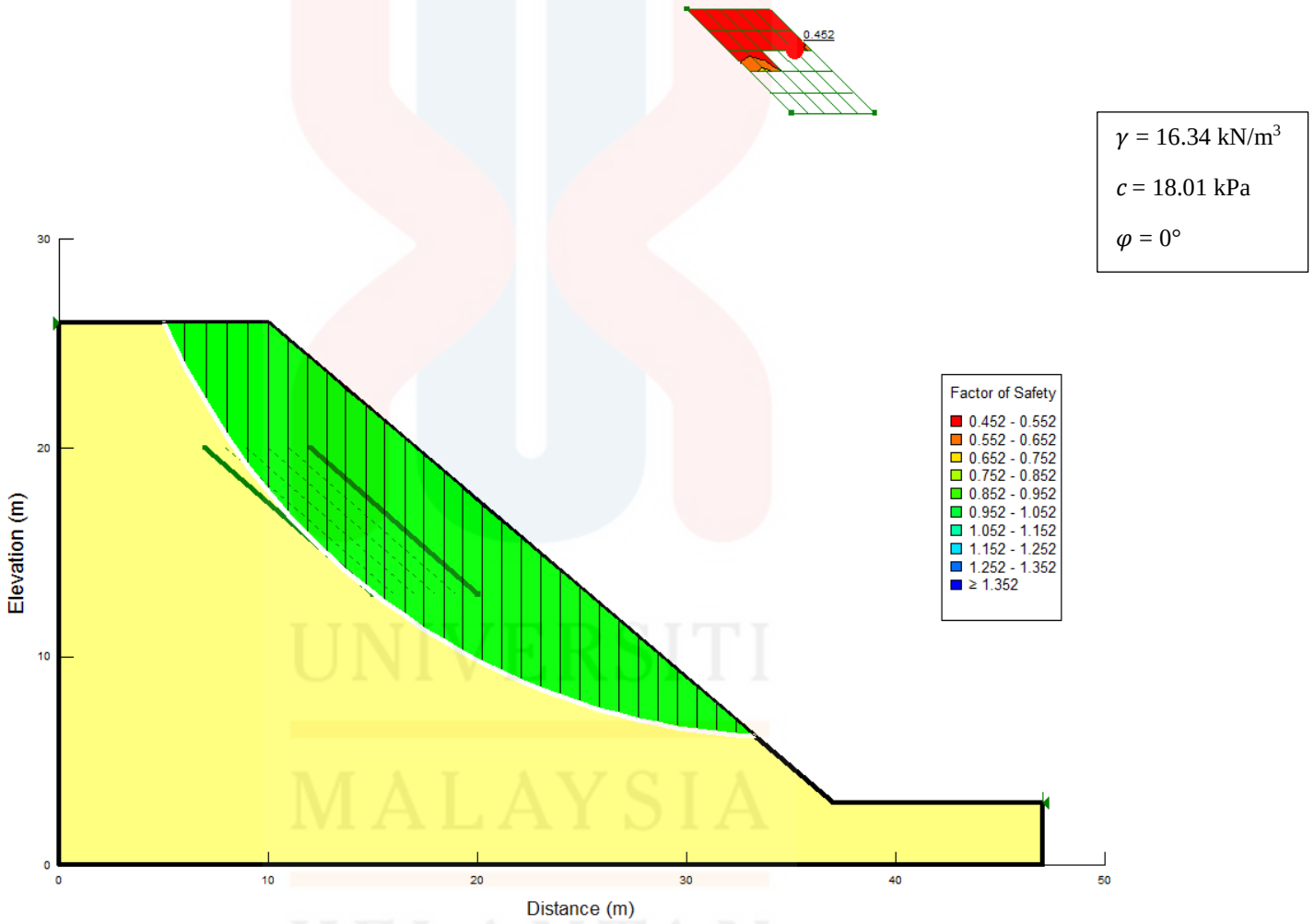

Figure 5.7: Slope model for slope 4 with critical slip surface.

Chapter 6

CONCLUSION AND RECOMMENDATION

6.1 Conclusion

As a conclusion, the geological map of Kuala Balah, Jeli, Kelantan with scale of 1:25 000 was updated. The lithology observed include fine-grained granite, granodiorite, fine-grained biotite granite, quartzite, fine-grained gneiss, coarse-grained quartz-plagioclase gneiss, shale, mudstone and metasandstone. All of these lithology are categorized into four group that can be mapped in the geological map. These groups are granite and gneiss; interbedded sandstone, mudstone and shale; granite intrusion and alluvium. Due to the previous extreme flood in 2014, the villages in the mapped are vanished and no longer exist. The only villages left are Kampung Kuala Balah, Kampung Kula and Kampung Batu Lembu.

Slope failure inventory of Kuala Balah, Jeli, Kelantan was produced according to the availability of the cut-slope failure. The parameters included slope geometry, mode/ type of failure, failure geometry, origin of soil/ rock, cause of failure, type of slope stabilization protection and vegetation cover of failure was measured during engineering mapping. Most of cut-slope failure have weathering grade of five and originated from shale. The type of failures are slump and rotational slide. All of the slopes are protected with vegetation and some of them are protected with Gabion retaining wall. The causes of the failure are weathering process and the rainfall.

Slope stability analysis for soil cut-slope by Slope/ W software was carried out. The lowest factor of safety for the selected slopes are determined. The properties of soil have been measured for the classification of soil. Moisture content test, plastic and liquid limits test, particle size distribution and laboratory vane shear test was carried out. The moisture content of soils are range in 23.38% to 41.69%. The soils have plastic limit range in 34.5 to 51.5, liquid limit of 41.2 to 74.7 and plasticity index of 5.1 to 35.4. From the particle size distribution test, there are only two soil samples have more than 50% of fine sand and six soil samples have more than 50% of silt. The average undrained shear strength from laboratory vane shear strength test range from 4.99 kPa to 48.64 kPa. There are only three types of soil classified which are sandy silty clay, sandy lean clay and sandy fat clay. The factor of safety determined by constructed the slope model are 2.548, 0.620, 0.339 and 0.452 for slope 1 to slope 4 respectively. It indicated there is only one stable slope and three of the slopes are unstable slopes.

6.2 Recommendation

For the geological mapping, it should be start earlier to avoid time constraint. The general knowledge of geological mapping has to improve to prevent the uncertainty of the geological features.

The laboratory test of soil, the laboratory vane shear strength test could be change to triaxial test to obtain the shear strength of the soil but not the average undrained shear strength. By the traxial test, the cohesion and angle of

friction of soil can be found by plotting the Mohr-Coulomb failure envelope. The more accurate value of cohesion and angle of friction can be obtained to increase the accuracy of the determination of factor of safety. Slope/ W is a recommended software used to determine the factor of safety. It is easy to use and the model problems can be solved within minutes.

Based on the factor of safety determined from Slope/ W software, there is three unstable and fail slope. The mitigation measure should be done to avoid the affect to accessibility of the road. Although all the slopes are covered by vegetation and one of them has Gabion retaining wall, the further stabilization protection have to be done as soon as possible especially before raining season. This is because most of the slope failure in Malaysia caused by rainfall. In Kelantan between November to January is monsoon season when heavy rainfall would lead to the slope failure in this particular area.

REFERENCE

Abdullah, I., & Setiawan, J. 2003. The kinematics of deformation of the Kenerong Leucogranite and its enclaves at Renyok waterfall, Jeli, Kelantan. Bulletin of the *Geological Society of Malaysia*, *46*, 307-312.

Adnan, N. A. 2010. *Quantifying the impacts of climate and land use changes on the hydrological response of a monsoonal catchment* (Doctoral dissertation, University of Southampton).

ASTM, D. 2006. 2487, Standard practice for classification of soils for engineering purposes (Unified Soil Classification System). *Annual Book of ASTM Standards*, 249-260.

ASTM, D. 2000. 4648-00, Standard Test Method for Laboratory Miniature Vane Shear Test for Saturated Fine-Grained Clayey Soil.

Aziman, M., & Husaini, O. 2001. Influence of discontinuity sets on slope failures at Pos Selim Highway, Malaysia. *Proceedings of Annual Geological Conference, Perak, Malaysia*, 237-242. Geological Society of Malaysia.

Azman A. Ghani. 2009. Plutonism. In. Hutchison, C.S. & Tan, N.K.D. (eds). *Geology of Peninsular Malaysia*, 211-232. Malaysia: The University of Malaya and the Geological Society of Malaysia.

Azman, A. Ghani. 2000. Mantled feldspar from the Noring granite, Peninsular Malaysia: petrography, chemistry and petrogenesis. *Bulletin of the Geological Society of Malaysia, 44*, 109-115.

Budhu, M. 2007. *Soil Mechanics and Foundations 2nd ed*. United States of America: John Wiley & Sons, Inc.

Caran, C. S., Woodruff Jr, C. M., & Thompson, E. J. 1981. Lineament Analysis and Inference of Geologic Structure--Examples from the Balcones/Ouachita Trend of Texas. *Geological Circular 82-1*, 59-69.

Chow, W. S. & Mohamad, Z. 2003. Debris slide at Kampung Chinchin, Gombak, Selangor. *Bulletin of the Geological Society of Malaysia, 46*, 51-58.

Cruden, D. M. & Varnes, D. J. 1996. Landslides: investigation and mitigation. Chapter 3-Landslide types and processes. *Transportation research board special report*, 247.

Dearman, W. R., 1991. *Engineering geological mapping. In*. Aziman, M., & Husaini, O. 2001. Influence of discontinuity sets on slope failures at Pos Selim Highway, Malaysia. In *Proceedings of Annual Geological Conference, Perak, Malaysia*, 237-242.

Geological Map of Kelantan State. 2010. Department of Minerals and Geoscience Malaysia

Duncan, J. M. 1996. Soil slope stability analysis. In. Turner, A. K. & Schuster, R. L. (eds). *Landslides investigation and mitigation*, 337-370. United States of America: Transportation Research Board.

Foo, K. Y. 1983. The Palaeozoic sedimentary rocks of Peninsular Malaysia—stratigraphy and correlation. In *Workshop on stratigraphic correlation of Thailand and Malaysia* (pp. 1-19).

Fossen, H. 2010. Structural Geology and Structural Analysis. In. *Structural Geology*, 1-18. United States of America: Cambridge University Press, New York.

Hashim, M. M. M., & Akhir, J. M. Lineament mapping using Landsat TM image in the eastern part of Gua Musang-Cameron Highland road.

Hassan, A. A. G. 2004. *Growth, structural change and regional inequality in Malaysia*. In. Adnan, N. A. 2010. Quantifying the impacts of climate and land use changes on the hydrological response of a monsoonal catchment (Doctoral dissertation, University of Southampton).

Head, K. H. 1980. *Manual of soil laboratory testing Vol. 1: Soil classification and compaction tests.* Great Britain: Engineering Laboratory Equipment Limited.

Highland, L. 2004. *Landslide types and processes* (No. 2004-3072). U.S. Department of the Interior & U. S. Geological Survey.

Hungr, O., Evans, S. G., Bovis, M. J., & Hutchinson, J. N. 2001. A review of the classification of landslides of the flow type. *Environmental & Engineering Geoscience*, *7*(3), 221-238.

Hussin, H., Jamaluddin, T. A., & Deraman, M. F. 2015. Mode of Slope Failure of Moderately to Completely Weathered Metasedimentary Rock at Bukit Panji, Chendering, Kuala Terengganu. *Journal of Tropical Resources and Sustainable Science*, *3*, 5-12.

Hutchison, C. S. 1977. Granite emplacement and tectonic subdivision of Peninsular Malaysia. *Bulletin of the Geological Society of Malaysia*, *9*, 187-207.

Hutchison, C. S. 2009a. Regional Geological Setting. In. Hutchison, C.S. & Tan, N.K.D. (eds). *Geology of Peninsular Malaysia*, 31-40. Malaysia: The University of Malaya and the Geological Society of Malaysia.

Hutchison, C. S. 2009b. Tectonic Evolution. In. Hutchison, C.S. & Tan, N.K.D. (eds). *Geology of Peninsular Malaysia*, 309-330. Malaysia: The University of Malaya and the Geological Society of Malaysia.

Hutchison, C. S. 2014. Tectonic evolution of Southeast Asia. *Bulletin of the Geological Society of Malaysia*, *60*, 1-18.

Jamaluddin, T. A. 1990. Geologi kejuruteraan Lebuh raya Timur-Barat penekanan kepada penstabilan cerun. In. Hussin, H., Jamaluddin, T. A., & Deraman, M. F. 2015. Mode of Slope Failure of Moderately to Completely Weathered Metasedimentary Rock at Bukit Panji, Chendering, Kuala Terengganu. *Journal of Tropical Resources and Sustainable Science*, *3*, 5-12.

Jamaluddin, T. A. 2006. Human factors and slope failures in Malaysia. *Bulletin of the Geological Society of Malaysia*, *52*, 75-84.

Jamaluddin, T. A., & Deraman, M. F. 2000. Relict Structures and Cut Slope Failures in Highly to Completely Weathered Rocks Along Jalan Tg. Siang, Kota Tinggi,

Johor. *Proceedings of the Geological Conference of the Geological Society of Malaysia*, 305-312. Geological Society of Malaysia.

Khoo, T. T., & Tan, B. K. 1983. Geological evolution of peninsular Malaysia. In *Proceedings of the Workshop on Stratigraphic Correlation of Thailand and Malaysia* (Vol. 1, pp. 253-290). Geol. Soc. Thailand and Geological Society Malaysia Bangkok.

Lee, C. P. 2009. Palaeozoic Stratigraphy. In. Hutchison, C.S. & Tan, N.K.D. (eds). *Geology of Peninsular Malaysia*, 55-86. Malaysia: The University of Malaya and the Geological Society of Malaysia.

Low, T. H., Ali, F., & Ibrahim, A. S. 2012. An investigation on one of the rainfall-induced landslides in Malaysia. *Electronic Journal of Geotechnical Engineering*, **17**, 435-449.

Metcalfe, I., & Azhar, H. H. 1995. Implications of new biostratigraphic data for stratigraphic correlation of the Permian and Triassic in Peninsular Malaysia. *Geological Society of Malaysia Bulletin*, *38*, 173-177.

Metclafe, I. 2000. The Bentong-Raub Suture Zone. *Journal of Asian Earth Sciences*, 18, 691-712.

Monroe, J. S., Wicander, R. & Hazlett, R. W. 2006. Mass Wasting. In. *Physical Geology: Exploring the Earth 6th ed*. 424-455. Thomson Brooks/ Cole.

Ng, K. Y. 2012. *Rainfall-Induced Landslides in Hulu Kelang Area, Malaysia* (Doctoral dissertation, UTAR).

People Distribution Information. 2013. Official Website Kota Bharu Municipal Council Islamic City. (Online) (30 April 2016). http://www.mpkbbri.gov.my/c/document_library/get_file?uuid=f069f86e-6738-4bac-b244-d4c6899c3c8d&groupId=20005

Raj, J. K. 2000. Rainfall and slope failures in the granitic bedrock areas of Peninsular Malaysia. *Proceedings of the Annual Geological Conferences, Pulau Pinang, Malaysia*, 275-282. Geological Society of Malaysia.

Ritter, M. E. 2006. The Physical Environment: an Introduction to Physical Geography. (Online) (31 October 2016). http://www.earthonlinemedia.com/ebooks/tpe_3e/title_page.html

Robert, B. J. & Jerome, V. D. 1988. Engineering Properties of Rocks. In. *Principles of Engineering Geology*. 126 – 212. Canada: John Wiley & Sons, Inc.

Shuib, M. K. 2009a. Major Faults. In. Hutchison, C.S. & Tan, N.K.D. (eds). *Geology of Peninsular Malaysia*, 249-269. Malaysia: The University of Malaya and the Geological Society of Malaysia.

Shuib, M. K. 2009b. Structures and Deformation. In. Hutchison, C.S. & Tan, N.K.D. (eds). *Geology of Peninsular Malaysia*, 271-308. Malaysia: The University of Malaya and the Geological Society of Malaysia.

Singh, D. S., Chu, L. H., Teoh, L. H., Loganathan, P., Cobbing, E. J., & Mallick, D. I. J. 1984. The stong complex: A reassessment. *Bulletin of the Geological Society of Malaysia*, *17*, 61-77.

Stability modeling with SLOPE/W. 2012. Canada: GEO-SLOPE International Ltd.

Streams and Drainage Systems. 2015. Tulane University. (Online) (20 November 2016). http://www.tulane.edu/~sanelson/eens1110/streams.htm

Subinoy, G. (eds). 2013. Landslide Evaluation and Mitigation. In. *Engineering Geology*, 466- 489. India: Oxford University Press.

Tanot Unjah, Ibrahim Komoo & Hamzah Mohamad. 2001. Inventori sumber warisan geologi dan landskap Negeri Kelantan. *Proceedings of Annual Geological Conference, Pulau Pangkor, Perak, Malaysia*, 279-286. Geological Society of Malaysia.

West, T. R. (eds). 2010. Landslides, Subsidence, and Slope Stability. In. *Geology Applied to Engineering*. 281-319. Illinois: Waveland Press. Inc.

APPENDIX-A: Nomenclature of Slopes

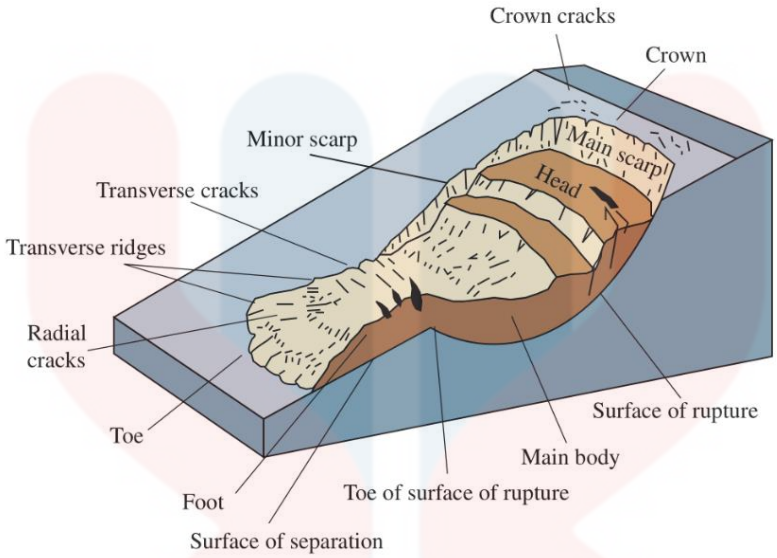

Crown: Steep, bare or sparsely vegetated slope form which the landslide is staring and remain material that still in place, basically undisplaced and adjacent to the highest parts of the main scarp.

Foot: Portion of the displaced material that has moved beyond the toe of the surface of rupture and overlies the original ground surface.

Head: The upslope portion or upper parts of the landslide along the contact between the displaced material and the main scarp.

Main body: Part of the displaced material of a landslide that overlies the surface of rupture between the main scarp and the toe of the surface of rupture.

Main scarp: Steep surface on the undisturbed ground at the upper edge of the landslide, caused by movement of the displaced material away from the undisturbed ground. It is visible part of the surface of rupture.

Minor scarp: Steep surface on the displaced material of a material of a landslide produced by differential movements within the displaced material.

Surface of rupture: Surface which forms or has formed lower boundary of the displaced material of a landslide below the original ground surface.

Surface of separation: Part of the original ground surface overlain by the foot of a landslide.

Toe: Downslope portion of a landslide usually curved margin of the displaced material of a landslide, it is the most distant from the main scarp.

Toe of surface of rupture: Intersection (usually buried) between the lower part of the surface of rupture of a landslide and the original ground surface.

APPENDIX-B: Type of Slope Failure

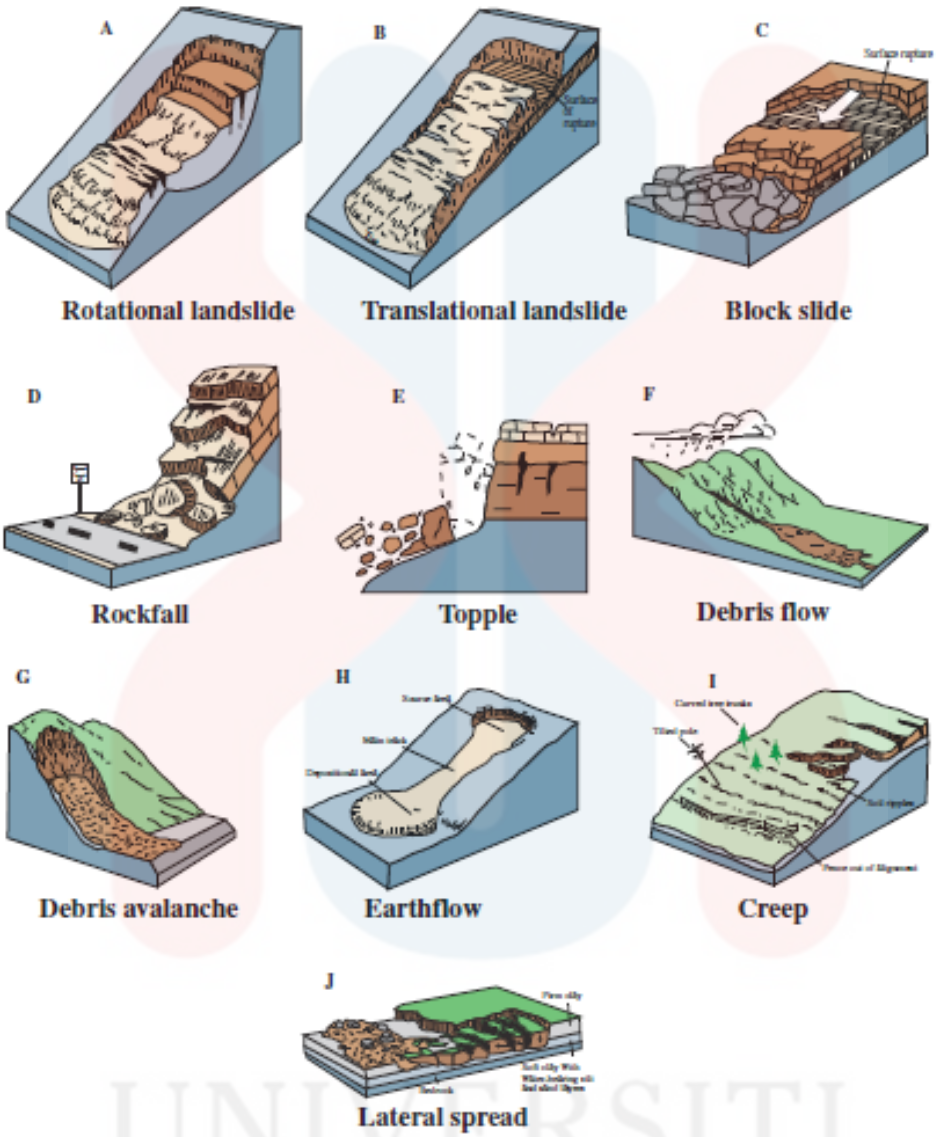

APPENDIX-C: Soil Classification Flow Chart (Source: ASTM Standards)

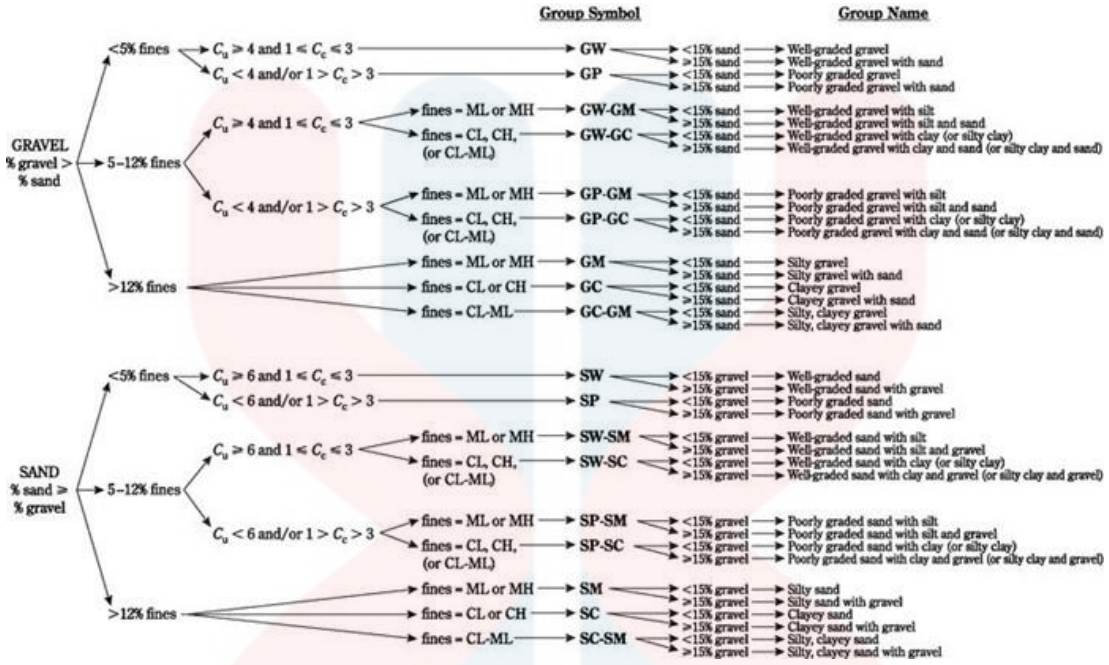

Coarse-grained soil

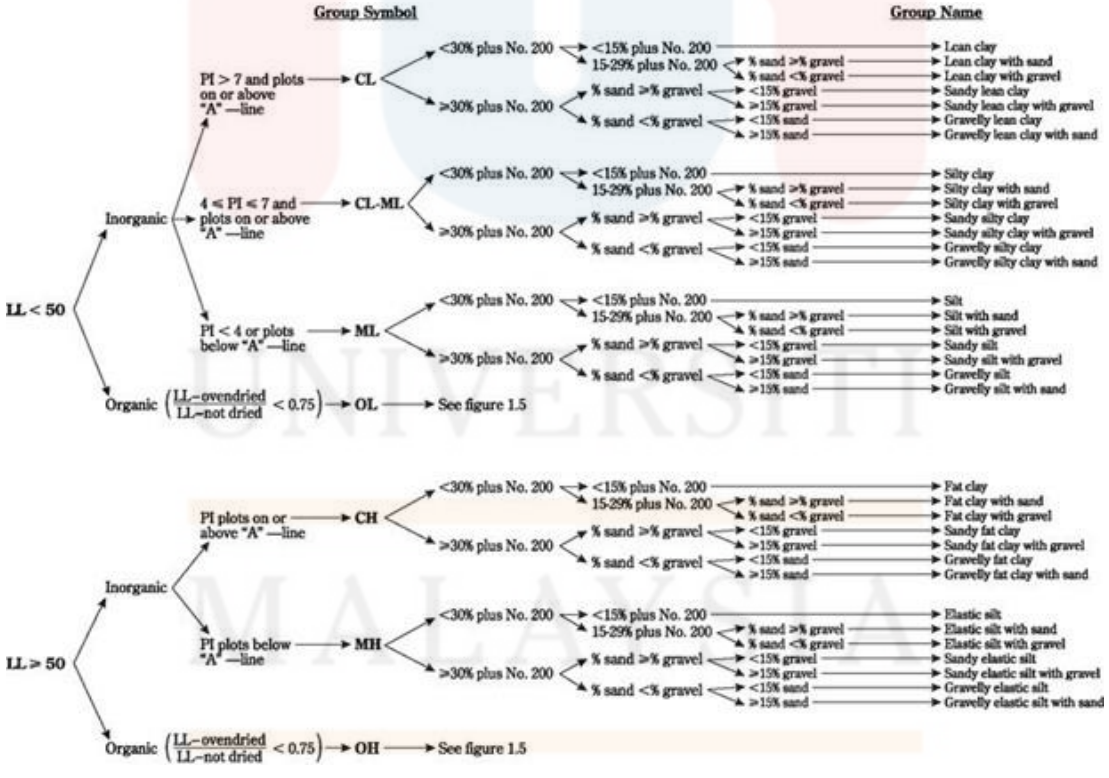

Fine-grained soil

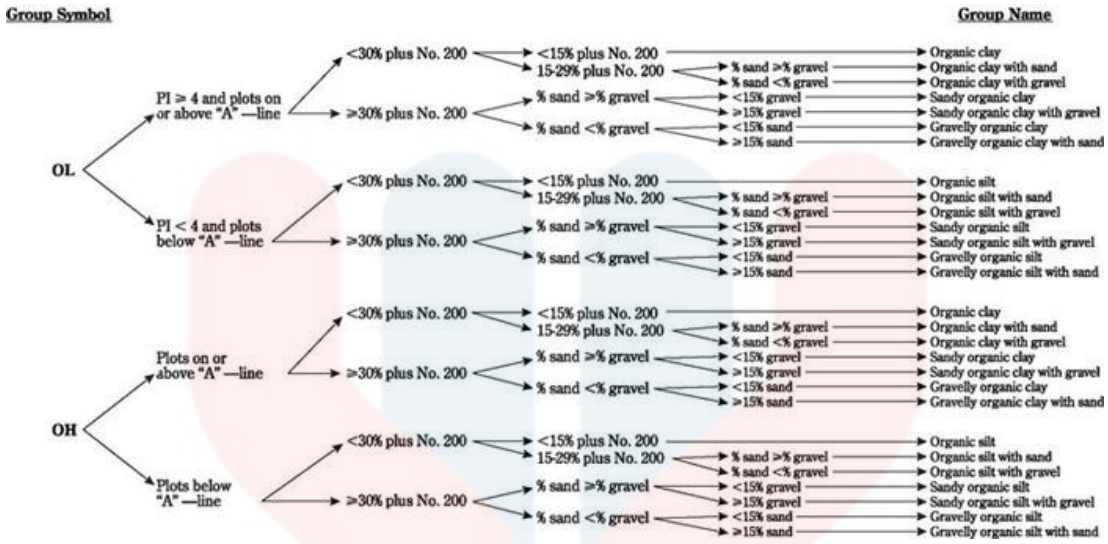

Fine-grained organic soil

APPENDIX-D: Method to Produce Thin Section of Rock Sample

a. Preparing the sample

Preparing the rock sample that target to make thin section and decide which part is going to be cut. A mark is plotted on the rock with the presence of the mineral and texture of the rock that ready to be observed. The different cuts will show the different rock fabric. The cutting of the rock for thin section usually on a plane perpendicular to any planar fabric.

b. Cutting

By using masonry saw, the rock can be cut into 4 cm x 2.5 cm and about 1 cm of thickness to obtain a flat surface. The size of cut rock is reduce to slightly smaller than a thin section.

c. Grinding

This process is to remove any saw marks from the cutting. The grinding process must start from the coarsest grinding disk. The grinding disk must clean and without any grains that can destroy the rock sample. When with the finer grade grinding disk, the specimen has to grinding slowly to avoid the broken of the specimen.

d. Polishing

Polishing process is to eliminate the traces of cutting and to obtain a flat surface as smooth as possible. A very flat piece of metal or glass about 70 mm – 100 mm diameter act as the substrate of the polishing tool. The light pressure and grind is use until all the scratches are gone.

e. Slide Mounting

The polished surface is stick onto a clean glass microscope slide with colourless and isotropic glue (epoxy). The epoxy is spread on rock specimen and placing slide on it, frosted down side. The slide is moving around to expel bubbles and extra epoxy. The extra epoxy is prevent to use because it will become a messy job.

f. Final Cutting

After the rock specimen is stuck onto the glass microscope slide, the process of final cutting is carry out to obtain the thinnest slice as possible about 0.3 cm thick by using the masonry saw.

g. Trimming

The trimming process is includes thinning and grinding process. The rock specimen is grinding again to about 30 microns thick and grind away all the cutting marks.

h. Final polish

In this step, the epoxy and rock specimen is polish until as clear as possible. It must be avoid that the glue will be start to peel off at this stage.

i. Covering

The rock specimen has to be wash or scrub to make sure there is no any leaving of polishing residue. The similar isotropic glue (epoxy) is use for the slide covering. The epoxy is drop onto the rock specimen and the slide is pace on it. The cover is moving to spread the epoxy and remove the bubbles. After the cover glass is well stuck, the excess epoxy is clean up.

APPENDIX-E: Photos

Photo E1: Slope failure 1 covered by vegetation

(Coordinate: N 05° 24’ 44.0”, E 101° 55’ 54.2”)

Photo E2: Exposed part of slope failure 1

(Coordinate: N 05° 24’ 44.0”, E 101° 55’ 54.2”)

Photo E3: Slope failure 2 and 3

(Coordinate: N 05° 24’ 41.9”, E 101° 55’ 55.1”)

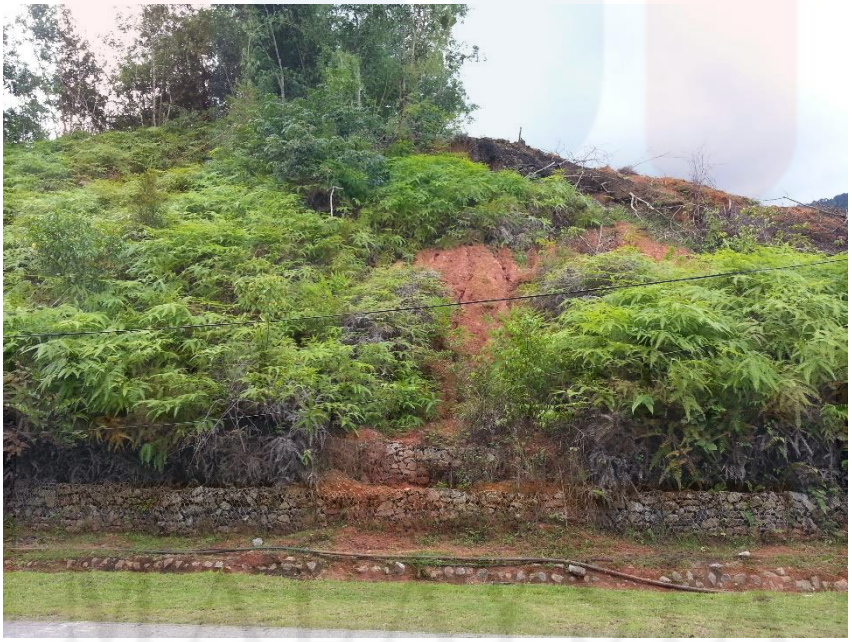

Photo E4: Slope failure 4

(Coordinate: N 05° 24’ 33.1”, E 101° 56’ 07.3”)

Photo E5: Slope failure 5

(Coordinate: N 05° 24’ 09.3”, E 101° 56’ 16.5”)

Photo E6: Slope failure 6

(Coordinate: N 05° 24’ 00.6”, E 101° 56’ 45.0”)

Photo E7: Slope failure 7

(Coordinate: N 05° 24’ 25.3”, E 101° 56’ 22.1”)

Photo E8: Slope failure 8

(Coordinate: N 05° 24’ 25.5”, E 101° 56’ 20.9”)

APPENDIX-F

Photo F1: Soil sample from field

Photo F2: Moisture content laboratory test

Photo F3: Particle size distribution test

Photo F4: Particle size distribution test

Photo F5: Soil sample from plastic limit test

Photo F6: Soil sample preparation for vane shear strength test

Photo F7: Soil sample for vane shear strength test

Photo F8: Laboratory vane shear strength test (Test at Politeknik Kota Bharu)

Photo F9: Liquid limit test (Test at Politeknik Kota Bharu)

APPENDIX- G: Laboratory Test Results

Results of plastic limit from laboratory test

No. of sample	Mass of evaporating dish (g)	Mass of evaporating dish + wet soil (g)	Mass of evaporating dish + dry soil (g)	Mass of dry soil (g)	Mass of water loss (g)	Moisture content (%)	Plastic limit
1	20.08	44.30	37.88	17.80	6.42	36.1	36.1
2	22.62	47.79	41.34	18.72	6.45	34.5	34.5
3	22.92	48.10	39.54	16.62	8.56	51.5	51.5
4	22.12	48.55	40.58	18.46	7.97	43.2	43.2
5	24.92	50.76	43.87	18.95	6.89	36.4	36.4
6	23.66	51.48	42.09	18.43	9.39	50.9	50.9
7	21.75	47.32	40.22	18.47	7.10	38.4	38.4
8	22.92	49.35	41.04	18.12	8.31	45.9	45.9

Results of liquid limit from laboratory test

Sample No.1

Test number	No. of blows	Mass of container (g)	Mass of container + wet soil (g)	Mass of container + dry soil (g)	Mass of dry soil (g)	Mass of water loss (g)	Moisture content (%)
1	42	0.40	10.80	8.05	7.65	2.96	38.7
2	30	0.40	14.80	10.50	10.10	4.02	39.8
3	22	0.40	12.30	8.81	8.41	3.49	41.5
4	14	0.40	11.50	8.10	7.70	3.40	44.2
5	12	0.40	12.60	8.76	8.36	3.84	45.9

Sample No.2

Test number	No. of blows	Mass of container (g)	Mass of container + wet soil (g)	Mass of container + dry soil (g)	Mass of dry soil (g)	Mass of water loss (g)	Moisture content (%)
1	31	0.4	12.3	8.63	8.23	3.67	44.6
2	24	0.4	10.3	7.15	6.75	3.15	46.7
3	19	0.4	9.1	6.25	5.85	2.85	48.7
4	15	0.4	8.7	5.86	5.46	2.72	49.8
5	11	0.4	12.7	8.50	8.10	4.20	51.9

Sample No.3

Test number	No. of blows	Mass of container (g)	Mass of container + wet soil (g)	Mass of container + dry soil (g)	Mass of dry soil (g)	Mass of water loss (g)	Moisture content (%)
1	48	0.5	11.1	7.08	6.58	4.02	61.1
2	36	0.5	9.6	6.05	5.55	3.55	64.0
3	28	0.6	10.8	6.76	6.16	4.04	65.6
4	19	0.6	11.5	7.09	6.49	4.41	68.0
5	14	0.6	12.5	7.47	6.87	5.03	73.2

Sample No.4

Test number	No. of blows	Mass of container (g)	Mass of container + wet soil (g)	Mass of container + dry soil (g)	Mass of dry soil (g)	Mass of water loss (g)	Moisture content (%)
1	50	0.3	11.0	7.49	7.19	3.51	48.8
2	35	0.4	14.9	10.00	9.60	4.90	51.0
3	25	0.3	16.5	11.01	10.71	5.49	51.3
4	17	0.4	12.1	7.98	7.58	4.12	54.4
5	11	0.4	11.6	7.62	7.22	3.98	55.1

Sample No.5

Test number	No. of blows	Mass of container (g)	Mass of container + wet soil (g)	Mass of container + dry soil (g)	Mass of dry soil (g)	Mass of water loss (g)	Moisture content (%)
1	51	0.4	9.3	5.85	5.45	3.45	63.3
2	45	0.4	11.8	7.31	6.91	4.49	65.0
3	32	0.5	10.4	6.24	5.74	4.16	72.5
4	22	0.6	12.6	7.36	6.76	5.24	77.5
5	14	0.6	13.1	7.45	6.85	5.65	82.5

Sample No.6

Test number	No. of blows	Mass of container (g)	Mass of container + wet soil (g)	Mass of container + dry soil (g)	Mass of dry soil (g)	Mass of water loss (g)	Moisture content (%)
1	54	0.6	9.1	5.91	5.31	3.19	60.1
2	42	0.3	8.5	5.32	5.02	3.18	63.3
3	34	0.6	10.4	6.45	5.85	3.95	67.5
4	21	0.3	10.1	5.89	5.59	4.21	75.3
5	15	0.6	9.3	5.33	4.73	3.97	83.9

Sample No.7

Test number	No. of blows	Mass of container (g)	Mass of container + wet soil (g)	Mass of container + dry soil (g)	Mass of dry soil (g)	Mass of water loss (g)	Moisture content (%)
1	52	0.50	10.10	6.42	5.92	3.68	62.2
2	42	0.40	10.30	6.31	5.91	3.99	67.5
3	34	0.40	8.80	5.29	4.89	3.51	71.8
4	25	0.30	10.30	5.96	5.66	4.34	76.7
5	12	0.40	14.00	7.92	7.52	6.08	80.9

Sample No.8

Test number	No. of blows	Mass of container (g)	Mass of container + wet soil (g)	Mass of container + dry soil (g)	Mass of dry soil (g)	Mass of water loss (g)	Moisture content (%)
1	46	0.50	12.90	8.86	8.36	4.04	48.3
2	37	0.40	10.70	7.22	6.82	3.48	51.0
3	31	0.40	13.20	8.79	8.39	4.41	52.6
4	24	0.40	11.30	7.47	7.07	3.83	54.2
5	14	0.50	11.60	7.41	6.91	4.19	60.6

Graph of Moisture Content against No. of Blows for Sample 1 to Sample 8

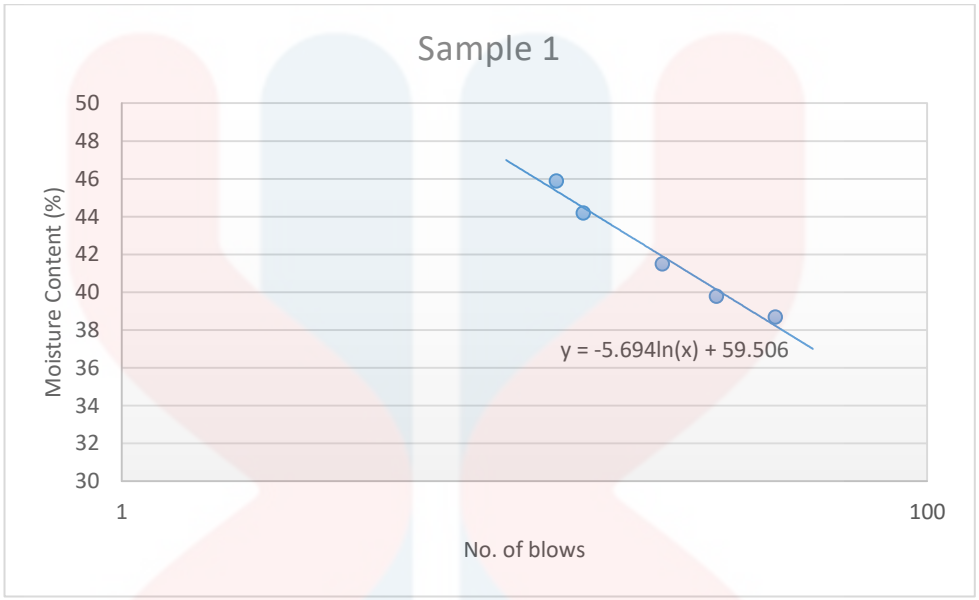

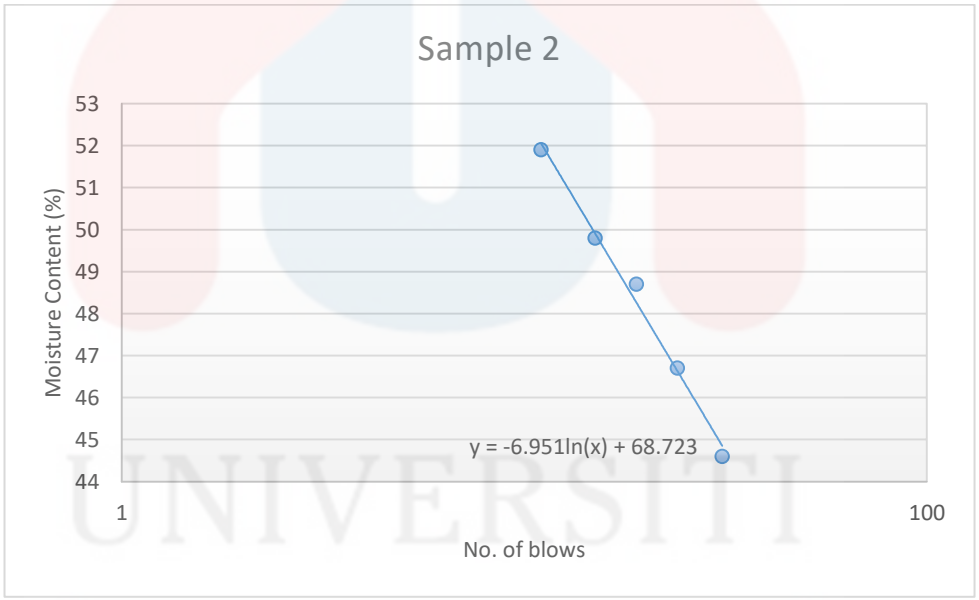

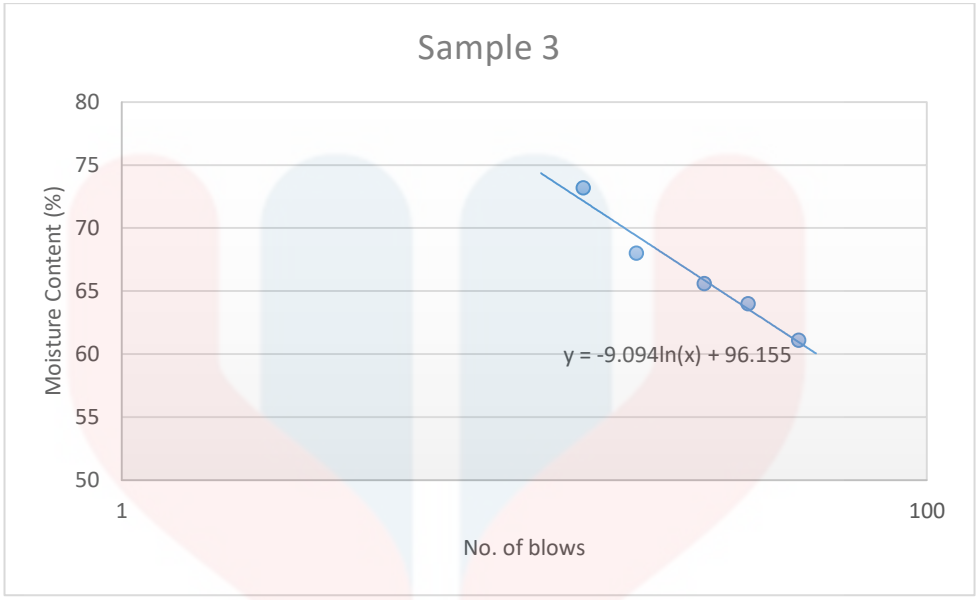

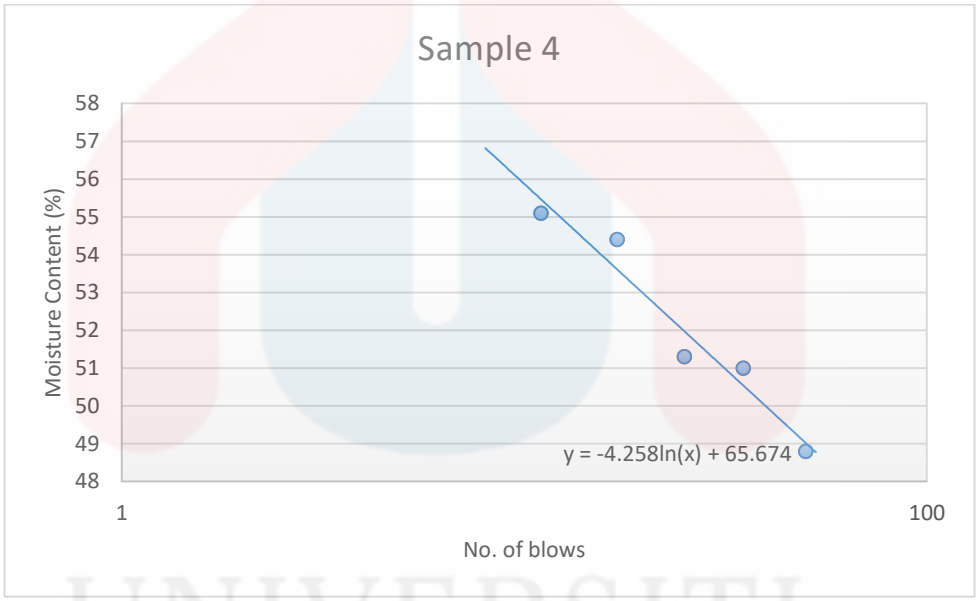

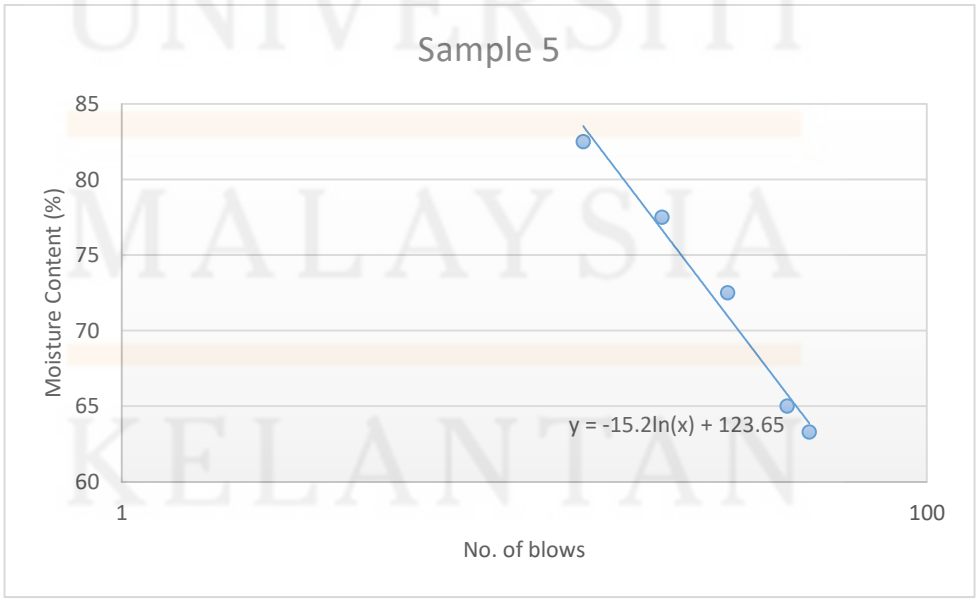

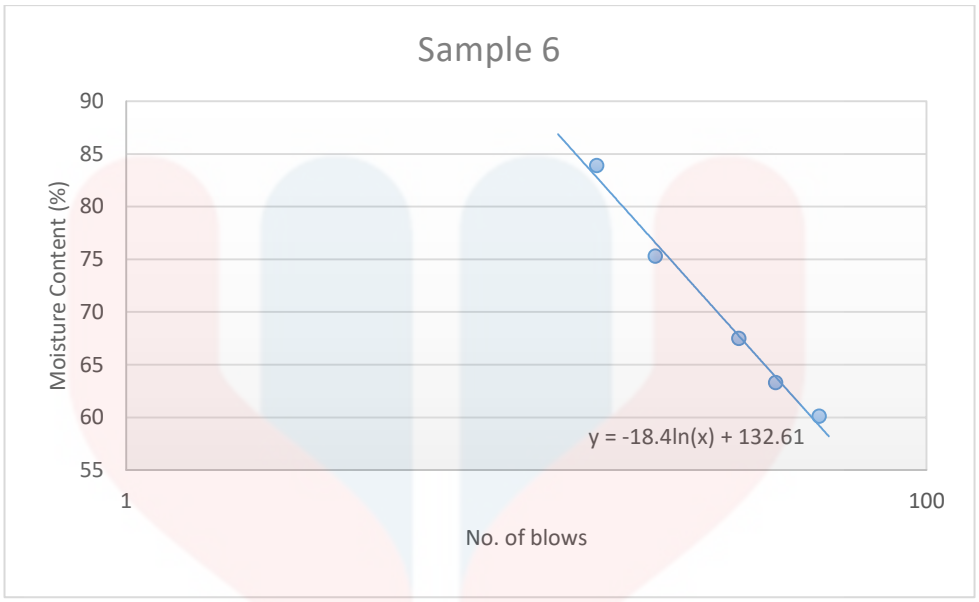

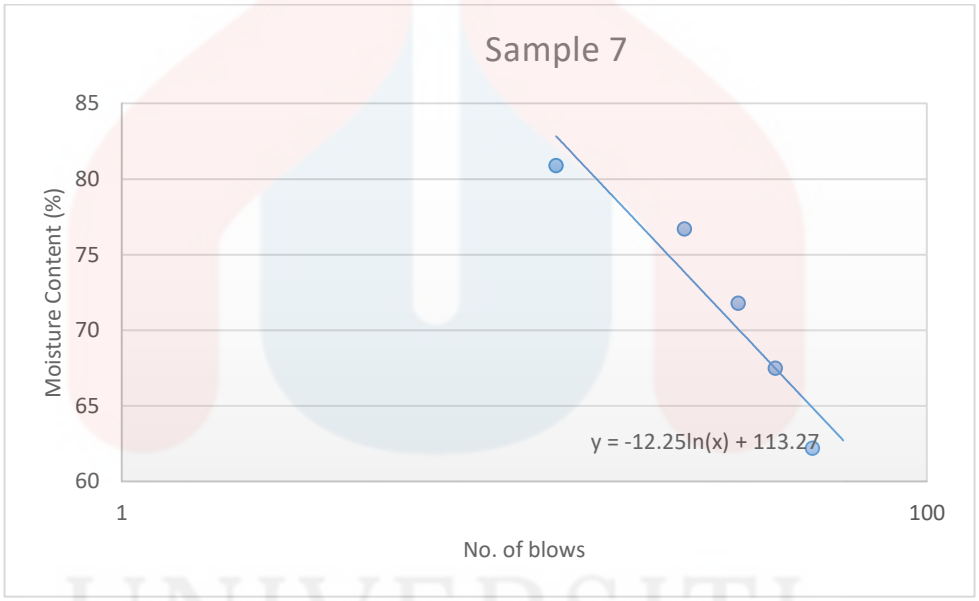

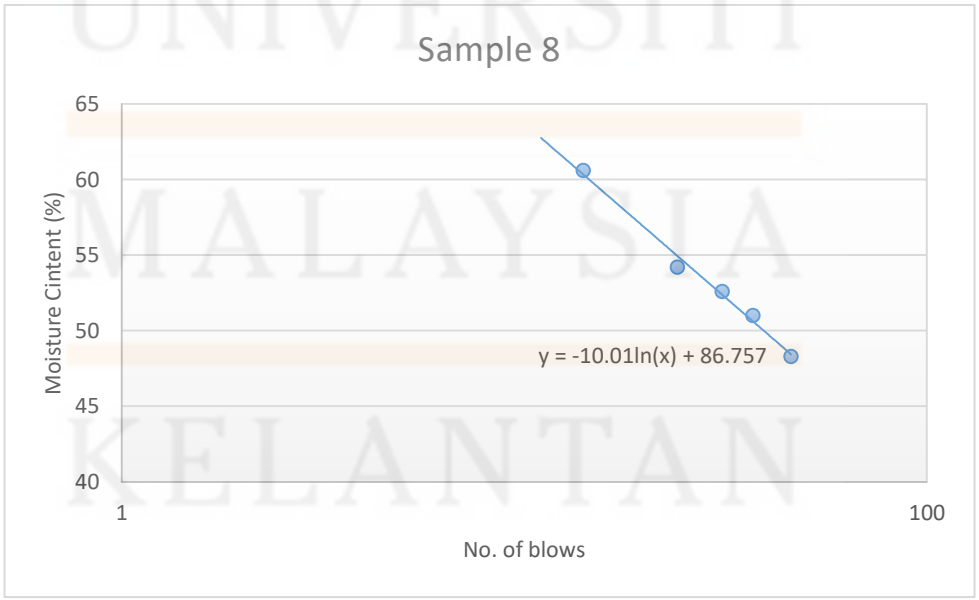

APPENDIX-H: Graph of Particle Size Distribution

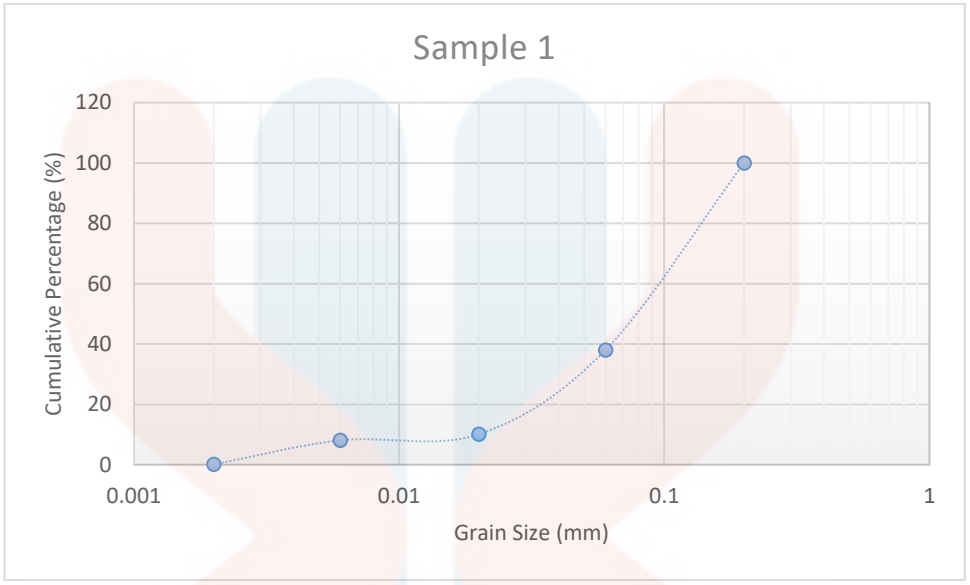

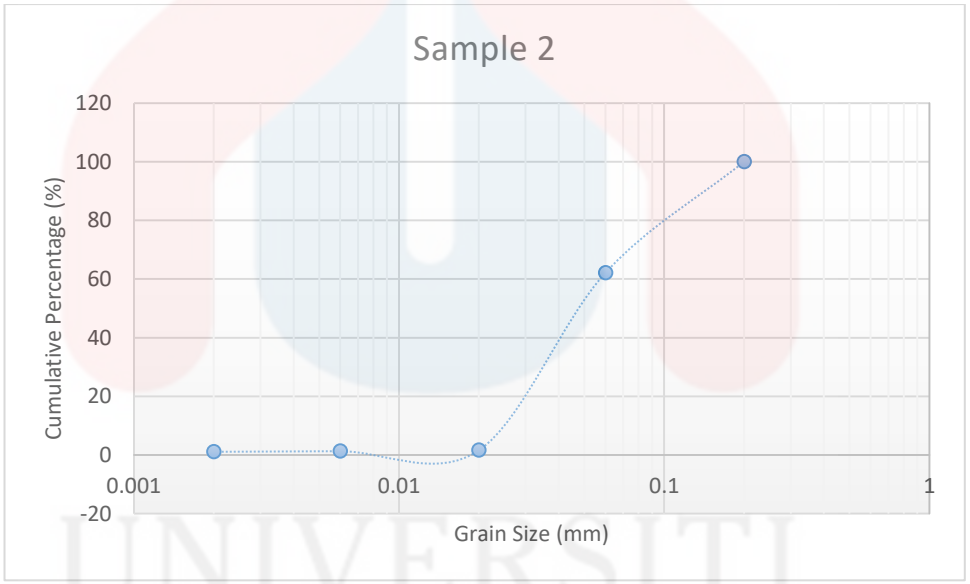

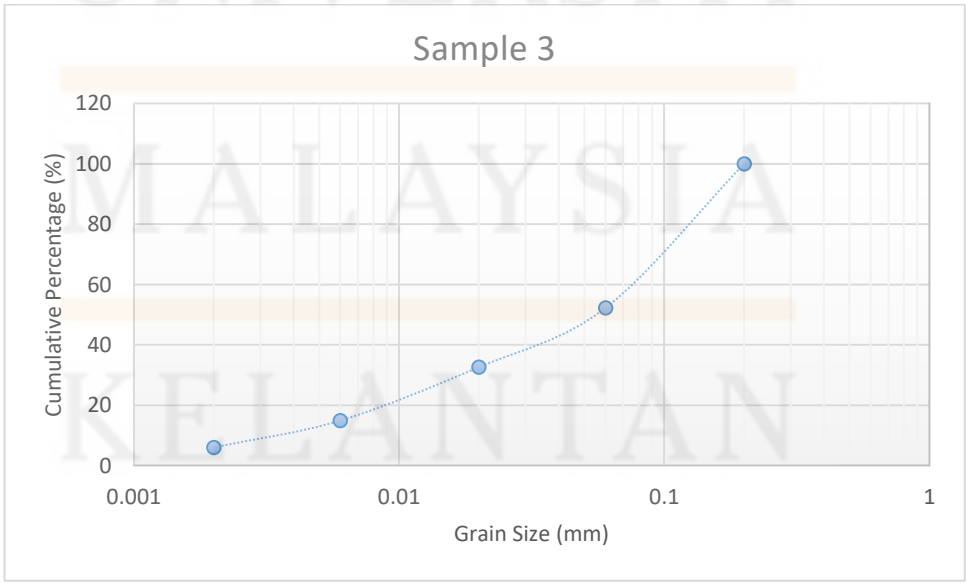

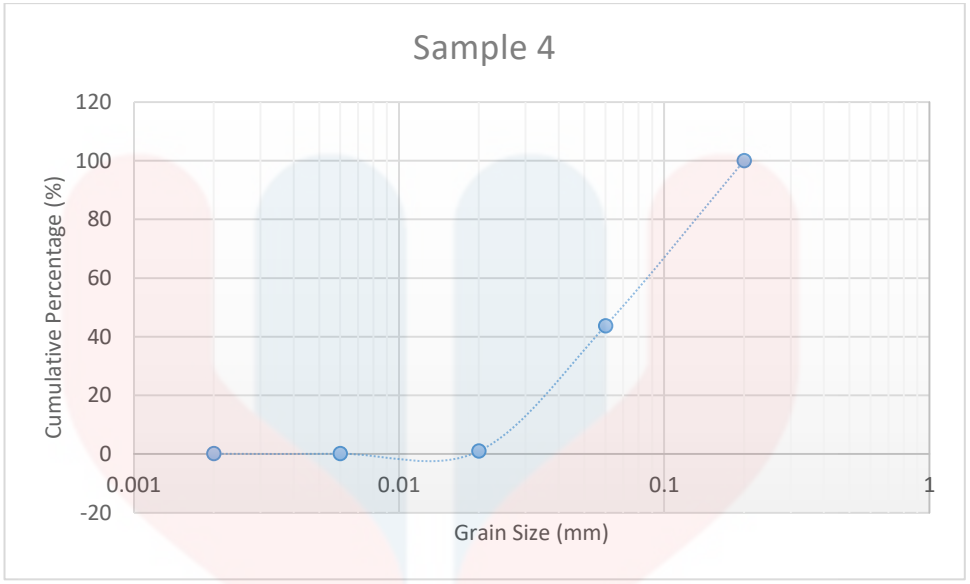

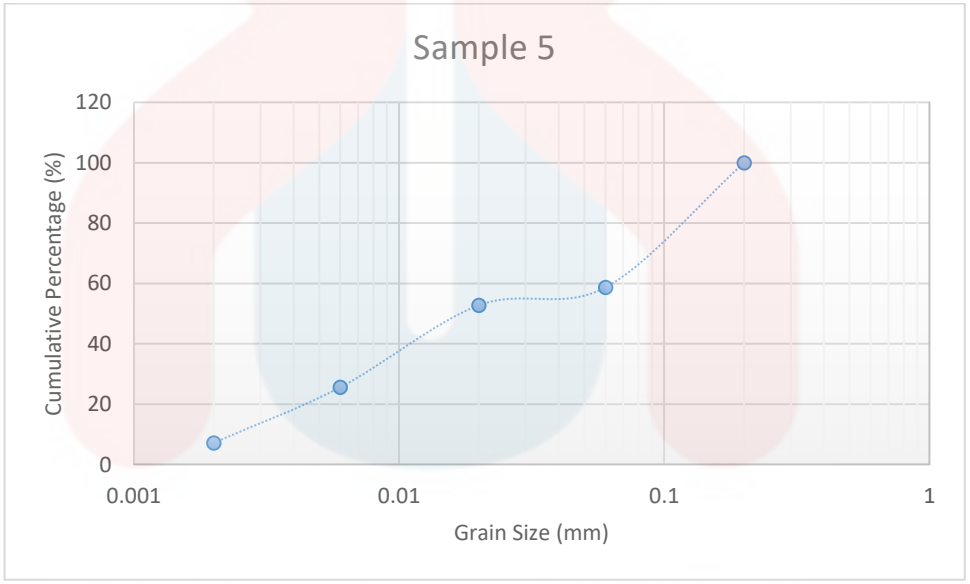

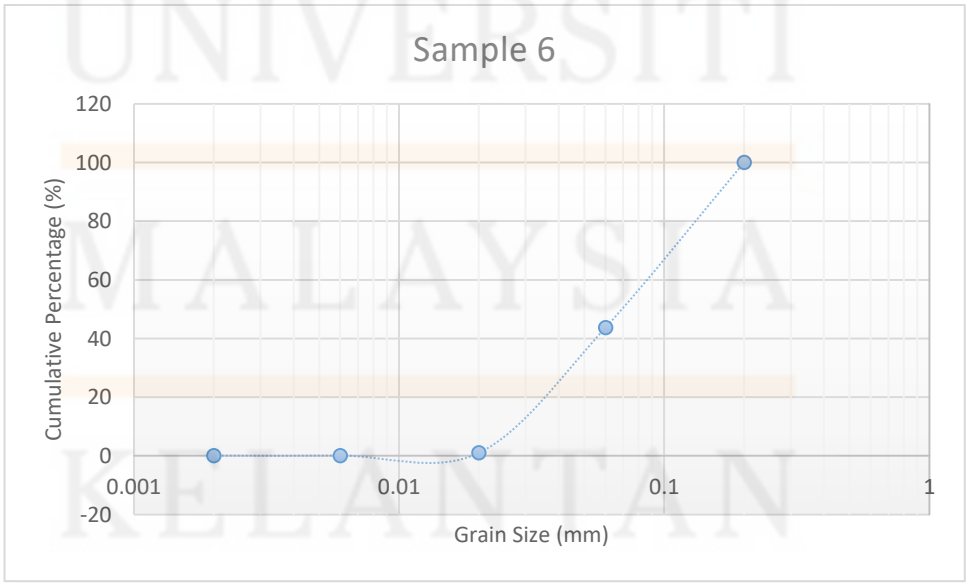

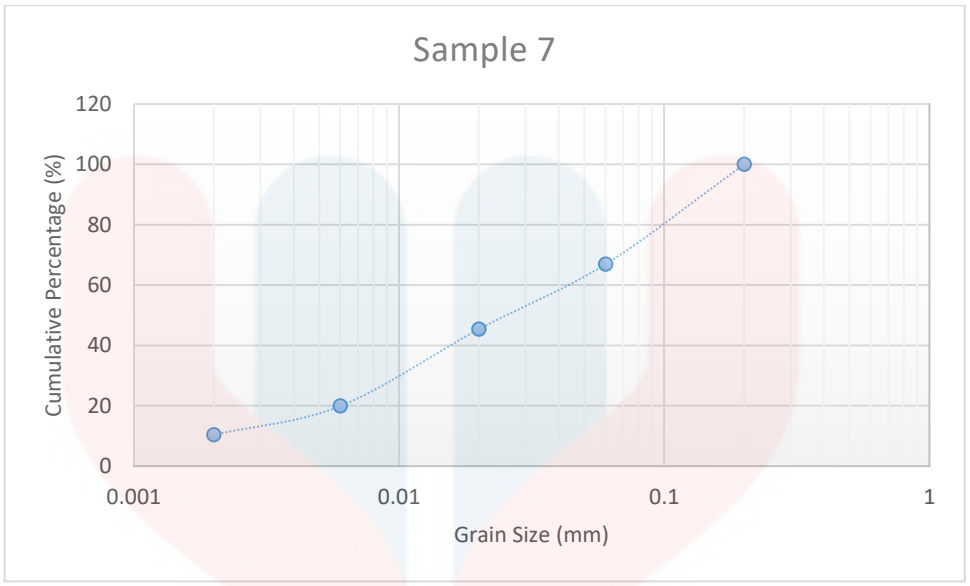

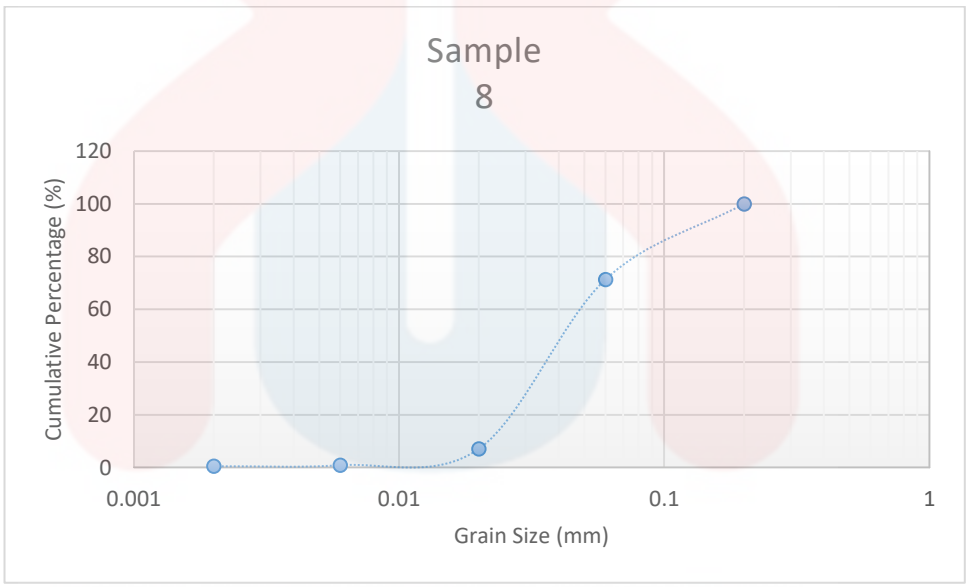

APPENDIX-I: Laboratory Vane Shear Test Results and Moisture Content of Sample in Laboratory Vane Shear Test

No. of sample	Initial torque angle (°)	Final torque angle (°)	Difference in torque angle (°)	Applied torque, T (kgcm)	Average undrained shear strength, C_u (kg/cm^2)	Average undrained shear strength, C_u (kPa)
1	168	337	169	3.0251	0.4776	46.84
2	168	192	24	0.4296	0.0678	6.65
3	172	266	94	1.6826	0.2657	26.06
4	165	277	112	2.0048	0.3165	31.04
5	165	220	55	0.9845	0.1554	15.24
6	165	183	18	0.3222	0.0509	4.99
7	166	231	65	1.1635	0.1837	18.01
8	167	231	64	1.1456	0.1809	17.74

Diameter of vane blade = 1.2 cm Height of vane blade = 2.4 cm $K = 6.33$ cm^3

Vane blade constant, $K = \pi \left(\frac{D^2 H}{2} + \frac{D^3}{6}\right)$

Example : Vane blade constant, $K = \pi \left(\frac{D^2 H}{2} + \frac{D^3}{6}\right)$

$$= \pi \left(\frac{1.2^2 \, x \, 2.4}{2} + \frac{1.2^3}{6}\right)$$

$$= 6.33 \text{ cm}^3$$

Moisture Content of Sample in Laboratory Vane Shear Test

No. of sample	Mass of container (g)	Mass of container + wet soil (g)	Mass of container + dry soil (g)	Mass of water loss (g)	Mass of dry soil (g)	Moisture content (%)
1	32.0	45.3	41.2	4.1	9.2	44.6
2	0.6	10.7	7.7	3.0	7.1	42.3
3	0.3	6.9	4.9	2.0	4.6	43.5
4	33.6	81.3	59.3	22.0	25.7	85.6
5	0.3	12.7	8.6	4.1	8.3	49.4
6	30.7	66.8	50.4	16.4	19.7	83.2
7	30.7	57.0	49.1	7.9	18.4	42.9
8	32.8	60.7	50.0	10.7	17.2	62.2

Spring Calibration of Spring No.2

Torque (kgcm)	Degree	Torque (Nm)	Degree
0.25	14	0.025	14
0.50	28	0.050	29
1.00	56	0.100	57
1.50	84	0.150	86
2.00	112	0.200	114
2.50	140	0.250	143
3.00	168	0.300	171

(Source : Manufacture)